DEVELOPING REGIONAL SEISMIC DATABASES FOR IMPROVING EVENT LOCATION AND GROUND TRUTH DATA SETS IN ASIA

Michael L. Begnaud, Julio C. Aguilar-Chang, Aaron A. Velasco, Lee K. Steck

Los Alamos National Laboratory

Sponsored by National Nuclear Security Administration
Office of Nonproliferation Research and Engineering
Office of Defense Nuclear Nonproliferation
Contract No. W-7405-ENG-36

ABSTRACT

Seismic event location remains one of the most crucial elements in monitoring for nuclear explosions. Recent development of a two-dimensional (2-D) empirical travel-time technique allows for correcting for unmodeled velocity structure, thus improving typical seismic event location using station corrections and/or a 1-D velocity model. However, this technique requires ground truth information, which can be in the form of known explosion locations and well located teleseismic events. To develop a ground truth data set, we rely on existing catalogs and our own travel-time information.

Many global and regional seismic catalogs with earthquake information for Asia are used in location studies. Each catalog contains origin and arrival information that may or may not overlap with the other catalogs. In order to obtain the most accurate earthquake locations, all available arrival information should be combined into a single data set, including derived travel times from digital stations. We have developed a seismic location database for the China region, combining origin and arrival information from a number of global catalogs, including the prototype International Data Center (pIDC) Reviewed Event Bulletin (REB), United States Geological Survey (USGS) Earthquake Data Reports (EDR), International Seismic Centre (ISC), as well as several regional catalogs. Regional arrivals obtained from digital data in Asia are also included. We also include ground truth information from previous research efforts for nuclear test sites and regional mining information. This merged database will provide detailed arrival data from which to produce more accurate locations.

Global and regional origin and arrival catalogs are merged using ORLOADER, a software package developed at Lawrence Livermore National Laboratory for combining individual seismic event catalogs into a master database. The program keeps identification numbers unique and uses a hierarchy table to select preferred origins. The master arrival table will also be analyzed for redundant arrivals based on a pre-approved author hierarchy. Certain catalogs are known to have errors in arrival times from truncation and machine versus manual picking. Traits such as this form the basis for determining a suitable hierarchy of criteria to allow removal of duplicate information. The final location database will thus have the most accurate arrival information available and be used to select appropriate information for various seismic location studies and/or ground truth catalogs.

We will determine how this new database improves location in the China region by relocating the events and observing how many arrivals remained defined in the solution versus the number from the original catalogs. Preliminary analysis indicates that locations will be improved for those events with few original defining phases and/or a large azimuthal gap.

OBJECTIVE

With the multitude of earthquake catalogs available to researchers, a determination of which catalog to use for locations, depths, arrivals, etc. is necessary. Errors are observed in many global and regional catalogs that can propagate into earthquake relocations and cause numerous problems with related research. Separate catalogs also contain varying degrees of accuracy on such data as arrival picks and station coordinates.

Of crucial importance to monitoring for nuclear explosions all over the earth is the process of event location/relocation. The use of empirical travel-time correction surfaces has greatly improved the accuracy of regional seismic locations. However, adequate ground truth information is required to create these surfaces. Global earthquake catalogs may rely on many common stations for their data, but many do not include similar stations of interest. By combining arrival information from many catalogs and using only the "best" information, ground truth information should be improved, resulting in more accurate seismic locations.

We have developed a seismic location database for the China region, combining origin and arrival information from many common global catalogs [e.g., International Data Center (IDC) Review Event Bulletin (REB), International Seismic Centre (ISC), United States Geological Survey (USGS) Earthquake Data Reports (EDR)] as well as regional and local catalogs from various institutions and researchers. Also included is ground truth information from research efforts around nuclear test sites and mines in the region of interest.

RESEARCH ACCOMPLISHED

Data Acquisition and Merging

As a first step in the merging of global catalogs and the compilation of arrival time information, new seismic information is automatically downloaded in the form of daily and weekly seismic bulletins (ASCII text files) via FTP transfers from open sources, such as the USGS EDR and IDC REB. These text files are parsed through a number of programs to convert the seismic data from their original catalog formats to CSS3.0 format flat data files. For example, we use modified versions of programs EDR2DB and REB2DB (distributed by BRTT as the Antelope software) to convert the EDR and REB seismic bulletins to CSS3.0 style flat files. After the data are converted and loaded into the database, several SQL scripts are run to quality control (QC) the data, identifying and correcting any problems with the data. Such QC checks include verifying that all data were loaded, fixing any duplicate entries based on pre-determined database table constraints, and enabling database table constraints (primary and unique keys) to ensure data integrity.

A method is needed to merge the origin information so each event has only one preferred location. We use the database utility ORLOADER (developed at Lawrence Livermore National Laboratory) to merge all of the bulletin data into a global table. This utility analyzes origin information and combines different catalog origins into an event and preferred origin based on location and origin time. All of the database identification numbers are renumbered and kept consistent with the arrival information also included in the seismic bulletins.

The merged event and origin information is now used to tie all of the in-house digital waveform files (formatted as Seismic Analysis Code, or SAC, files) to the events in the global merged database. All of the waveform holdings are QC'd and duplicate and incomplete/missing waveforms and SAC header information are dealt with. The SAC headers contain information on the arrival, station, and event location associated with the waveform and are updated using Perl scripts to correspond with the global tables.

Once the waveforms are tied to the database, in-house Perl scripts are run to create WFDISC, WFTAG, ASSOC, and ARRIVAL database tables that contain data about our waveform holdings and Los Alamos National Laboratory (LANL)-generated phase picks. ORLOADER is then run to merge LANL phase arrivals and waveform information with the global tables. A schematic of the data acquisition and merging process is shown in Figure 1.

Developing the Location Database

The majority of earthquake location programs that utilize some type of CSS3.0 schema tables (database or flat file) require there to be one origin entry per event in the ORIGIN table. In addition, all of the arrivals should point to one origin via the ASSOC table. The process of merging catalogs results in EVENT and ORIGIN tables, where there are several origins for any given event. Many ARRIVAL tables, which have duplicate phase picks for the same event but different origins, are now merged. In order to correctly relocate any of these events, specific rules for arrivals must be adhered to, such one *P* phase used per station, per event. With the large number of duplicate arrivals, a method needs to be developed to select appropriate phases from robust catalogs.

Using merged global tables, we developed a method to create ASSOC and ARRIVAL database tables that have the proper phase names for use with location programs such as EvLoc (Bratt and Bache, 1988; Nagy, 1996) and MatSeis (Harris and Young, 1997). The ASSOC table contains only the preferred origin location for a given event (one event can have one or more origin locations; each location corresponds to a different author, such as USGS EDR, IDC REB; etc.), based on a pre-determined LANL-generated ranking table, which ranks preferred authors to origin locations based on that author's location and time estimate uncertainties. The ASSOC table also has the phase arrivals from all sources (global bulletins, regional catalogs, LANL picks) associated with the preferred origin of an event.

Seismic phases in the ASSOC table are renamed so that all phases associated with a given event have unique descriptive names [this is a requirement of the EvLoc (libloc) program used in the location effort]. The renaming of the seismic phases follows a pre-determined ranking scheme, in which LANL arrival picks are ranked highest, and takes place following the ranking based on phase pick author and phase names.

A common problem is the phase-naming convention for *P* and *S* arrivals. Many catalogs name the *P* phases just *P*, not necessarily a *Pn* if needed (same for the *S* arrivals). Originally, we assumed we could group all of the *P* phases, all of the *Pn*, etc. and remove duplicates. However, many times one catalog would name the same *P* phase a *P* and another would name it a *Pn*, even if the arrival times were the same or very similar for that station. Therefore, it is necessary to analyze the *P*, *Pn*, *S*, and *Sn* phases and choose the correct arrival to rename to *P* or *S*.

To account for these phase discrepancies, all of the *P*, *Pn*, and *Pg* phases for a given station/event are grouped by author rank and time. If, by chance, there were any combination of the three phases for the same station/event, the phase with the minimum time for that author (if it was the highest ranking) would be selected as the "*P*", including any azimuth and/or slowness measurements. We assume that the first P-type arrival was made from the first break in the waveform and, therefore, has the best chance of being an accurate pick. By renaming the phase to *P*, we allow the velocity model in the location program to determine if the time corresponds to a *P*, *Pn*, or *Pg* phase.

We did not want to actually remove the other P-type phases from the table, so they were renamed to append the rank number at the end of the phase, thereby removing the phase from the location procedure, but leaving it in the database for possible later use or comparison. For more complex phases such as pP, PmP, etc., this process of renaming the duplicate phase to add the rank number was all that was modified. The user could later choose whether or not to include more complex phases in the solution. An example of the phase renaming method is shown in Table 1. The renaming of phases is necessary in order to provide the best distinct phase arrival times to the programs used in the location effort. By doing this, we are compiling a database with the "best" phase arrivals, so that for a given event at a given station, there is only one *P*, *Pn*, and *Pg* phase.

After phases have been renamed and distinct names given, we create synthetic arrival times based on the preferred origin. These times are then used to modify the time residual field in the ASSOC table so it is accurate for the given origin. The field for number of defining phases is also updated to be consistent with the actual number of phase chosen for location. The azimuth and slowness measurements are also updated. These updates permit the researcher to choose events for relocation that have a minimum number of defining phases, time residual, and/or azimuthal gap.

Relocation Results

We will utilize the location database to test effectiveness in relocating large sections of the LANL merged catalog. A first test will relocate approximately 156 events for a region around the Mw=7.5 Tibet event of 08NOV1997, with

manually-picked LANL *P* and *S* arrivals as well as global catalog arrivals having a station-event distance ranging from 5.5 to over 30 degrees. The Tibet event provides a unique ground truth test due to the presence of a related surface rupture identified by Inferometric Synthetic Aperture Radar (InSAR) (Peltzer *et al*., 1999) and the determination of the Tibet event as associated with a vertical strike/slip fault (Velasco *et al*., 2000). We will test whether the location database produces relocations that better align with this surface rupture.

Figures 2 and 3 show preliminary relocations using *P* and *S* travel-time correction surfaces for USGS EDR origins/arrivals only and LANL location database origins/arrivals, respectively. The main shock is located at the center area of the surface rupture. Using the EDR arrivals only, the main shock does not transfer to the surface rupture. However, in other studies, the main shock does transfer to the rupture, using and correcting only the *P* phases (Steck *et al*., 2001).

For the location database, the number of events has increased as well as the number of stations and phases. Typically, improvement is readily observed for those events that, in standard catalogs, had few defining phases and/or large azimuthal gap. Relocating using the correction surfaces appears to produce events that align more on the rupture, and moves the main shock closer to the rupture. Again, the shear phases have inconsistencies through most catalogs and do tend to introduce more error in the locations. There is still considerable scatter in the relocations, but this probably is due in large part to the sparse nature of the data.

Other location methods have been tested with the location database, including application of the double-difference location algorithm HYPODD (Waldhauser and Ellsworth, 2000), using the location produced with the *P* and *S* corrections as the starting point (see *Steck et al*, this Proceedings).

CONCLUSIONS AND RECOMMENDATIONS

With the multitude of global, regional, and local catalogs, it is necessary to develop methods to incorporate all available arrival time data into one main catalog in order to create the most accurate set of travel times for use in seismic location. Merging datasets permits all available arrivals to be accessible to the researcher, where specific choices can be made about which authors and arrivals to use for the location process. Duplicate and/or redundant arrival information must be removed from the database so location algorithms have distinct phases for events and stations. The location database typically results in improved origin accuracy as well as an increased number of arrivals for an event. This method can improve locations considerably for events with few arrivals and/or large azimuthal gap.

REFERENCES

Bratt, S. R. and T. C. Bache (1988). Locating events with a sparse network of regional arrays, *Bull. Seism. Soc. Am.*, **78**, 780-798.

Harris, M. and C. Young (1997). MatSeis: a seismic GUI and toolbox for MATLAB, *Seis. Res. Lett.*, **68**, 267-269.

Nagy, W. (1996). New region-dependent travel-time handling facilities at the IDC: Functionality, testing, and implementation details, *SAIC Tech Rep. 96/1179*, 57 pp.

Peltzer, G., F. Crampé, and G. King (1999). Evidence of nonlinear elasticity of the crust from the Mw7.6 Manyi (Tibet) earthquake, *Science*, **286**, 272-276.

Steck, L. K., A. A. Velasco, A. H. Cogbill, and H. J. Patton (2001). Improving regional seismic event location in China, *Pageoph*, **158**, 211-240.

Velasco, A. A., C. J. Ammon, and S. L. Beck (2000). Broadband source modeling of the November 8, 1997 Tibet (Mw = 7.5) earthquake and its tectonic implications, *J. Geophys. Res.*, **105**, 28,065-28,080.

Waldhauser, F., and W. L. Ellsworth (2000). A double-difference earthquake location algorithm: Method and application to the Northern Hayward Fault, California, *Bull. Seism. Soc. Am.*, **90**, 1353-1368.

Table 1. Example of phase renaming for example event #100 at example station XYZ.

Phase pick author	Rank	Original phase			Renamed phase		
		time 1	time 2	time 3	time 1	time 2	time 3
LANL	1	Pn	Pg		P	Pg	
REB	2	Pg	P	Pn	Pg2	P2	Pn
EDR	3	Pn	P	Pg	Pn3	P3	Pg3

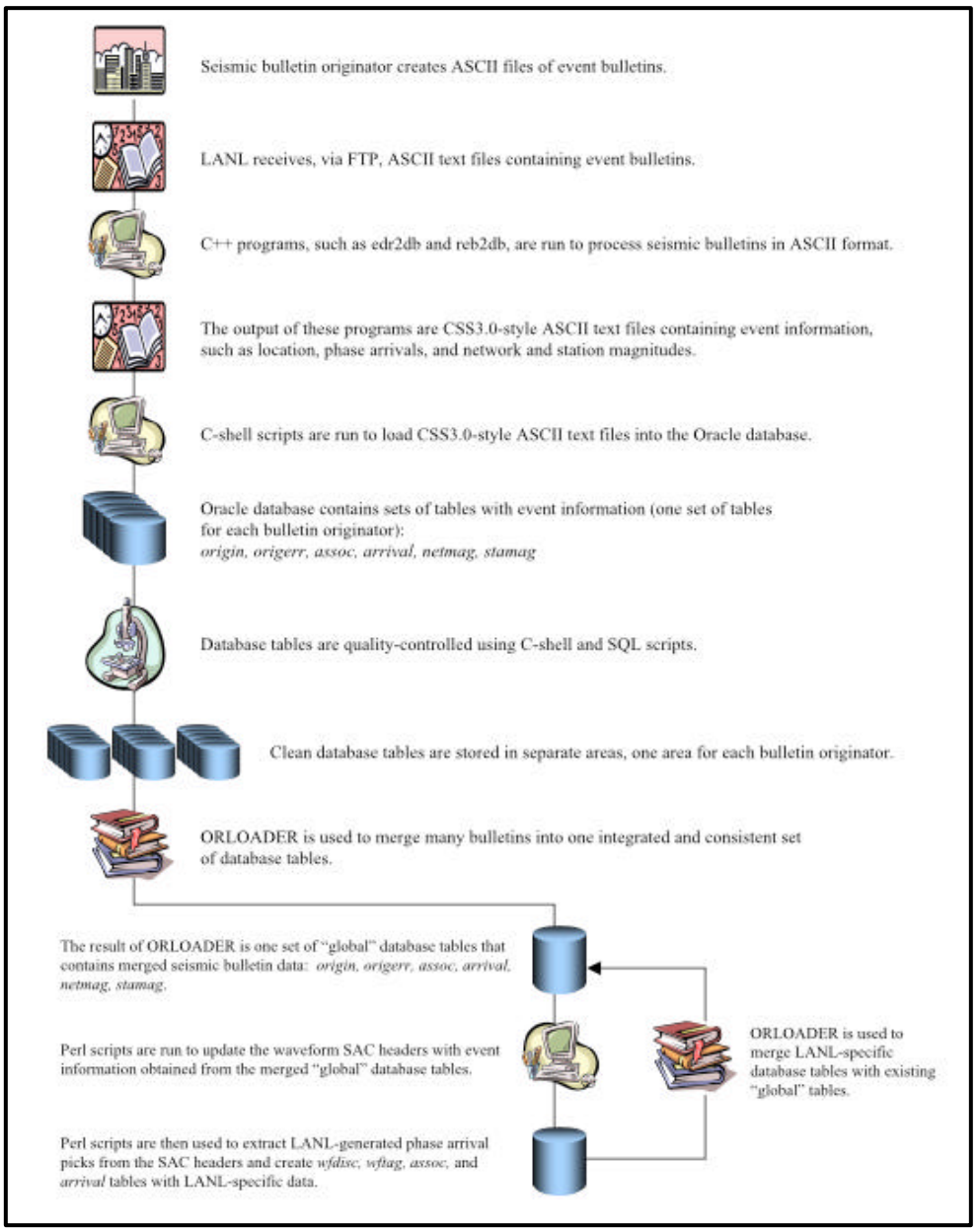

Figure 1. Flow chart for LANL seismic catalog merging process.

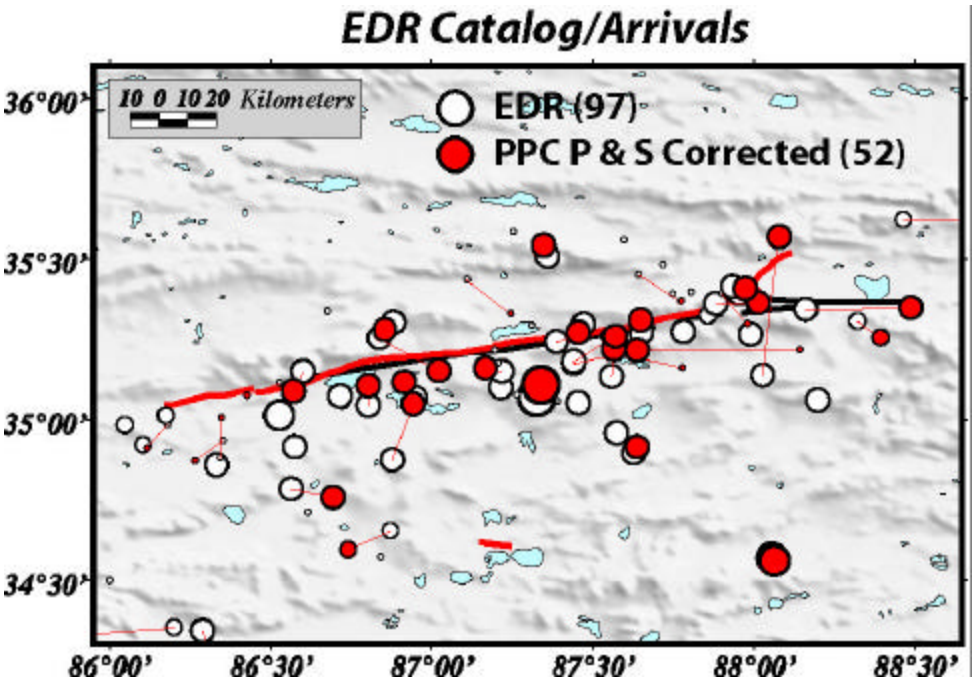

Figure 2. Relocations of Tibet events around a surface rupture using EDR catalog locations and arrivals only. Red line is surface rupture, black line is mapped fault. Both P and S phase travel time correction surfaces were used in the relocation. The main shock (largest event near center of rupture) does not relocate on the rupture (the event was determined to be a vertical strike/slip mechanism, see text).

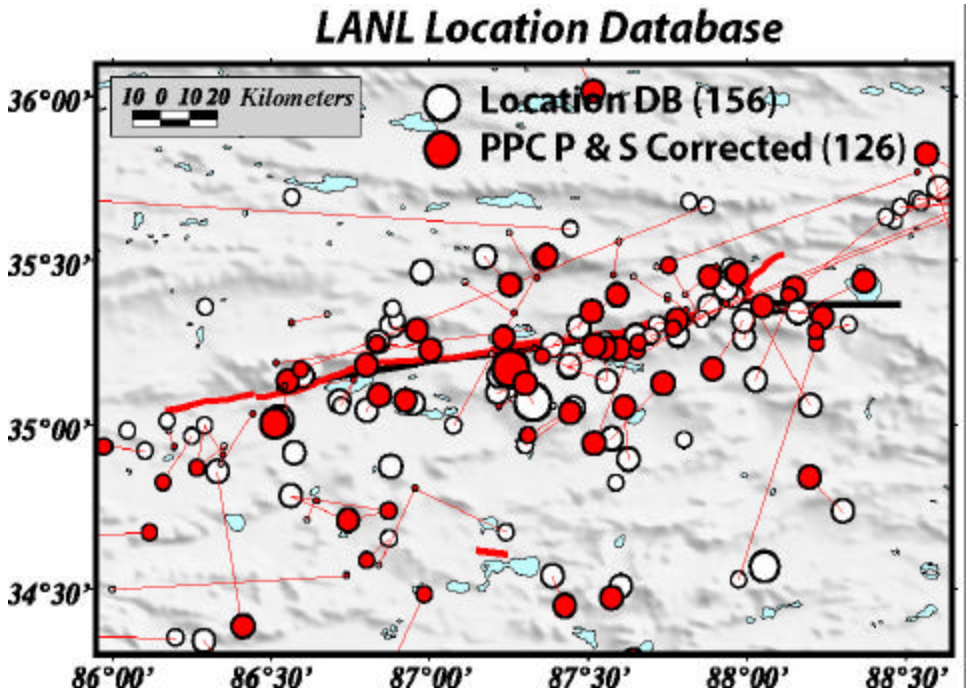

Figure 3. Relocations of Tibet events around a surface rupture using LANL location database origins and arrivals. Refer to Figure 2. The number of events in the area has increased relative to the EDR catalog. The main shock relocates much closer to the surface rupture and many other events align more along the rupture and produce more event clusters.

DEVELOPMENT OF AUTOMATED MOMENT TENSOR SOFTWARE AT THE PROTOTYPE INTERNATIONAL DATA CENTRE

Margaret Hellweg,[1] Douglas Dreger,[1] Barbara Romanowicz,[1] Jeffry Stevens[2]

University of California, Berkeley, Seismological Laboratory;[1] Science Applications International Corporation[2]

Sponsored by Defense Threat Reduction Agency

Contract No. DTRA01-00-C-0038

ABSTRACT

We are implementing the seismic moment tensor software used at the Berkeley Seismological Laboratory (BSL) for routinely monitoring earthquake strain release (Romanowicz *et al*., 1993; Pasyanos *et al*., 1996) on the test bed at the Center for Monitoring Research (CMR, formerly the Prototype International Data Centre (PIDC). The discrimination of nuclear explosions from naturally occurring earthquakes is difficult, particularly for moderate magnitude events. By providing a general representation of the seismic source, the moment tensor allows us to characterize its radiation in terms of isotropic and compensated linear vector dipole (CLVD) patterns in addition to the double couple radiation expected from typical tectonic earthquakes. The software package from BSL determines moment tensors for an event using two separate procedures: a complete waveform (CW) time-domain method as well as a spectral method applied to the surface wave (SW) recordings. During the past year, we have completed the implementation of the code package at CMR. This has involved major reworking of the waveform extraction package *mtisshell* to provide data pre-processing so that other programs such as the Seismic Analysis Code (SAC) or sapling ([a BSL processing module], Pasyanos, 1996) are no longer necessary. In addition, we have improved the estimation of signal-to-noise ratio for data used in the surface wave inversion to exclude noisy data that skews the inversion results. To illustrate the application, we present the inversion results from both methods for events with mb 5.4 in a test interval occurring between 19 July 1999 and 16 October 1999. The waveform data for input are taken from the very sparse network of the primary stations of the International Monitoring System (IMS), while the Greens functions (CW) are calculated using the IASPEI-91 velocity model and mode information for the SW code is derived from model 1066. We compare the results of both inversion methods with information given in the Harvard Centroid Moment Tensor (CMT) catalog and that in the moment tensor catalog of the US Geological Survey (USGS).

To improve its integration into the routine system, we are continuing to test and tune the procedure. Although the results for events in the test interval in some regions of the Earth are good, there are several regions where they could be improved. We show the effects of performing the inversions using theoretical information calculated on the basis of other Earth models. In addition, for selected events, we show how the addition of data from auxiliary stations improves the station coverage and thus the inversion results. On the basis of velocity structure and waveform data collected as part of the Advanced Concept Demonstration (ACD) centered on Lop Nor, we intend to investigate and demonstrate the advantages of Greens functions and mode calculations based on a regional velocity model and investigate the resolution of the two methods for moderate events, recorded well in the ACD region.

OBJECTIVE

Through moment tensor inversion, we can use broadband waveforms from modern broadband digital seismic stations to derive a robust estimate of source magnitude (M_w) for an event as well as information about its mechanism and its depth. In addition, the moment tensor results that are obtained using either primary stations of the International Monitoring System (IMS) or both primary and auxiliary stations will provide an important database of details about the seismic sources. This information will benefit other programmatic objectives such as the calibration of velocity and attenuation structure at both global and regional scales. Thus seismic moment tensors are a potentially powerful method for screening observed seismicity to identify anomalous events, those which are shallower than is typical and which have unusual, non-double couple radiation patterns (e.g. Patton 1988; Dreger and Woods, 2002). Such events may be flagged to be analyzed in greater detail. While previous work has demonstrated that moment tensors of nuclear explosions are different than those of tectonic earthquakes (Patton, 1988; Stump and Johnson, 1984; Vasco and Johnson, 1989), it was often difficult to resolve a purely isotropic source with regionally recorded long-period data (Patton, 1988). In contrast, recent experience indicates that anomalous radiation from nuclear explosions or non-tectonic seismic events may be identified with a relatively sparse network of broadband stations (e.g. Dreger and Woods, 2002; Dreger *et al*., 2000). These studies have identified significant deviation from double-couple type seismic radiation, but come up short in actually resolving the physical processes which give rise to the non-double-couple seismic radiation.

The moment tensor formalism was first developed more than 20 years ago (e.g. Mendiguren, 1977), and has been since applied successfully in various settings for the study and/or routine cataloguing of moderate to large earthquakes on the global scale, using either waveforms in the time-domain (e.g. Dziewonski *et al*., 1981) or surface-wave spectra in the frequency domain (e.g. Romanowicz, 1982; Romanowicz and Guillemant, 1984). When the signal-to-noise ratio is good, data from a single, three-component station are sufficient to obtain a moment tensor solution for a large, purely double-couple earthquake at teleseismic distances (Ekstrom *et al*., 1986). The same is true for regional distances, where a robust estimate of the seismic moment tensor of a moderate earthquake may be determined with data from a single, three-component station (e.g. Dreger and Helmberger, 1991; Fan and Wallace, 1991; Walter, 1993). For large earthquakes recorded teleseismically, relatively low frequency data can be used. In such cases, it is not necessary to know the propagation corrections with great accuracy. The use of standard 1D reference models of the Earth and, more recently, 3D models obtained from global tomography generally give acceptable solutions. More recently, as sparse regional broadband networks become more common, moment tensor inversion procedures have been adapted for application to smaller events observed at regional distances. In such cases, waves with periods between 15 and 40 s are used in the inversions. They are more sensitive to complex crustal structure, and propagation corrections must therefore be estimated more accurately using appropriate regional models. At U.C. Berkeley, we have developed and implemented two independent approaches for estimating the moment tensor of moderate earthquakes at regional distances (Romanowicz *et al*., 1993). They have been automated within the framework of our real-time program (Gee *et al*., 1996) to routinely provide reliable estimates of earthquake size, mechanism and depth in quasi-real time (Pasyanos *et al*., 1996).

In the time-domain moment tensor inversion procedure, the CW method, the complete long-period waveform from the initial P-wave through the surface wavetrain is used (Dreger and Romanowicz, 1994; Pasyanos *et al*., 1996; Fukuyama *et al*., 1998; Fukuyama and Dreger, 2000). This method functions quite well in a region as complex as California for monitoring seismicity 30 to 700 km from stations with only a few calibrated velocity models. One of the models we use describes the relatively fast wave propagation in the thick Sierra block, the second describes propagation through the relatively slow and thin California Coast Ranges (Pasyanos *et al*., 1996). Recently, a third model has been developed to improve results for events occurring offshore of Cape Mendocino (Tajima *et al*, 2000). While a satisfactory solution may often be derived using three-component data from a single station, in practice we use data from several stations to improve the azimuthal coverage of the focal sphere (Pasyanos *et al*., 1996).

The second moment tensor method used at U.C. Berkeley, the SW method, is a frequency-domain, surface wave approach, adapted from the two-step method of Romanowicz (1982). The use of surface waves, the largest of the regional phases, allows us to extend the analysis to smaller seismic events. For this procedure, calibrated fundamental-mode surface wave phase velocities between 10-60 sec period are used to calculate propagation corrections (Pasyanos *et al*., 1996). We are able to analyze events down to magnitude 3.5 using data from stations of the Berkeley Digital Seismic Network between 100 to 500 km from the epicenter. When azimuthal coverage is acceptable this method performs quite well.

The purpose of this project is to adapt and implement the two procedures in use at U.C. Berkeley for nuclear monitoring purposes. The initial goal for this software is the automatic determination of moment tensors on a global scale for events with magnitudes greater than M = 5.5. For a specific region, we will attempt to achieve reliable results for lower magnitudes through the use in the inversions of velocity structures adapted for the region as well as data from additional regional broadband stations. Later releases of the software will incorporate calibration information for several regions of interest, which will allow moment tensors to be determined for events with magnitudes greater than M ~ 4.

RESEARCH ACCOMPLISHED

We have developed and installed an automated processing system for the moment tensor package on the testbed at the Center for Monitoring Research (CMR). The flowchart in Figure 1 gives an overview of the automatically executed processing steps. For a given Julian date, events are selected for processing on the basis of information extracted from the database tables containing the reviewed event bulletin (REB). For our tests, we have chosen the interval from 19 July (day 200) to 16 October (day 290) 1999. If an event has a body-wave magnitude greater than 5.4 and depth shallower than 200 km, it is included in the processing. Table 1 lists the events in the testbed database with these characteristics. In addition to hypocentral information, the process automatically extracts from the database tables a list of the primary stations equipped with broadband sensors, which were used in producing the REB, along with event-station azimuths and distances. Several important events with REB $m_b < 5.4$ have been added to improve coverage, and to improve the testbed dataset for calibration purposes.

For those seismic stations, waveform data are extracted separately for the two inversion routines and preprocessed using the program *mtisshell*. The data intervals are chosen on the basis of group velocity. For the CW method, data lie within an interval having group velocities between 200 km/s and 2 km/s, and only includes stations located less than 5000 km from the epicenter. Data for the SW method are in an interval defined by group velocities between 4.5 km/s and 2 km/s. During the data extraction process, basic data quality tests are performed. If one or more components from a station has gaps in the selected interval or the interval for which data is present is shorter than requested, data from that station are excluded. For data to be used in the SW inversion, a second quality check is performed after they have been extracted. The power for the surface waves in the band of interest, usually between 100 s and 20 s, is compared with the power of the noise in an interval before the arrival of the P-wave from the event (group velocities between 200 km/s and 15 km/s). If the signal-to-noise ratio in power is lower than 100 for the Z, R or T components, data from that station are excluded from the inversion. The maps in Figure 2 show the primary stations, which provided waveform data for the events in the test. As is shown in Figure 1, the preprocessing depends on the inversion algorithm. For both methods, means and trends are removed from the data and they are then resampled to 1 sps. The instrument response is deconvolved and the records are rotated to directions radial (R) and transverse (T) to the event-station direction. While the data for the CW inversion is bandpass-filtered to extract the band to be used in the inversion, the filter limits for the SW data lie well outside the band of interest in order to exclude very long period noise without affecting the data to be inverted.

In addition to the waveform data, the CW method requires Greens function files for the fundamental fault orientations and movements (Dreger and Helmberger, 1991). The Greens functions used at U.C. Berkeley are calculated from the regional velocity models using *FKPROG*, a program for frequency-wavenumber calculation regional waveforms (Saikia, 1994). *FKPROG* treats the velocity model as a planar, not spherical structure, which is an acceptable assumption for near-regional distances of up to 700 km as in California. For the application of *FKPROG* to event-station distances up to 5000 km, as in the testbed implementation, the assumption is no longer valid. Initial tests of the CW method with Greens functions calculated directly from the radially symmetric iasp91 velocity model for the Earth (Kennett and Engdahl, 1991) were unsuccessful. Typically, time differences between phases in the Greens functions were too short to achieve good fits. We applied a flattening algorithm (Müller, 1973, Müller, 1977) to the iasp91 velocity model before calculating a new set of Greens functions. The agreement between the travel times in the Greens function synthetics for a given distance and the data for events at that distance from a station improved. Our analysis of the broadband waveform fits, and comparisons of derived moment tensor solutions with those reported by either Harvard or the USGS indicate that this flattening correction produces a robust set of Greens functions.

The upper map in Figure 2 shows the moment tensors calculated using the CW method and Greens functions based on a flattened iasp91 velocity model (blue) and on a flattened PREM velocity model (green, Dziewonski and Anderson, 1981). For comparison, the moment tensors given for these events in the Harvard CMT (brown) and USGS (red) catalogs are also shown. For events in the southwest Pacific Ocean, the moment tensors derived by the CW method differ from those given by both the Harvard and USGS catalogs. However, data for each of these events were only available for one primary station less than 5000 km from the epicenter, STKA. The solutions calculated by the CW method are consistent with the waveforms from this station. Were data from one or more other stations available, the additional constraints would probably improve the agreement with the standard catalogs. Figure 3A shows the moment tensor difference function (Pasyanos *et al*, 1996) comparing the results from the CW inversions using iasp91 and PREM Greens functions with Harvard CMT catalog moment tensors and with each other, while Figure 3B plots the ratios of the calculated moments to the catalogs' moments and between the different Greens functions. While there is some variation between the ratios of the moments, they cluster around 1. This indicates that the estimate of the moment using the CW method is reliable. On the whole, the agreement between the moment tensors from the CW method and Harvard CMT are not very good when described using the moment tensor difference function (Figure 3A).

The Hector Mine event (Origin ID 20595122, October 16, 1999) is a good example on which to investigate these differences. The map in Figure 4A shows the location of the Hector Mine event (star) and the primary stations of the network of the International Monitoring System (IMS) for which broadband data was extracted from the testbed database (filled blue inverted triangles). Data from the two broadband primary stations closest to the epicenter, NV32 and PD31 (open blue inverted triangles), were excluded because the interval stored in the waveform database was too short. Figure 4B shows the waveform fits and the moment tensor resulting from the automatic inversion of data filtered in a passband between 20 s and 50 s using Greens functions derived from the iasp91 velocity model. While the waveform fits do not look very bad, the moment tensor is the opposite of those given by the Harvard CMT and USGS catalogs and the total reduction in variance is only 18 percent. We investigated the waveforms and instrument information given for the four primary stations. It appears that the instrument response functions stored in the database for the stations ULM and IL31 have reversed polarity. Figure 4C shows the results for the same four stations, when the instrument response has been corrected. In addition, we have used a filter passband between 33 s and 100 s, more appropriate for the size of the Hector Mine earthquake, and less susceptible to the influence of lateral heterogeneity.. The new moment tensor result agrees well with the catalog results and the variance reduction is better than 50 percent. For Figure 4D we have added data from three auxiliary stations of the IMS network (filled red inverted triangles) to the inversion. The data for stations ANMO and CCH was extracted from the database of the Incorporated Research Institutions in Seismology (IRIS), while data from YBH came from the archives of the Berkeley Seismological Laboratory. The stations YBH and ANMO are approximately the same distance from the epicenter as PD31. This inversion shows how the auxiliary stations can supply data from locations close to the epicenter while improving the coverage of the focal sphere.

Figure 2 also shows the moment tensors calculated using the SW method (lower map). Again, the moment tensors calculated using modes derived from two velocity models, 1066b (blue, Gilbert and Dziewonski, 1975) and the PREM velocity model (green) can be compared with the moment tensors given in the Harvard CMT (brown) and USGS (red) catalogs. Fewer of the events selected from the catalog are present on this map than the upper map for the CW method. Moment tensors were calculated only for events if high quality, three-component data were available for more than 2 stations, that is data with no gaps, of a sufficient length between group velocities of 4.5 km/s and 2.0 km/s, and with a signal-to-noise ratio in power greater than 100. Figure 3C shows the moment tensor difference function comparing the results from the SW inversions using 1066b and PREM modes with Harvard CMT catalog moment tensors and with each other, while Figure 3D compares the calculated moments. While the mechanisms for some events agree well with the catalog values, for others, they are completely different. This is also apparent in the plot of the moment tensor difference function (Figure 3C), where it is clear that the results from the 1066b inversion are basically the same as those from the PREM inversion (plusses). Clearly, the values of the moments determined for these events are low, compared with the Harvard CMT catalog (Figure 3D), on average a factor of 7 lower. This is independent of the model used, as the average for the ratios of the moments determined using the 1066b model and PREM is about 1 (plusses).

Figure 5 shows the results of the surface wave inversion of the Hector Mine event (origin ID 20595122, 16 October 1999). The phase and amplitude fits are shown for all stations and frequencies used to produce the result given on the right hand side of the figure. Just as the reversed polarity of the instrument correction for stations ULM and IL31

affected the solution for the CW method, it will have an effect on the results of the surface wave method. We must determine which other stations may have similar problems. We are also investigating the cause of the low estimate of events' moments calculated in the course of the inversion.

CONCLUSIONS AND RECOMMENDATIONS

The automatic procedure to determine moment tensors has been implemented on the testbed at the Center for Monitoring Research. The procedure selects events from the reviewed event bulletin and calculates moment tensors, the events' depths and moments using the complete waveform and surface wave methods developed at U.C. Berkeley. Results from a set of earthquakes with $m_b > 5.4$ and depth shallower than 200 km that occurred between 19 July and 16 October 1999 demonstrate both the effectiveness of the procedure, as well as the areas where improvement is necessary. We have calculated the results of each method, the CW method and the SW method, using synthetic information calculated from two global velocity models. We are investigating solution differences that are apparently due to the choice of velocity model. Initial observations suggest that for the CW method, the differences in the automatic solutions usually result from incorrect alignment with the Greens function. When solutions are reviewed, and the alignment of the waveforms and the Greens function adjusted, the results are much more consistent for the two models.

One of the most basic problems we encountered in the development process relates to the amount and quality of the data used in the inversions. For the methods to function well, the waveform data must have a high signal-to-noise ratio and no gaps or glitches. In many regions of the world, for example the southwest Pacific Ocean, there are very few primary stations. The results of the inversion could be improved by using recordings from auxiliary stations of the IMS network equipped with broadband instruments. Unfortunately, for the test interval, it is impossible to go back and retrieve such data to add in to the inversion. We have been using recent events to test feasibility of using data from auxiliary stations in the moment tensor procedure. In practice, data from auxiliary stations are used in producing the REB, however, generally only very short intervals of data are requested from the stations. These intervals are not long enough to be useful for moment tensor inversions. We recommend that intervals starting at the event origin time and ending with the end of the surface wave train be requested from auxiliary stations with broadband instruments within 50 degrees of the event and stored in the waveform database for use with the moment tensor code. If it is not possible to handle the resulting volume of data, we suggest that at least 1 sps data be stored.

Recently, the Center for Monitoring Research has been collecting waveform data from earthquakes and nuclear explosions in and around Lop Nor as part of an advanced concept demonstration (ACD). Figure 6 shows a set of 175 earthquakes recorded between 1995 and 2002 as well as 25 nuclear explosions dating from 1966 to 1996. As an example of the calibration of the automatic moment tensor procedures for a specific region, we are planning to use this data along with the 3D velocity structure given by CUB1.0 (Anatolik *et al*, 2001). We will compare the moment tensor results with those determined by Bukchin *et al* (2001).

REFERENCES

Anatolik, M., G. Ekström, A. M. Dziewonski, L. Boschi, B. Kustowski, and J Pan (2001), Multi-Resolution Global Models for Teleseismic and Regional Event Location, *23rd Seismic Research Review: Worldwide Monitoring of Seismic Explosions*, Jackson Hole, WY, October 1-5.

Kukchin, B. G., A z. Mostinsky, A. A. Egorkin, A. L. Levshin, and M. H. Ritzwoller (2001), Isotropic and Nonisotropic Components of Earthquakes and Nuclear Explosions on the Lop Nor Test Site, China, *Pure Appl. Geophys.*, **158**, 1497-1515.

Dreger, D. and D. V. Helmberger (1991), Complex Faulting Deduced from Broadband Modeling of the 28 February 1990 Upland Earthquake (M_L=5.2), *Bull. Seism. Soc. Am.*, **81**, 1129-1144.

Dreger, D. and B. Romanowicz (1994), Source Characteristics of Events in the San Francisco Bay Region, *USGS Open-file report, 94-176*, 301-309.

Dreger, D. (1997), The Large Aftershocks of the Northridge Earthquake and their Relationship to Mainshock Slip and Fault Zone Complexity, *Bull. Seism. Soc. Am.*, **87**, 1259-1266.

Dreger D. and B. Woods (2002), Regional Distance Seismic Moment Tensors of Nuclear Explosions, *Tectonophysics*, in press.

Dreger, D. S., H. Tkalcic, and M. Johnston (2000), Dilational Processes Accompanying Earthquakes in the Long Valley Caldera, *Science*, **288**, 122-125.

Dziewonski, A. M., T.-A. Chou, and J. H. Woodhouse (1981), Determination of Earthquake Source Parameters from Waveform Data for Studies of Global and Regional Seismicity, *J. Geophys. Res.*, **86**, 2825-2852.

Dziewonski, A. M. and D. L. Anderson (1981), Preliminary Reference Earth Model, *Phys. Earth Plan. Int.*, **25**, 297-356.

Ekstrom, G., A. M. Dziewonski, and J. Steim (1986), Single station CMT:Application to the Michoacan, Mexico, Earthquake of September 19, 1985, *Geophys. Res. Lett.*, **13**, 173-176.

Fan, G. and T. Wallace (1991), The Determination of Source Parameters for Small Earthquakes from a Single, very Broadband Seismic Station, *Geophys. Res. Lett.*, **18**, 1385-1388.

Fukuyama, E., M. Ishida, D. Dreger, and H. Kawai (1998), Automated Seismic Moment Tensor Determination by Using OnLine Boadband Seismic Waveforms*, Jishin*, **51**, 149-156.

Fukuyama, E. and D. Dreger (2000), Performance Test of an Automated Moment Tensor Determination System, *Earth Planets Space*, **52**, 383-392.

Gee, L., D. Dreger, D. Neuhauser, R. Uhrhammer, and B. Romanowicz (1996), The REDI program, *Bull. Seism. Soc. Am.*, **86**, 936-945.

Gilbert, F. and A. M. Dziewonski (1975), An Application of Normal Mode Theory to the Retrieval of Structural Parameters and Source Mechanisms from Seismic Spectra, *Phil. Trans. Roy. Soc. Lon.*, **278**, 187-269.

Kennett, B. L. N. and E. R. Engdahl (1991), Traveltimes for Global Earthquake Location and Phase Identification, *Geophys. J. Int.*, **105**, 429-465.

Mendiguren, J. (1977), Inversion of Surface Wave Data in Source Mechanism Studies, *J. Geophys. Res.*, **82**, 889-894.

Müller, G. (1973), Theoretical Body Wave Seismograms for Media with Spherical symmetry; Discussion and Comparison of Approximate Methods, *J. Geophysics*, **39**, 229-246.

Müller, G. (1977), Earth-Flattening Approximation for Body waves Derived from Geometric Ray Theory; Improvements, Corrections and Range of Applicability, *J. Geophysics*, **42**, 429-436.

Pasyanos, M. (1996), Regional Moment Tensors and the Structure of the Crust in Central and Northern California, *Ph.D. Thesis, University of California, Berkeley*, 261p.

Pasyanos, M., D. Dreger and B. Romanowicz (1996), Toward Real-Time Estimation of Regional Moment Tensors, *Bull. Seism. Soc. Amer.*, **86**, 1255-1269.

Patton, H. J. (1988), Source Models of the Harzer Explosion from Regional Observations of Fundamental-Mode and Higher Mode Surface Waves, *Bull. Seism. Soc. Am.,* **78**, 1133-1157.

Pechmann, J. C., W. R. Walter, S. J. Nava, and W. J. Arabasz (1995), The February 3, 1995, ML 5.1 Seismic Event in the Trona Mining District of Southwestern Wyoming, *Seis. Res. Lett.*, **66**, 25-34.

Romanowicz, B. (1982), Moment Tensor Inversion of Long Period Rayleigh Waves: A New Approach, *J. Geophys. Res.*, **87**, 5395-5407.

Romanowicz, B. and Ph. Guillemant (1984), An Experiment in the Retrieval of Depth and Source Parameters of Large Earthquakes Using Very Long Period Rayleigh Wave Data, *Bull. Seism. Soc. Am.*, **74**, 417-437.

Romanowicz, B., M. Pasyanos, D. Dreger, and R. Uhrhammer (1993), Monitoring of Strain Release in Central and Northern California Using Broadband Data, *Geophys. Res. Lett.*, **20**, 1643-1646.

Saikia, C. (1994), Modified Frequency-Wavenumber Algorithm for Regional Seismograms using Filon's Quadrature: Modeling of Lg Waves in Eastern North America, *Geophys. J. Int.*, **118**, 142-158.

Stump, B. W., and L. R. Johnson (1984), Near-Field Source Characterization of Contained Nuclear Explosions in Tuff, *Bull. Seism. Soc. Am.*, **74**, 1-26.

Tajima, F., D. S., Dreger, and B. Romanowicz (2000), Modeling of the Transitional Structure from Ocean to Continent in the Mendocino Region using Broadband Waveform data, *EOS*, **81**, no. 48 (Fall meeting supplement).

Vasco, D. and L. Johnson (1989), Inversion of Waveforms for Extreme Source Models with Application to the Isotropic Moment Tensor Component, *Geophys. Journ. Royal Astr. Soc.,* **97**, 1-18.

Walter, W. R. (1993), Source Parameters of the June 29, 1992 Little Skull Mountain Earthquake from Complete Regional Waveforms at a Single Station, *Geophys. Res. Lett*., **20**, 403-406.

Table 1. Events of test interval, July 19 – October 16, 1999

OriginID	Date	Lat	Lon	Depth	m_b %	Region
20537870	1999 7 19 2:17:09.150	-28.561	-177.424	70	5.64	Kermadec
20541908	1999 7 26 1:33:15.178	-5.210	152.076	16	5.68	New Britain
20542430	1999 7 28 0:16:59.480	-28.606	-177.322	34	5.47	Kermadec
20542756	1999 7 28 10:08:18.210	-30.239	-177.774		5.81	Kermadec
20553840	1999 8 12 5:44:56.157	-1.595	122.667		5.56	Sulawesi
20555310	1999 8 14 0:16:54.100	-5.840	104.674	102	5.87	S. Sumatra
20559538	1999 8 17 0:01:37.795	40.772	30.092		5.59	Turkey
20560647	1999 8 20 10:02:18.146	9.260	-84.165		5.46	Costa Rica
20561207	1999 8 22 12:40:42.345	-16.095	168.213		5.94	Vanuatu
20568654	1999 9 7 11:56:49.481	38.161	23.544		5.50	Greece
20576492	1999 9 18 21:28:34.048	51.264	157.499	50	5.61	Kamchatka
20576889	1999 9 17 14:54:46.930	-13.815	167.446	169	5.72	Vanuatu
20577664	1999 9 20 17:47:29.732	23.548	121.012		5.94	Taiwan MS*
20577672	1999 9 20 17:57:19.559	23.852	121.217	43	5.42	Taiwan AS*
20578273	1999 9 20 18:11:50.377	23.811	121.136		5.83	Taiwan AS*
20578492	1999 9 22 0:14:42.005	23.747	121.091	33	5.45	Taiwan AS
20581262	1999 9 25 23:52:53.459	23.774	121.158	37	5.46	Taiwan AS
20582713	1999 9 29 4:42:55.319	1.907	125.195	158	5.37	Molucca Passage
20582842	1999 9 29 18:01:28.201	-30.763	-71.902		5.43	Central Chile
20583432	1999 9 30 16:31:09.188	16.083	-96.800		5.95	Oaxaca
20590301	1999 10 10 7:03:01.547	-1.960	134.100		5.48	W. Irian
20591829	1999 10 13 1:33:38.755	54.691	-161.136	13	5.54	Alaska Pen
20595122	1999 10 16 9:46:45.597	34.541	-116.361		5.35	Hector Mine

% Given in the testbed database

* No MT solutions determined due to data overlap

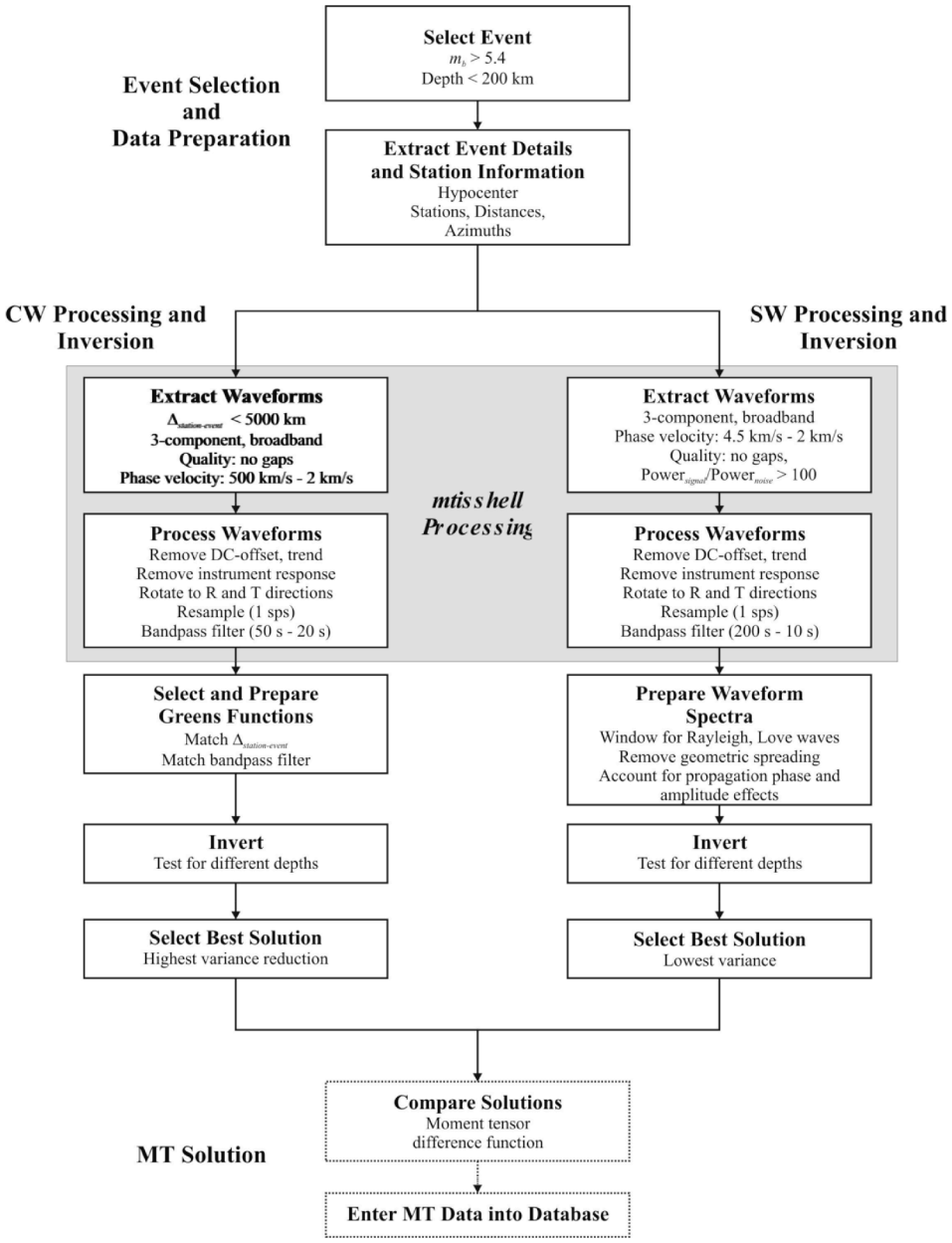

Figure 1. Flowchart describing the automated moment tensor data selection and processing procedure. Event selection parameters are given which characterize the events described in the following text.

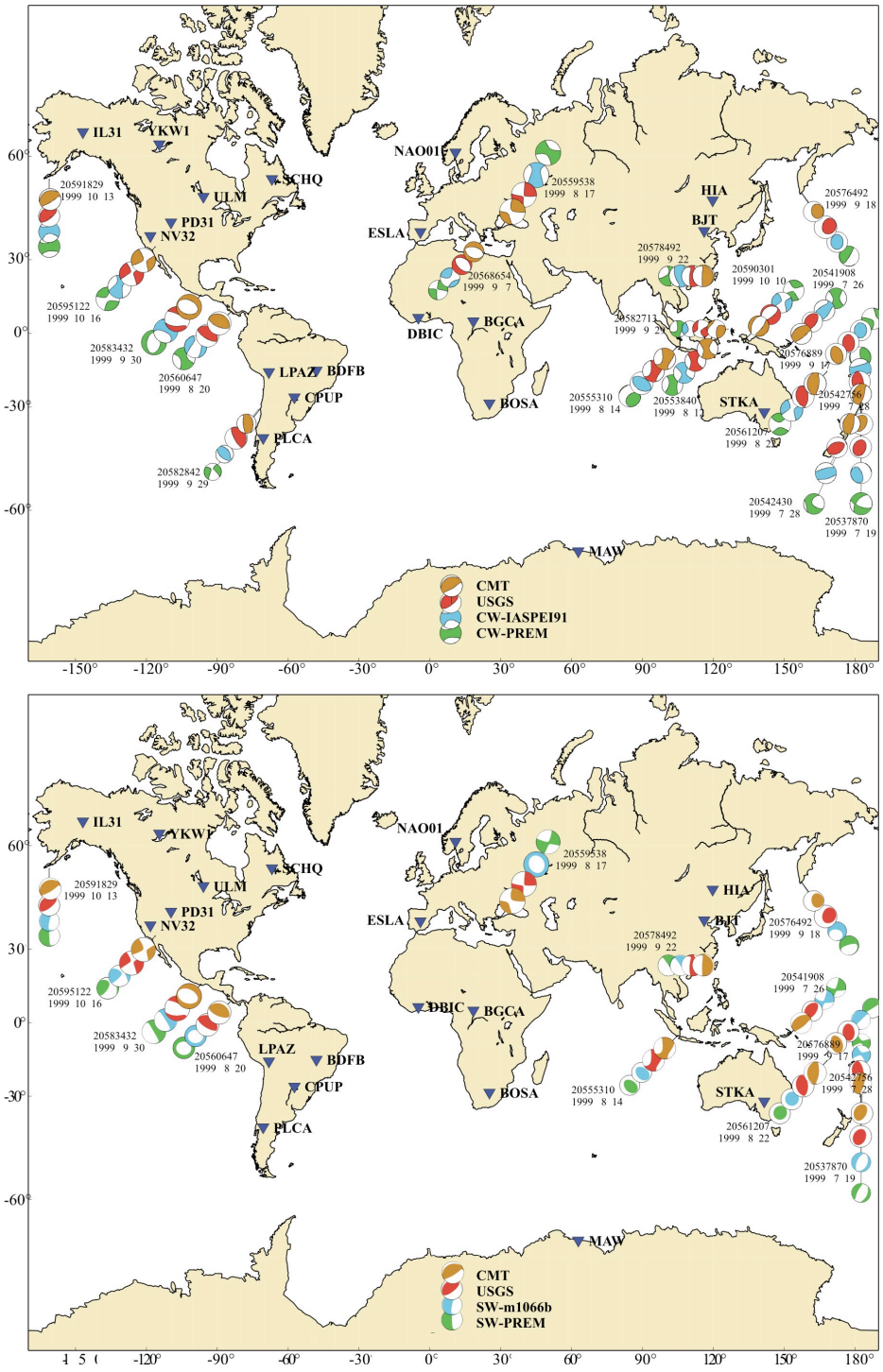

Figure 2. Maps showing the inversion results for the events of the test interval. Inverted triangles mark the locations of stations used in the inversions. The upper map compares results from the CW method using Greens functions based on the iasp91 **(blue) and the PREM (green) velocity models with moment tensors from the Harvard CMT (brown) and USGS (red) catalogs. The lower map compares moment tensors generated by the SW method using modes calculated from the velocity models 1066b (blue) and PREM (green) with those from the Harvard CMT (brown) and USGS (red) catalogs.**

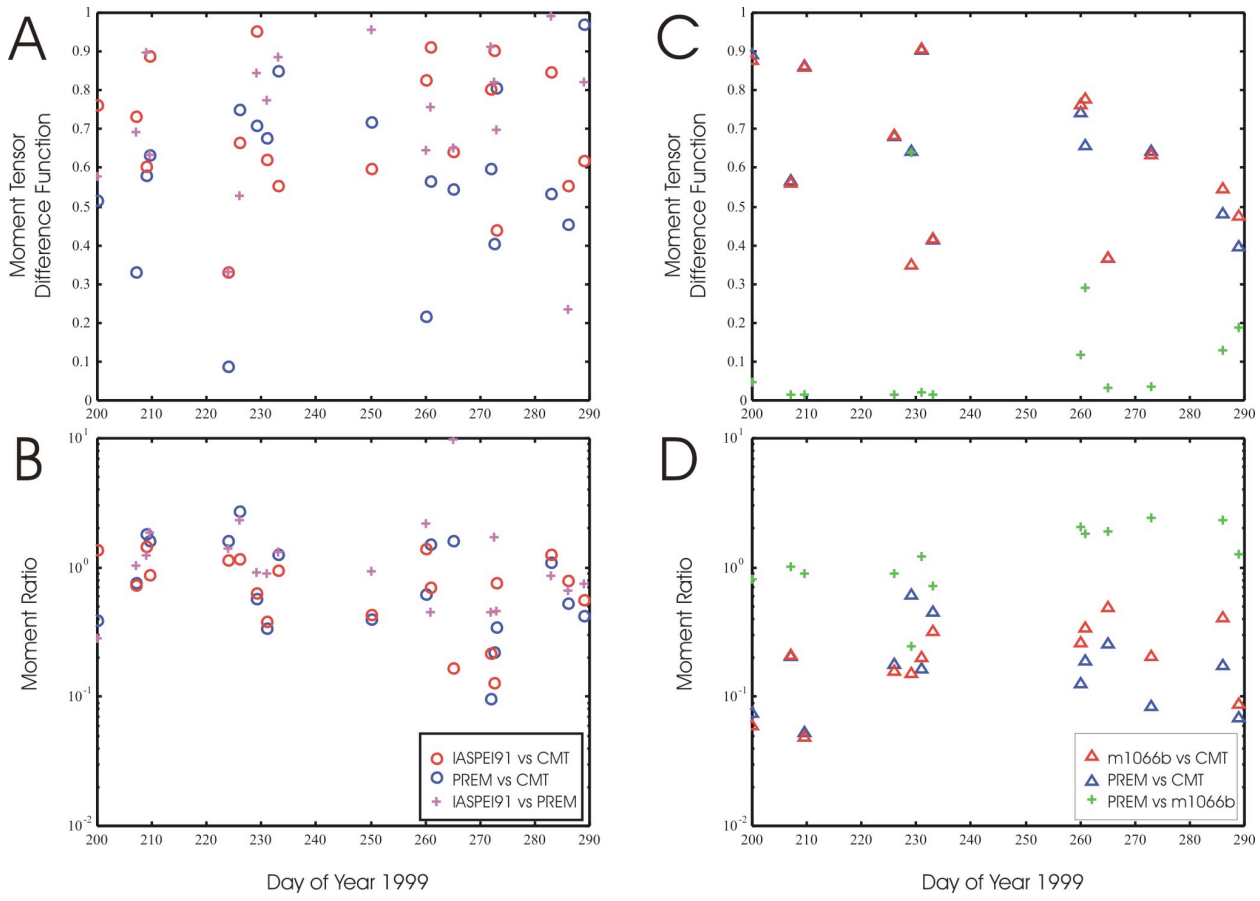

Figure 3. Quantitative comparison of moment tensor solutions from CW (A, B) and SW (C, D) with Harvard CMT results. A and C show the moment tensor difference function (Pasyanos *et al*, 1996). If the difference function is less than 0.5, the moment tensors are similar. B and D show the ratio between the moment of the event calculated using the various methods.

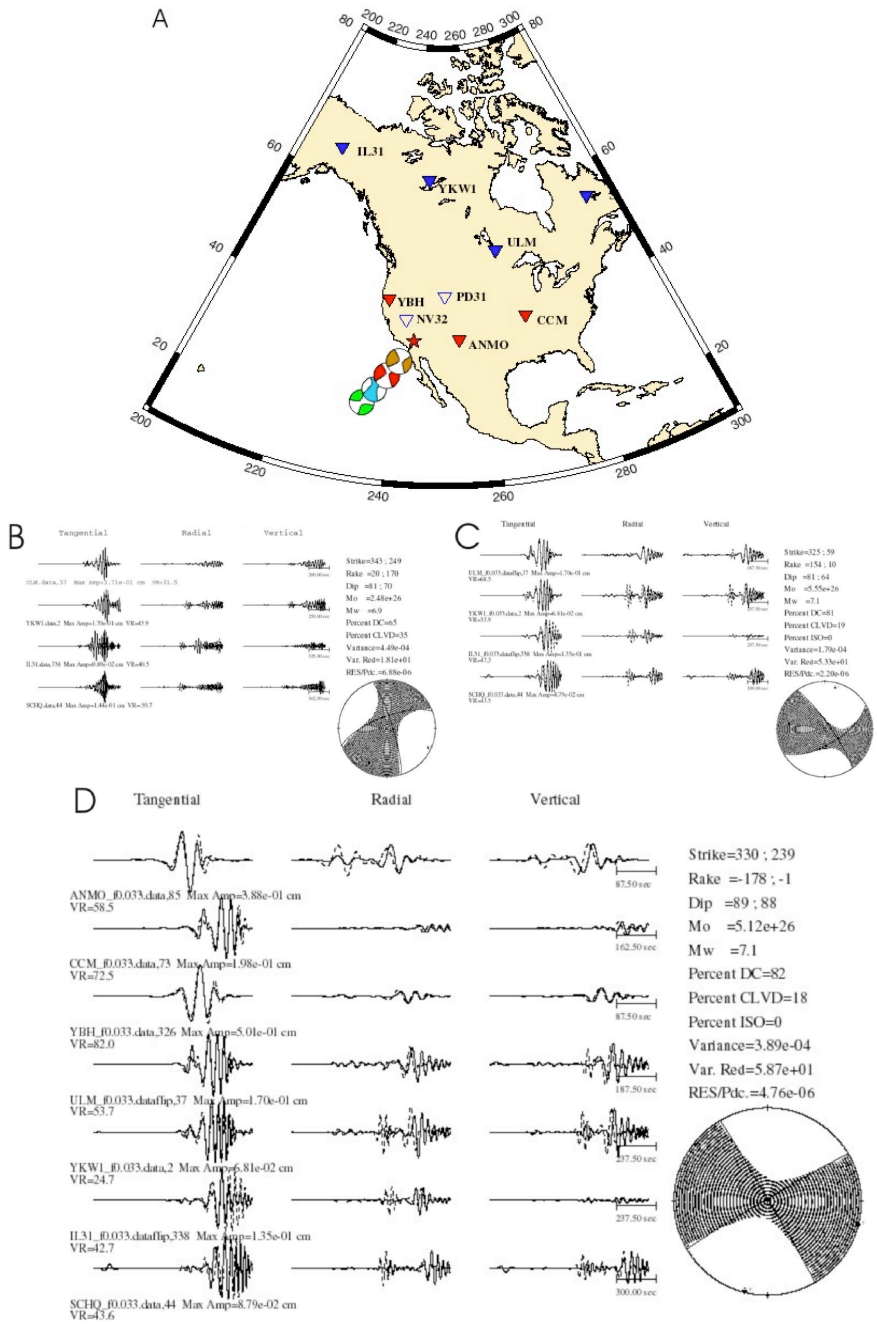

Figure 4. Complete waveform inversion of the Hector Mine event (origin ID 20595122, October 16, 1999). (A) The star shows the epicentral location. Data for the primary stations (filled blue inverted triangles) IL31, YKW1, ULM and SCHQ were extracted from the database. Data from primary stations (open blue inverted triangles) NV32 and PD31 were rejected as being too short. To improve and check the CW inversion, we requested data from the auxiliary stations (filled red inverted triangles) YBH, ANMO and CCM. This data was not available in the testbed database. The moment tensors are as given in Figure 2. (B) Automatic moment tensor solution. (C) Revised moment tensor solution. (D) Moment tensor solution including data from auxiliary stations. See text for discussion.

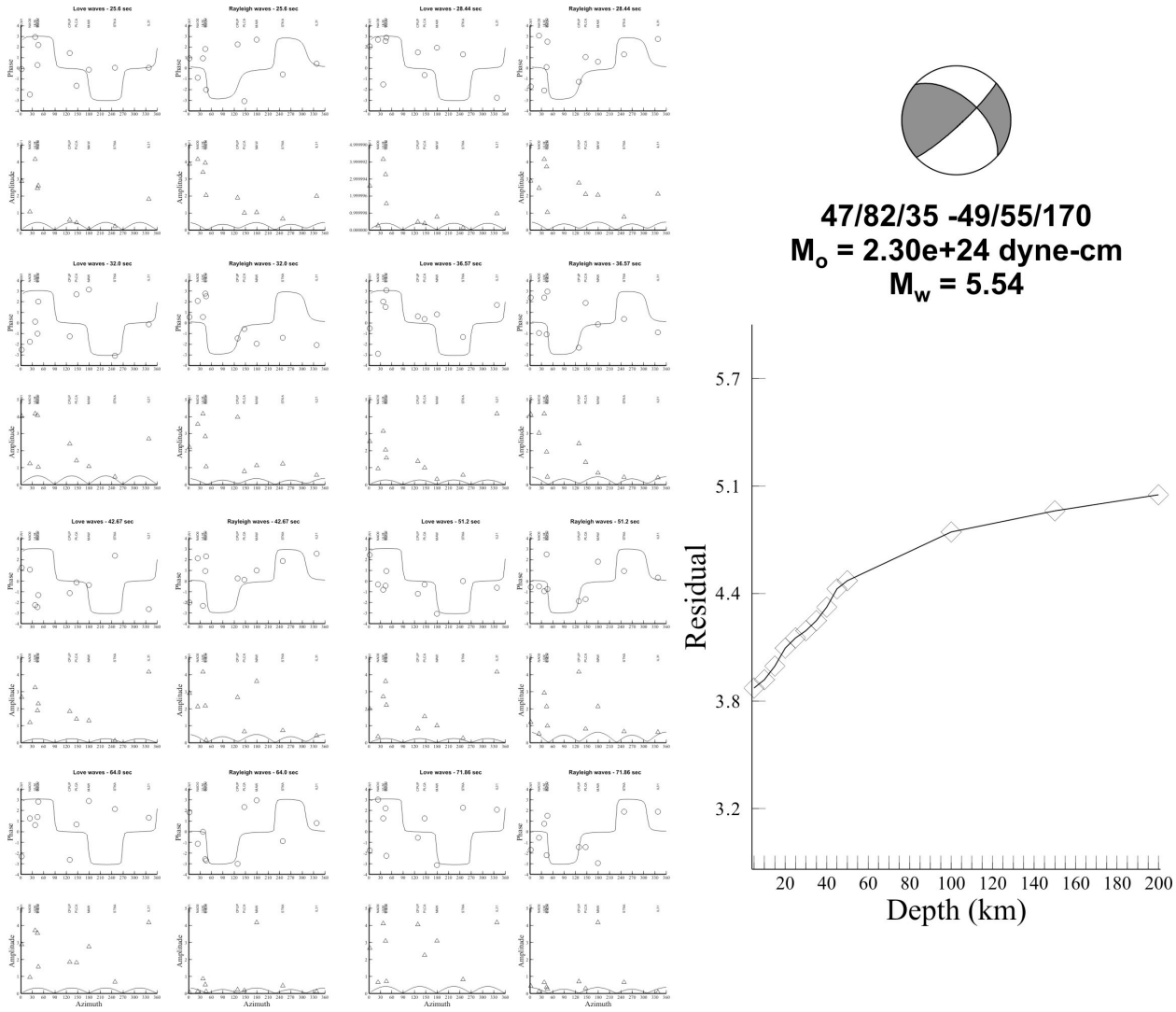

Figure 5. Surface wave inversion of the Hector Mine event (origin ID 20595122, October 16, 1999). The plots on the left show the phase and amplitude fits for the stations and frequencies used to generate the automatic solution. The plot on the right shows the source mechanism and the residuals. For this event, the best solution is found for a depth of 5 km, the shallowest depth used.

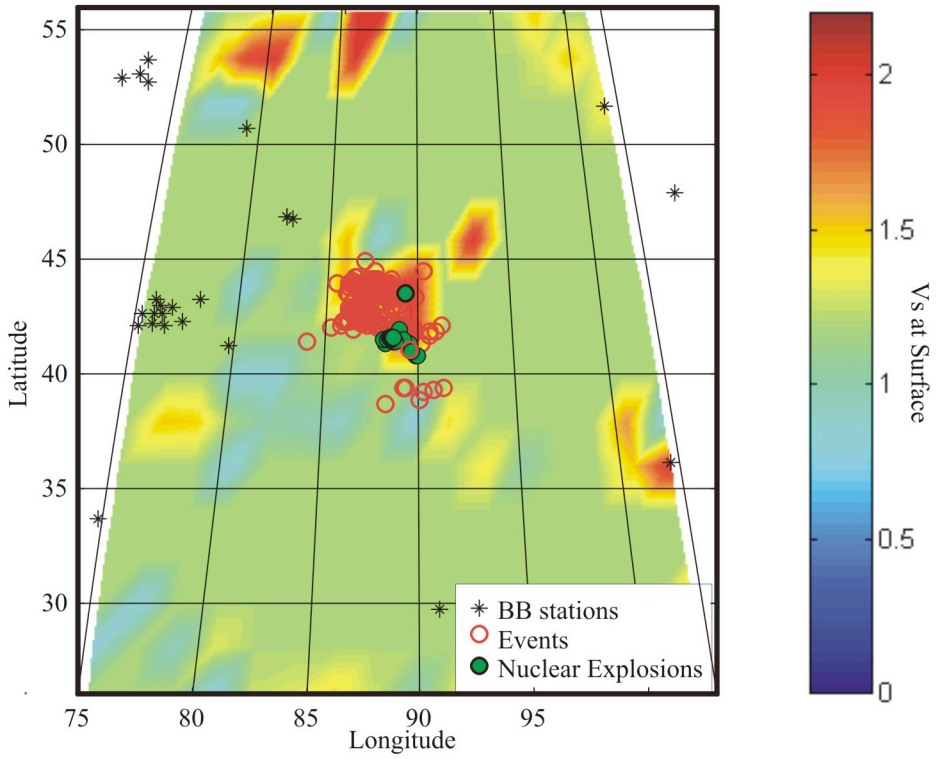

Figure 6. Lop Nor, the advanced concept demonstration region. Waveforms for 200 events, among them 25 nuclear explosions, have been collected for this region. The recordings come from 54 stations equipped with broadband instruments. The color map shows the S-wave velocity at the surface given by the model CUB1.0.

REGIONAL SEISMIC THRESHOLD MONIORING

T. Kværna, E. Hicks, J. Schweitzer, and F. Ringdal

NORSAR

Sponsored by Defense Threat Reduction Agency

Contract No. DTRA01-00-C-0107

ABSTRACT

A database comprising a total of 45 events, selected to provide the best possible ray path coverage of the Barents Sea and adjacent areas, was compiled and reanalyzed in a consistent manner. This resulted in new regional attenuation relations for Pn and Sn, together with a preferred average velocity model to be used for predicting the travel times of regional phases. We have now applied these attenuation relations to investigate a regional threshold monitoring scheme for the Barents Sea area.

A grid system with an approximately 100-km grid spacing was deployed for the Barents Sea region, and the observations at the arrays, ARCES, SPITS, FINES and NORES, were then used for calculating threshold magnitudes for each of the grid points. During an interval without seismic signals, the threshold magnitudes showed large variations over the region, and, in particular, in the vicinity of each array. However, for the region around the island of Novaya Zemlya, the variations are modest, varying around a mean of magnitude 2.1-2.2.

In order to investigate in more detail the variations in threshold magnitudes for the Novaya Zemlya region, we deployed a dense grid with an areal extent of about 500 x 500 km around the former Novaya Zemlya nuclear test site. For each of the grid nodes, we calculated magnitude thresholds for the two-hour time interval 00:00 - 02:00 on 23 February 2002. At 01:21:12.1 there was an event with a magnitude of about 3, located about 100 km northeast of the former nuclear test site.

Regions of different sizes were constructed by selecting grid points within different radii from the former nuclear test site. Average, minimum and maximum threshold magnitudes were calculated for circular regions with radii of 20, 50, 100 and 200 km, respectively.

The most important result is that even for a target region with radius as large as 100 km, the variations in threshold magnitudes are all within 0.2 magnitude units. This applies both for the time interval with the event and for background noise conditions. For the investigated station geometry, it will therefore be meaningful to represent the monitoring threshold of the entire Novaya Zemlya region with the values of a single target point, together with the *á priori* determined uncertainty bounds.

We can therefore conclude that the experimental site-specific threshold monitoring which has been run daily by NORSAR for the past 5 years, aiming at the Novaya Zemlya test site, can be used with only minor adjustments to assess the threshold within 100 km of the site. This monitoring has shown that between 16 August 1997 and 23 February 2002, the threshold level has been consistently below 2.5, except during “interfering” large regional or teleseismic events located well outside the target region.

For areas with larger variations in threshold magnitudes, like in the vicinity of the arrays, a 100-km radius target region will obviously show larger differences between the maximum and minimum values. Examples illustrating this point will be shown.

OBJECTIVE

The main objective of this research is to develop and test a new, advanced method for applying regional seismic array technology to the field of nuclear-test-ban monitoring. To that end, we address the development and testing of a method for optimized seismic monitoring of an extended geographical region, using a sparse network of regional arrays and three-component stations. Our earlier work on optimized site-specific threshold monitoring serves as a basis for the development of this new method. Emphasis of the research is on algorithms that can be efficiently applied in a real-time monitoring environment, that are using primarily automated processing, and that can be readily implemented in an operational Comprehensive Nuclear-Test-Ban Treaty (CTBT) monitoring system.

RESEARCH ACCOMPLISHED

Travel times and attenuation relations for regional phases in the Barents Sea region

A database containing 45 events in the Barents Sea region (Figure 1) has been compiled and analyzed with the aim of evaluating crustal models, travel times, and attenuation relations in the context of performing regional detection threshold monitoring of this region. The 45 events are mostly located around the circumference of the study area due to the virtually aseismic nature of the Barents Sea itself. Regional Pn and Sn phases were observable for most events in the database, while Pg and Lg phases were only observable for events with ray paths that do not cross the tectonic structures in the Barents Sea. This corroborates a number of previous observations of Lg-wave blockage within the Barents Sea.

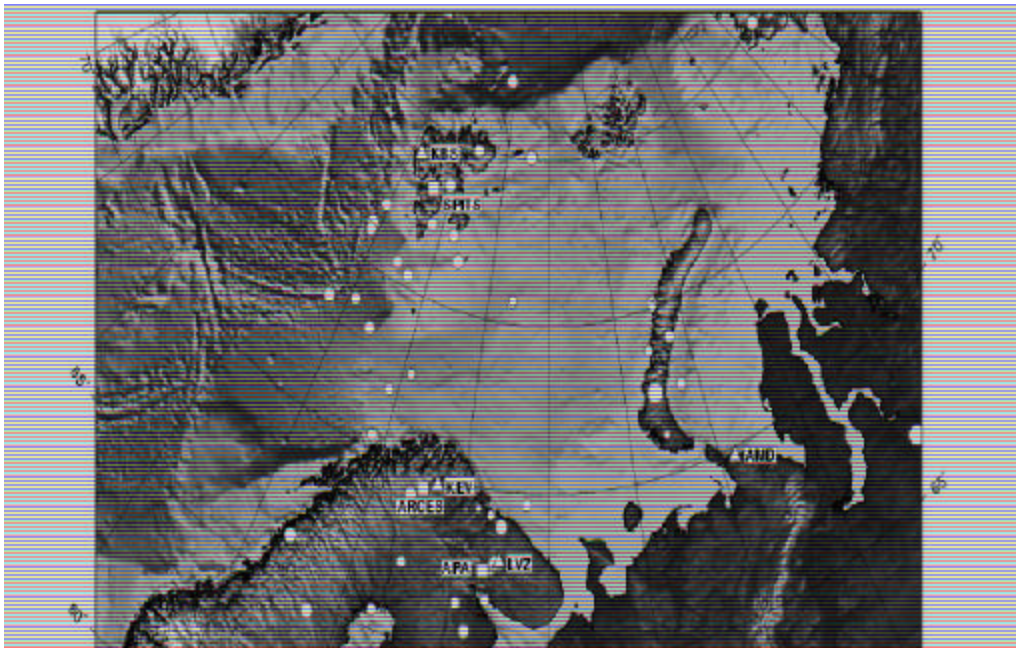

Figure 1. EVENTS (circles) and seismic stations used for deriving wave propagations characteristics of the Barents Sea and surrounding areas. Array stations are shown as squares, while three-component stations are shown as triangles. The symbol sizes for the events are proportional to the network magnitudes.

In order to estimate magnitudes, short-term average (STA) and spectral amplitude values were calculated in several frequency bands for all phase arrivals in the data base. There were no significant differences between spectral and STA amplitudes, so the latter were used since this parameter is more efficient to calculate in real-time processing. A joint inversion of the regional phases Pn, Pg, Sn and Lg was performed in order to determine attenuation relations specific for this region according to the relation given in Equation 1.

$$\mathbf{M_L} = \log \mathbf{A} - \log \mathbf{e} \cdot \alpha_{\mathbf{i}}^{0} \cdot \mathbf{f} + (\mathbf{a_i f} + \mathbf{b_i}) \log\left(\frac{200}{\Delta}\right) + \delta_{\mathbf{ik}} + 1.66 \qquad (1)$$

where A is observed STA amplitude within a frequency band with logarithmic center frequency f, Δ is epicentral distance, the α^0_i term represents the total attenuation for phase i out to the reference distance of 200 km, and a_i and b_i are phase-dependent attenuation constants. The inversion results for the parameters α^0, a and b are given in Table 1.

Table 1. The inversion results for the a, b and a0 coefficients (±1s) for Pn, Sn, Pg and Lg phases used in the attenuation relation (Equation 1).

Phase	a	b	α
P_n	-0.002 ± 0.023	2.340 ± 0.099	0.584 ± 0.030
S_n	0.141 ± 0.028	2.021 ± 0.110	0.419 ± 0.037
P_g	0.091 ± 0.084	0.851 ± 0.366	-0.538 ± 0.035
L_g	0.534 ± 0.062	-0.186 ± 0.123	-0.609 ± 0.063

Figure 2 shows a comparison between the phase magnitude residuals calculated using the relations and parameters of Jenkins *et al*. (1998) and our inversion results. Our results using the relations and parameters of Jenkins *et al*. (1998) revealed a relatively high scatter between individual station and phase magnitudes, and also some systematic inconsistencies, most notably magnitudes calculated from different frequency bands at the same station. Magnitudes calculated from STA values in the 2- to 4-Hz passband are mostly higher than magnitudes calculated in the 3- to 6-Hz passband, which again are generally higher than magnitudes calculated from the 4- to 8-Hz passband. The coefficients used in this case were determined using data from eastern North America, central Asia, and Australia. However, this relation is not primarily intended for local magnitude calculation, and some of the scatter in the magnitudes from Pg and Lg arrivals in particular may be due to the small distance for some of these observations, below the lower distance limit of 1.8° used by Jenkins *et al.* (1998).

Phase magnitudes calculated using Equation 1 and the parameters of Table 1 are shown to the right of Figure 2. These results show that the scatter (expressed as standard deviation) was significantly reduced compared to the original calculations. There is also no apparent frequency dependency in the magnitude residuals.

As an example we show in Table 2 the individual phase magnitude estimates of the 23 February 2002 event located on the northeastern coast of Novaya Zemlya. The consistency of these phase magnitudes is remarkably high.

Table 2. Phase magnitudes and network magnitudes for the 23 February 2002 event located on the northeastern coast of Novaya Zemlya, using the attenuation relations developed in this study.

Station	Phase	Distance	Magnitude
AMD	Pn	509	3.19
AMD	Sn	509	3.15
LVZ	Pn	1055	3.22
LVZ	Sn	1055	3.01
SPITS	Pn	1095	3.44
SPITS	Sn	1095	3.11
ARCES	Pn	1144	2.97
ARCES	Sn	1144	3.08
KBS	Pn	1197	3.16
KBS	Sn	1197	3.19
FINES	Pn	1850	3.17

Magnitude Type	Magnitude
Network Pn	3.19
Network Sn	3.11
Network All	3.15

Figure 3 shows comparisons of corrected network magnitudes compared to magnitudes calculated from individual phases. Although relative P and S magnitudes could be used as an aid in discriminating earthquakes and explosions, Figure 3 shows that regional path effects in this area also give rise to substantial differences in magnitude. This is particularly visible for Pn and Sn magnitudes, as they are available for events covering the entire region. Events that predominantly have ray paths within Fennoscandia have larger Sn magnitudes, while the opposite is true for events that have ray paths crossing the sediment basins of the Barents Sea (Novaya Zemlya/Kara Sea and the western Barents Sea/Mid-Atlantic ridge areas).

From this study, it is clear that Pn and Sn are the most useful phases for calculating magnitudes for events in the Barents Sea. In fact, Figure 3 shows that Pg and Lg are mainly observed at close epicentral distances (< 300 km). This situation is quite different from what we have previously found for the Scandinavian Peninsula and the Baltic Shield, where Lg is the dominant phase on the seismogram out to at least 1000 km. Thus, even for a stable continental region, one may expect quite significant regional variations in the magnitude correction factors.

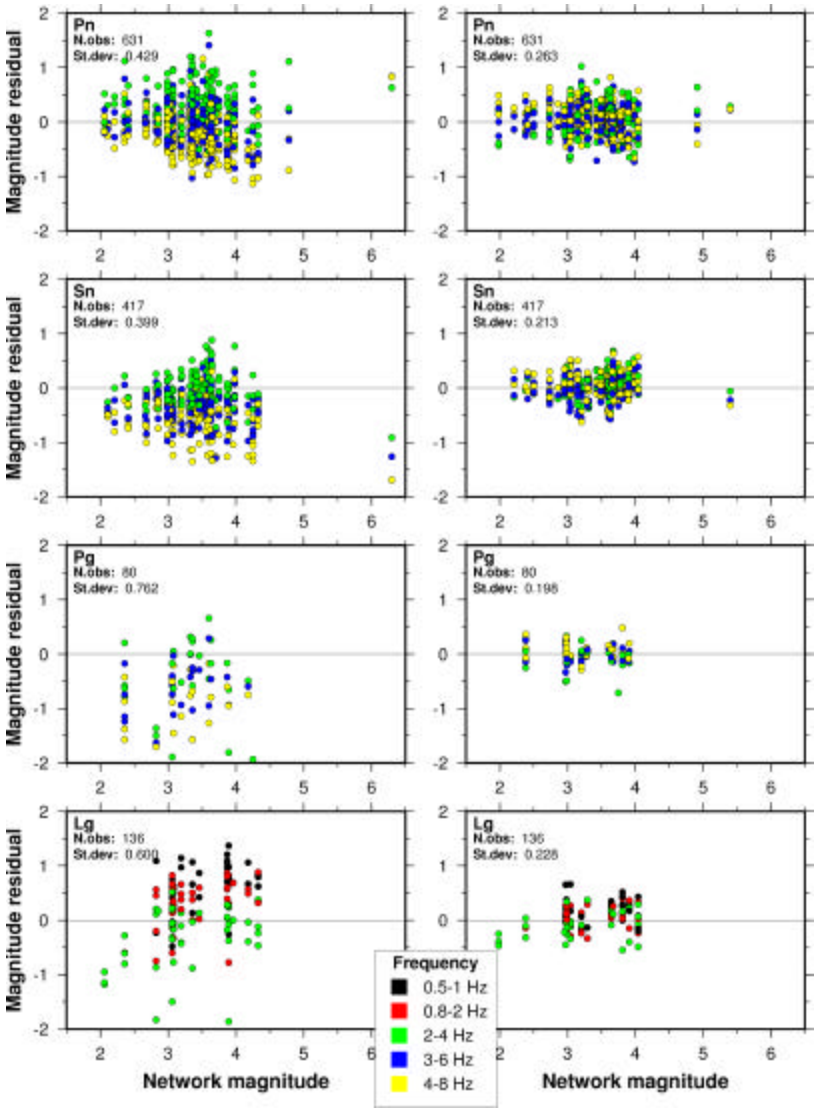

Figure 2. Magnitudes calculated using the relation from Jenkins *et al*. (1998) (left) and this study (right) from individual amplitude readings, plotted vs. network magnitudes for the 45 events. Note the significant reduction in scatter (St. Dev.) and also the absence of frequency-dependent effects when the relation from this study is used.

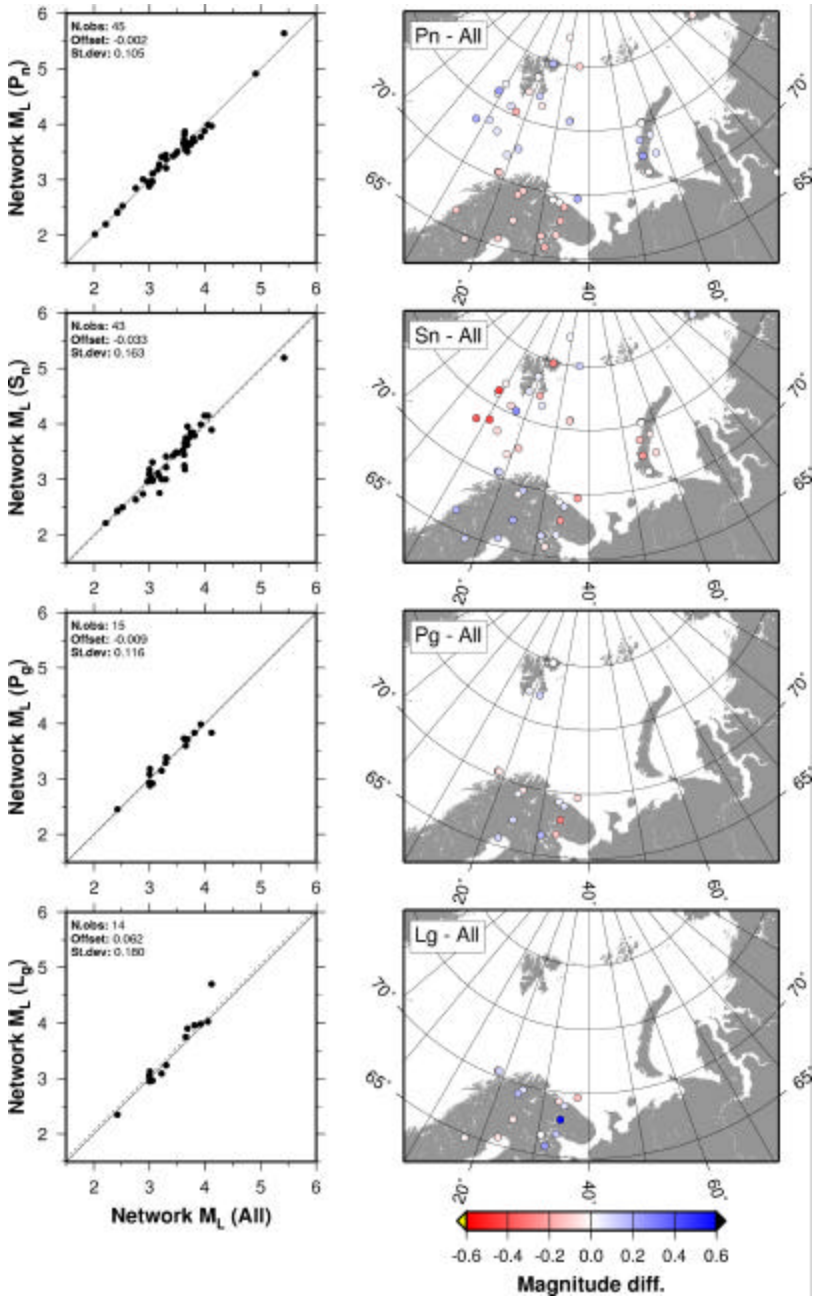

Figure 3. Network event magnitude comparisons and maps of the geographical distribution of the magnitude differences for individual phase magnitudes compared to network magnitudes. Note that Sn magnitudes are overestimated for events that have paths predominantly within the Baltic Shield, while events with paths that cross the Barents Sea have lower Sn magnitudes. Pg and Lg magnitudes appear to be quite stable within the limited distance range from which readings are available.

Regional Threshold Magnitudes

Using the developed attenuation relations described above, observations at the arrays ARCES, SPITS, FINES and NORES were used for calculating threshold magnitudes for a grid system covering the entire Barents Sea region. The grid spacing was approximately 100 km. Figure 4 shows the threshold magnitudes during a time instant without seismic signals. We find large variations over the region, and in particular when approaching each of the arrays. However, for the region around the island of Novaya Zemlya (NZ) the variations are modest, varying around a mean of magnitude 2.2.

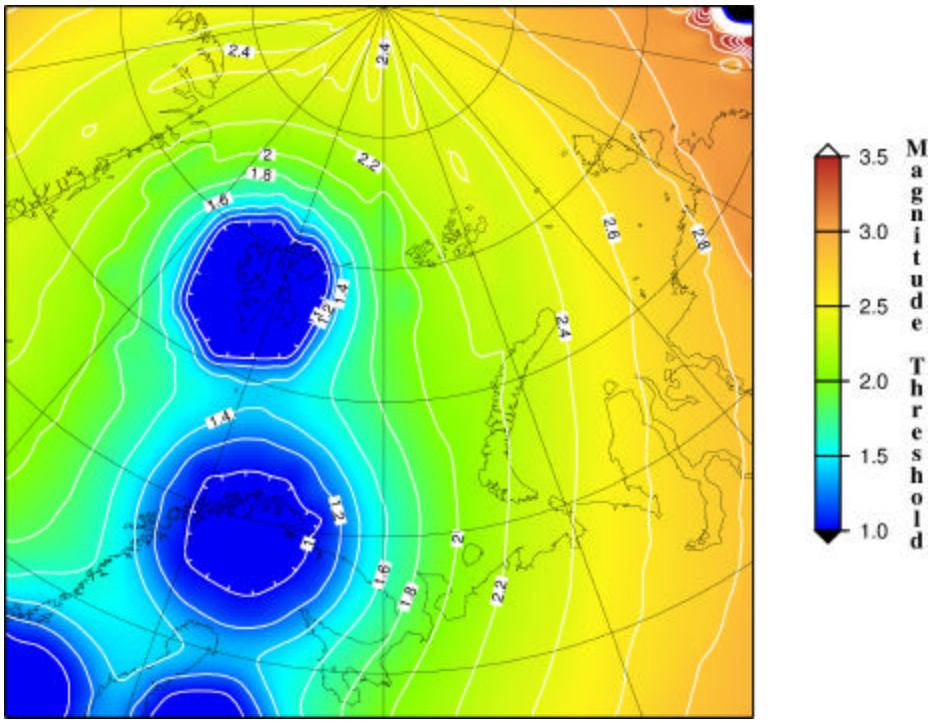

Figure 4. Threshold magnitudes for the time instant 2002-054:01.11.20.0. Notice the improved monitoring capability in the vicinity of each station. For distances above 1.5 degrees of each station, we have considered the Pn and Sn phases, whereas Pg and Lg have been used for distances less than 1.5 degrees.

In order to investigate in more detail the variations in threshold magnitudes for the Novaya Zemlya region, we deployed a dense grid with an areal extent of about 500 x 500 km as shown in Figure 5. For each of the grid nodes, we calculated magnitude thresholds for the two-hour time interval 00:00 - 02:00 on 23 February 2002. At 01:21:12.1 there was an event with a magnitude of about 3.2 (see Table 2), located about 100 km northeast of the former nuclear test site.

Regions of different sizes were constructed by selecting grid points within different radii from the former nuclear test site. Figure 6 (left) shows the variations in threshold magnitudes for a circular region with a radius of 20 km around the test site. The blue line shows the average threshold, whereas the red lines represent the minimum and maximum values. Figure 6 (right) shows similar curves for a region with radius 100 km.

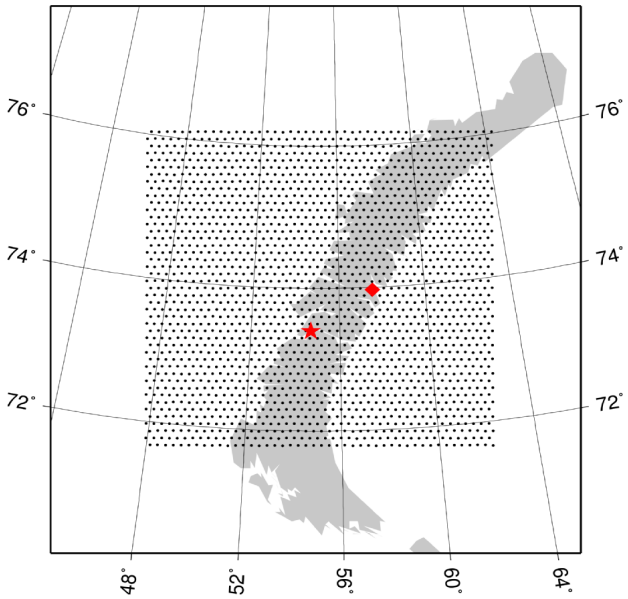

Figure 5. Dense grid deployment around Novaya **Z**emlya (grid spacing 11 km). The red star shows the location of the former nuclear test site, whereas the red diamond shows the location of the event on 23 February 2002 with origin time 01:21:12.1.

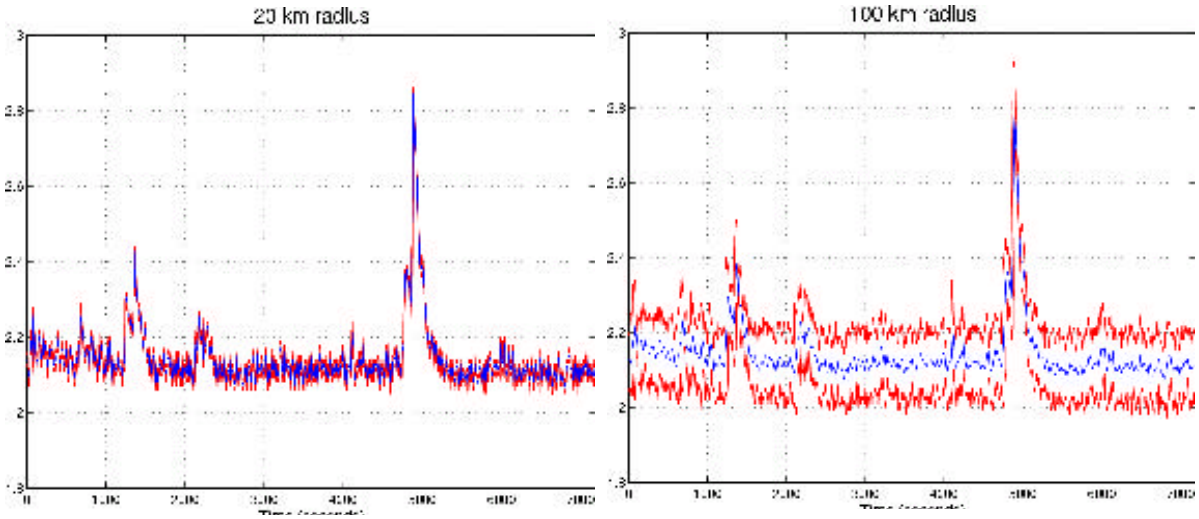

Figure 6. Threshold magnitudes for the time interval 00:00 - 02:00 on 23 February 2002 for 20-km (left) and 100-km (right) radius target regions centered around the former nuclear test site. The peak at about 5000 seconds corresponds to signals for the 3.2 event located about 100 km northeast of the test site.The blue line shows the average threshold, whereas the red lines represent the minimum and maximum values.

It is interesting to notice that even for a region with 100-km radius, the variations in threshold magnitudes are all within 0.2 magnitude units. For this particular configuration of the monitoring network relative to the target area, it will therefore be meaningful to represent the monitoring threshold of the entire region with the values of a single target point, together with uncertainty bounds as shown in Figure 6. For areas with larger variations in threshold magnitudes, like in the vicinity of the arrays, a 100-km radius target region will obviously show larger differences between the maximum and minimum values.

We would like to comment on the threshold magnitude of the peak corresponding to the event located northeast of the test site. In cases where an event actually occurs in the target region, the magnitude thresholds will often be biased slightly low. In Figure 6 we find a maximum value of about 2.9, whereas the event magnitude is estimated to be 3.15. In such cases a maximum-likelihood magnitude estimation algorithm should be activated. However, for small events with a size close to the threshold magnitudes, this bias will not be significant.

Regional threshold monitoring including the Amderma Station

The Kola Regional Seismic Center (KRSC) group in Apatity, Russia, has provided us with about three days of continuous data from the station in Amderma, located on mainland Russia, just south of the island of Novaya Zemlya. The data interval is centered around the origin time of the 23 February 2002 event located on the northeastern coast of Novaya Zemlya. In addition, data from the array in Apatity on the Kola Peninsula were included.

Figure 7 shows the threshold magnitudes during an instant without seismic signals, using the developed attenuation relations for Pn, Pg, Sn and Lg. We find large variations over the region, and in particular when approaching each of the arrays. With the Amderma Station included, we also find significant variations for the island of Novaya Zemlya, ranging from 1.4 at the southern tip to 2.2 at the northern tip. This implies that a regional threshold monitoring scheme for the NZ region has to be divided into geographical sub-regions having similar threshold magnitudes during background noise conditions.

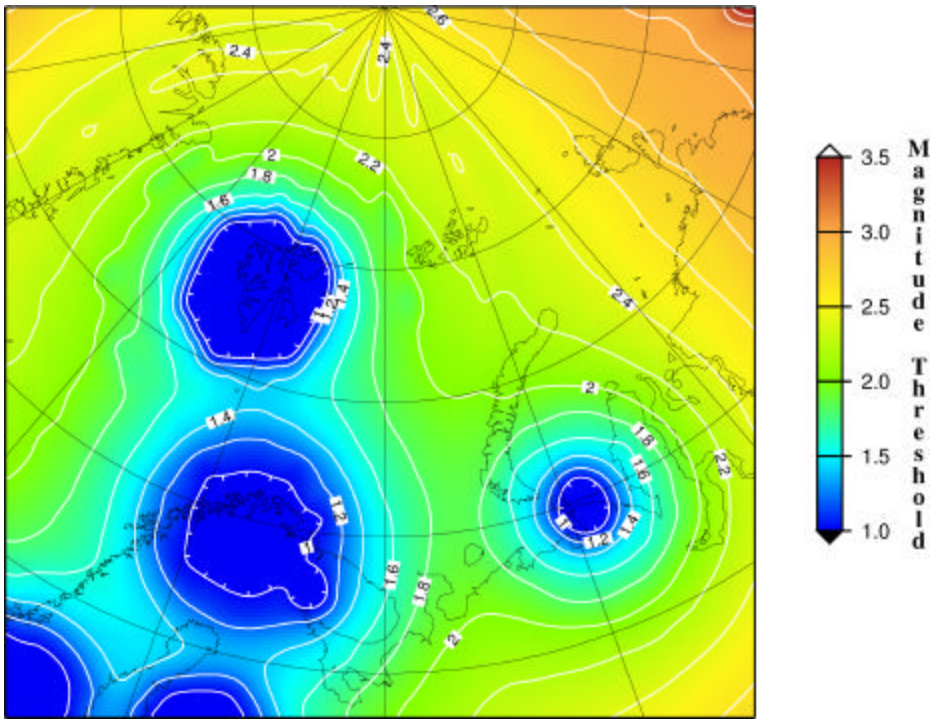

Figure 7. Threshold magnitudes for the time instant 2002-054:01.11.20.0, including data from the Amderma Station and the Apatity Array. Notice the improved monitoring capability in the vicinity of the Amderma Station as compared to the thresholds shown in Figure 4.

CONCLUSIONS AND RECOMMENDATIONS

The pattern of Lg arrivals and associated amplitudes supports the previously published indications that the deep sediment basins and Moho topography under the Barents Sea efficiently block Lg wave energy from crossing. From this, it is clear that Pn and Sn are the most useful phases for calculating stable and consistent magnitudes for events in the Barents Sea.

The 'BAREY' model from Schweitzer and Kennett (2002), based on a model for the Barents Sea area from Kremenetskaya *et al*. (2001), provides the smallest overall travel-time residuals when locating events within the vicinity of the Barents and Kara Seas.

The attenuation in the Barents Sea region differs somewhat from that observed in other stable tectonic regions, as evidenced by the fact that the coefficients given by Jenkins *et al.* (1998) for such regions do not give consistent magnitudes across frequencies, phases and stations for our amplitude observations from the events in the Barents Sea region.

Amplitude inversion has been used in this study to resolve new attenuation coefficients and station corrections for estimating magnitudes from STA amplitude observations for Pn, Pg, Sn and Lg phases in the Barents Sea region. The distance range of observations on which the Pg and Lg relations are based is limited; a future study using a greater number of continental events could most likely provide a relation for STA-based Lg magnitudes that is applicable at larger distances, albeit limited to paths within Fennoscandia.

The seismic station in Amderma can be tied in to the regional network in Fennoscandia and on the Svalbard Archipelago using an appropriate crustal model, and is able to provide important information regarding the location of events in the eastern parts of the Barents Sea and the Kara Sea (Schweitzer and Kennett, 2002). Magnitudes calculated at this station are, on the whole consistent, with the other observations.

For the time interval under study, the seismic arrays ARCES, SPITS, FINES and NORES provide an average monitoring capability of about magnitude 2.2 for the island of Novaya Zemlya. For a region with a 100-km radius around the former nuclear test site, the variations in threshold magnitudes are all within 0.2 magnitude units. It will therefore be meaningful to represent the monitoring threshold of the entire region with the values of a single target point, together with uncertainty bounds as shown in Figure 6.

In cases when data from the Amderma Station can be retrieved, we find significant variations in threshold magnitudes over the island of Novaya Zemlya, ranging from 1.4 at the southern tip to 2.2 at the northern tip. For the actual time interval, the monitoring capability for the former nuclear test site is lowered by about 0.3 magnitude units to about 1.9. This implies that a regional threshold monitoring scheme for the NZ region has to be divided into geographical sub-regions having similar threshold magnitudes during background noise conditions.

REFERENCES

Jenkins, R.D., T.J. Sereno, and D.A. Brumbaugh (1998), Regional attenuation at PIDC stations and the transportability of the S/P discriminant. AFRL-VS-HA-TR-98-0046, Science Applications International Corporation, San Diego, CA, USA.

Kremenetskaya, E., V. Asming, and F. Ringdal (2001). Seismic location calibration of the European Arctic, *Pure Appl. Geophys.* **158**, 117-128.

Schweitzer, J. and B.L.N. Kennett (2002), Comparison of location procedures - the Kara Sea event 16 August 1997, Semiannual Technical Summary, 1 July - 31 December 2001, NORSAR Sci. Rep. 2-2001/2002, Kjeller, Norway, 97-114.

GROUND TRUTH DATA IN INDIA AND CHINA FROM DENSE LOCAL NETWORKS AND CALIBRATION EXPERIMENTS

Walter D. Mooney and Shane Detweiler

US Geological Survey, Menlo Park

Sponsored by National Nuclear Security Administration
Office of Nonproliferation Research and Engineering
Office of Defense Nuclear Nonproliferation

Contract No. DE-A104-98Al79758

ABSTRACT

Obtaining and interpreting qualified, regional geologic and geophysical data from countries such as India and China has been an important scientific and technical goal for many years. To aid in this effort, the U.S. Geological Survey has been building relationships with comparable government organizations throughout Asia. Here we present preliminary results from this interaction in the form of ground truth and crustal structure information for India and China.

We have successfully developed a cooperative program with Indian scientists over the past several years. During that time, delegations from Indian geophysical laboratories have made multiple visits to Menlo Park, CA, bringing with them new seismic data and crustal structure information. We have been very pleased to achieve such unprecedented access to data and their interpretation. During the most recent visit, shallow seismic refraction data from NE India (Kutch region), near the epicenter of the 2001 Bhuj earthquake and in close proximity to the Indian nuclear test site, were processed and interpreted. Another highlight of this cooperation has been the release of aftershock data. This data has relocated hypocenters determined from 18 local seismic stations and were obtained during a visit to India.

We continue our ongoing program of collecting crustal structure and ground truth information from China as well. This effort has likewise been a great success as delegations from many organizations within China have shared data and offered cooperation over the years. We are currently reprocessing data from a 1000-km-long seismic refraction profile centered at 36° N and 104° E. There are 9 borehole chemical shots on this profile, each with 3000-4000 kg charges. The resulting P-wave and S-wave arrivals are excellent. The large borehole explosions will likely have been recorded at seismic monitoring sites, and will serve as valuable ground truth events. In addition, we are working with Chinese seismic network catalog data that provide excellent ground truth seismic events.

OBJECTIVE

This research is aimed at continued cooperation between the U.S. Geological Survey and counterpart agencies in Asia to exchange data and interpretations of crustal structure, and hypocentral locations. With our colleagues from the National Geophysical Research Institute (Hyderabad, India) and the China Seismological Bureau (Beijing, China), we have been successful at initiating and completing a number of seismic studies in areas that are of great importance for nuclear test monitoring. The 2001 Bhuj (western India) earthquake has triggered widespread discussion in the scientific community about the nature and the causes behind such intra-plate earthquakes, and this, in turn, has led to joint work agreements between the USGS and NGRI. This is fortuitous as the Kutch region is just south of the Indian nuclear test site, and the joint study has yielded access to previously unavailable data in the region. In China, we have focused on obtaining the crustal structure of the 1000-km-long Project 973 profile through central China. In addition, large explosions along this line at close proximity to receivers provide excellent ground truth events.

Here, we first make an effort to summarize the available information about the destructive 2001 Bhuj and other major earthquakes in Kutch and their tectonic setting. We shall also try to assess the basic data gaps that need to be filled for understanding the Kutch crustal structure, and thereby will be in a better position to characterize events that occur in the region. Following this, we will describe the area of China where we have newly available information.

RESEARCH ACCOMPLISHED

India

The Kutch region forms a crucial geodynamic part of western continental margin of the Indian sub-continent, and falls in the seismically active Zone-V outside the Himalayan seismic belt. It extends for approximately 250 km (E-W) and 150 km (N-S), and is flanked by Nagar Parkar Fault in the north and the Kathiawar Fault in the south (Fig. 1). The portion bounded between these two faults also contains several E-W trending major faults including the Katrol Hill Fault, Kutch Mainland Fault, Banni Fault, Island Belt Fault and Allah Bund Fault (Biswas, 1987).

The Kutch tectonic setting owes its origin to Mesozoic tectonic events initiated during the break-up of Gondwanaland and the northward drift of the Indian plate. The rift basin evolved as a consequence of this break-up and was controlled by a series of normal faults, which are still exposed in the region. Movement along these faults under an extensional regime produced a number of horsts and grabens.

The Kutch landscape can be categorized into four major E-W trending geomorphic zones (Malik *et al*., 2000). They are: the coastal zone - demarcating the southern fringe, the Kutch mainland - forming the central portion of the rocky uplands, Banni-Plains marked by raised mud flats, and the Great Rann in the north and the Little Rann in east comprising vast saline-waste land. The boundaries of these geomorphic zones are bounded by major faults. The rocky mainland is characterized by the uplifts exposing folded Mesozoic rocks. All the major uplifts are bounded, at least on one side, by a fault or a sharp monoclinal flexure, on the other side by gently dipping Tertiary strata and the peripheral plains that merge gently into the surrounding residual depression.

The Kutch Mainland Fault marks the northern fringe of the rocky mainland. This fault is a vertical to steeply inclined normal fault, but changes upwards into a high angle reverse fault (Biswas, 1987). The central part of the rocky mainland has been upthrown along the longitudinal Katrol Hill Fault (Malik *et al*., 2000).

The Mw=7.6 Bhuj, western India earthquake occurred early in the morning of January 26, 2001. The epicentral coordinates of the main shock obtained from teleseismic data as reported by the USGS to be 23.36°N and 70.34°E. The focus of the earthquake was placed at 22 km. Aftershocks outline an ENE trending south-dipping thrust (45°-50° dip) to great depths (20-30+ km). Later results show concentrated patches of relocated aftershocks that dip to the south between 6 and 37 km deep (Raphael *et al*., 2001). The long-period source time function shows a relatively simple source of about 15 seconds duration. Mori *et al*., (2001) report that the largest area of slip was close to the hypocenter. This asperity is about 10 km x 20 km with a maximum slip of about 10 meters for a rupture velocity of 2.9 km/s. The area of the fault is small for such a large event.

It is interesting to note that Antolik and Dreger's (2001) waveform inversion results also favor the presence of a second sub-event located at shallower depth above and slightly west of the rupture initiation containing as much as 6 m of slip. This sub-event occurs near an area of intense lateral spreading and ground deformation observed in the field, indicating the possible presence of shallow slip although the fault rupture appears not to have reached the surface. They, however, found the overall source parameters (short duration, high stress drop) in line with observations from other intra-plate earthquakes.

The recent Kutch event is about 50 km southeast of the 1819 Kutch (i.e. Allah Bund) event (Mw=7.8), which also originated on a thrust fault (Bilham, 1998). The inferred 50-70 deg N-dipping fault plane (slip>11m) beneath Allah Bund was unfavorably steep for reverse faulting, presumably requiring high fluid pressure in the nucleation zone, according to Bilham (1999). Rajendran and Rajendran (2001) concluded occurrence of another similar sized event 800-1000 years ago from paleo-liquefaction studies. Kaila *et al*. (1972) from statistical analysis computed a return period of 200 years, which is quite close to the time interval between 1819 and 2001 events. More recently, in 1956, a Mw=6.0 event occurred near Anjar town, which also had a thrust mechanism (Chung and Gao, 1995).

Looking at the possible origin of Kutch seismicity, we find that the focal mechanism studies of all the major earthquakes indicate thrust motions on nearly westerly striking planes and, as such, appear to reflect an approximately northerly compressive stress in the crust that would be expected with the ongoing northward collision of India into Eurasia. A change from rift-related extension to north-south compression probably occurred about 40 Ma ago, subsequent to the collision of India with Asia. Low-angle reverse faults exposed in this region provide geologic evidence for such a tectonic reversal, which is indicated also by the thrust-type focal mechanisms. The stress field oriented in the N-S to NNE-SSW direction is considered to be responsible for this reversal of movement and the ongoing deformation (Rajendran and Rajendran, 2001). As well, the Kutch region may be subjected to high and complex stress because of its proximity to the India, Arabia, Asia triple junction, which is located about 500km to the west (Gupta *et al*., 2001). An additional source of stress in the Kutch area might be loading by the Indus delta (Seeber *et al*., 2001).

A good velocity model will improve the hypocenter locations, and thereby identification of active faults. A well-planned seismic reflection study may also image the causative lower crustal fault of the 2001 event, which might have propagated down. If we can image the proper geometry of the fault system, we will be able to assess how the disposition of faults and their interconnection affect/perturb the ambient plate tectonic stress field.

At present, there is far too little information about the Kutch region to completely define the tectonic setting, however this has afforded us an excellent opportunity to share data and research techniques with our Indian counterparts. The data we present here are considered a continuing step in our efforts to work with the Indians. Several issues must be settled before an acceptable model for Kutch seismicity emerges, which will satisfy various observational data sets. We still lack a first order crustal velocity model of the Kutch region. Though we have some knowledge about the geologically mapped faults, we are totally unaware of the disposition of blind faults and thrusts in the crust. Very first information of immense importance is about the thickness, geometry and velocities of this complicated rifted crust. This information may tell us about the age of the crust and its later orogenic history. This will also tell us if there is any systematic difference in the crust between the seismogenic and non-seismogenic parts of the Kutch region. In turn, this information will aid us a great deal in creating accurate crustal models of the area for the purposes of nuclear test monitoring.

Velocity Modeling

In the Kutch region, seismic refraction data was collected, using two 60-channel DFS V recording stations up to a maximum shot-receiver distance of 48 km. The receiver spacing was maintained at 100 m, while the shot point interval was kept as 7 to 8 km. The shot holes drilled up to 20-30 m have been utilized to detonate high-energy explosives. The charge size varied from 50 to 500 kg, depending upon shot-receiver distance.

The data that had been selected for processing at USGS was initially processed at NGRI by utilizing only first arrival refraction data. No attempt was made to utilize near vertical and wide-angle reflection data. The hypocenters of the main and aftershocks of 2001 Bhuj earthquake reportedly lie mainly in the lower crust. After a detailed discussion, we have initiated an effort to reexamine data of some shot points, particularly for the seismic signatures coming from sub-basement features and the base of the crust. We have enhanced the signals of post 5s seismograms

by applying automatic gain control (AGC) and suitable band-pass filters. A few intra-crustal reflections and the reflections from the Moho could be clearly identified. As an experiment, we have subjected this data to stacking, and Kirchhoff pre-stack depth migration. This experiment was done for a small segment with 4 shot points in the vicinity of the 2001 epicentral area (segment C), in addition to the other two segments (B, A) shown in Fig. 1. For depth migration, the aftershock derived sub-basement velocity-depth function (Rastogi *et al*., 2001) has been utilized for the main segment between Anjar and Adhoi, falling in the epicentral area. The average velocity model derived from first arrival refraction data has been used for the column down to the basement. Since one can expect shallower depths to the Moho near the coast, some alterations have been made in the velocity models of other segments for depth migration. Care has been taken to only process subbasement reflection data, as the upper sectional details are restricted.

The 35-km-long main segment (C) of refraction profile between Anjar and Adhoi, shows significantly good reflectivity in the entire mid and lower crustal column (Fig. 2) with prominent reflection horizons at an average depth of 10 km,18-20 km and 30 km. The strong reflection horizon, identified as Moho, has a significant northward dip with depth of about 37 km at the southern end of the segment to almost 47 km at the northern end. At around common depth point (CDP) 200, one can notice a significant change in the pattern of Moho, with Moho assuming a thick lens-like structure. At the southern end of this lens, one can notice the emergence of a possible fault/thrust. From the surface this fault has a southward dip. Also, at the southern end of the segment one can notice the presence of a strong subcrustal reflector at a depth of ~ 57 km. The diffused and disturbed nature of reflectivity at the northern region of the profile has obliterated this reflector. The nearly 35-km-long southern coastal segment (A), depicts good reflectivity in the entire crust (Fig. 3), with the most prominent reflections occurring at an average depth of 5-6 km, and in patches at 10 km and 20 km. The third reflector horizon as a strong band of reflections has a clear eastward updipping trend, with the depth varying from 26 km at the western end to about 18 km at the eastern end of the profile. The Moho, identified as thick zone of 2-3 km thickness, is nearly horizontal all through the profile with an average depth of 35 km. As in the case of the main segment (C) one can notice reflectivity even at sub-Moho depths, with a reflection horizon at an average depth of ~ 47 km.

A close look at the Moho configuration along the three segments suggests that the subhorizontal Moho observed along segments A and B changes the pattern abruptly in the middle part of segment C, where the subsurface crustal structure is disturbed. Perhaps the most striking feature of segment C is the indication of two steeply dipping faults, which extend down to Moho (Fig. 2). The epicenter of 2001 main shock with a fault plane dipping south and a focal depth of 22 km lies very close to this segment.

Thin crust in the aseismic southern segment and a thick crust in the main segment suggest that the Kutch mainland uplift is probably associated with a crustal root, suggesting the significant role played by extensional and compressional tectonic activity. Data from the Banni basin is needed to have detailed subsurface configuration across the area.

China

We also investigate the tectonic process in the northern border of the Tibetan Plateau and the genetic mechanism of the 1920 M=8.6 Haiyuan earthquake, the largest earthquake in recent time in China. To accomplish this, we have interpreted data from what is known as “Project 973” (Funding for this project was established in 1997, March; thus “973.”). This project incorporated a 1000-km-long deep seismic sounding, teleseismic observation, and magnetotelluric sounding profiles. This “tri-combination profile” was the first profile of its kind in China.

The formation and evolution of the Tibetan Plateau is closely related to the convergence of the Indian and Eurasian continental plates. At about 45 Ma, the Indian subcontinent collided with Asia, and has since continued to underthrust at a rate of about 5 cm per year (Molnar and Tapponnier, 1975). As a result, the widest and highest continental deformation zone in the world has been formed. In contrast to the few tens of km wide oceanic deformation zones, the Tibetan Plateau extends into the interior of the plate for more than one thousand km from the plate boundary. The mechanisms of these two kinds of deformation zones are completely different. Therefore, it is of great interest to study the crustal structure of the Tibetan continental deformation zone.

Many investigations in the Tibetan region have been conducted with the efforts of Earth scientists from around the world. As a result, many models have been proposed to describe the evolution of Tibetan Plateau, including the

escape model (Molnar and Tapponnier, 1975; Tapponnier *et al*., 1990), the hydraulic pump model (Zhao and Morgan, 1985, 1987; Westaway, 1995), the underthrust model (Argand, 1924; Barazangi, 1989; Beghoul *et al*., 1993) and the accordion model (Dewey and Burke, 1973; England and Houseman, 1986; Wu *et al*., 1990). However, up to now, most of the field observations have been concentrated in the southern Tibetan region, and therefore most models are based on the data there. In northern Tibet, both observational and theoretical works are sparse and insufficient. Thus, the question remains as to the tectonic process that occur in the northern border of the Tibetan Plateau.

To investigate this question, the China Seismological Bureau, Research Center in Zhengzhou conducted a 1000-km-long geophysical profile crossing the northeastern border in 1999 (Fig. 4). Striking NE-SW, the seismic profile crosses the northeastern corner of Tibetan Plateau and penetrates into the Ordos Block, a very rigid and stable block in the North China Platform. Within the Tibetan Plateau, the profile passes across the Kunlun Fault that is bounded by the Kunlun and Qilian Blocks. The profile also passes through the epicentral area of the M=8.6 Haiyuan earthquake. Here we present the preliminary results from deep seismic sounding data of this profile.

Twelve shots were carried out at each of the 9 shot points along the profile, and for each shot 200 seismometers were deployed with 1-3 km spacing. Thus, a perfect overlapping and reversed observational system was formed.

Based on the characteristics of the recorded P-wave data, the following wave groups were identified: a diving wave (Pg) from the upper crust, reflected waves Pc and Pm from interface C and Moho discontinuity, respectively, and refracted wave Pn which penetrates into top of the upper mantle. The Pc wave, second only to the Pm wave in intensity, can be traced continuously. This indicates that interface C is a major interface of the crust. On these grounds, we deem that the crust can be vertically divided into the upper crust and the lower crust. In addition, we have observed some minor reflected phases, i.e. Pc1, Pc3, Pc4 and Pc5. However, most of these phases are weaker and less continuous than Pc, so the upper and lower crust can be further subdivided into inhomogeneous secondary layers.

The travel times of seismic waves were used to invert for the crustal velocity structures. First, the x^2-t^2 method was used to calculate the depth and average velocity of interface C and Moho discontinuity corresponding to each shot point. Then, the depth-velocity function for each shot point was extracted by 1-D inversion. On this basis, the initial model of 2-D velocity structure along the profile was constructed. The final 2-D velocity structure was ultimately revealed by travel time inversion. In the 2-D model calculation, a joint inversion technique was used for both interface location and velocity values (Zelt and Smith, 1992).

Since apparent seismic velocities are directly measured while the depth of refracting horizons are consecutively calculated (from the shallowest to deepest layer), seismic velocities generally have lower percent errors than interface depths. As is discussed by Mooney (1989), the errors for velocities and interface depths are about 3% and 10% respectively. Even so, the relative variation of velocities and interface depths, and the main features of the crustal structures can be seen from the velocity model.

Figure 5 presents the final 2-D velocity structure. The crust can vertically be divided into an upper crust and a lower crust, with interface C as the boundary. Lateral variation of the crust along the profile is considerable. On the whole, the crust gets gradually thicker from northwest to southwest. As the depth of interface C does not vary greatly along the profile, the variation of crustal thickness is mainly attributed to the gradual thickening of the lower crust from northwest to southwest. The Moho fluctuates significantly in the areas of the Maqin and Haiyuan blocks.

The number of secondary interfaces that exist in the upper and lower crust clearly varies along the profile. It increases gradually from northeast to southwest along the profile, indicating an increase of vertical heterogeneity of the crust.

Figure 5 also shows that a number of low velocity layers exist in the crust in the Maqin Region and one velocity layer exists near interface C in the Haiyuan Region. Moreover, in the vicinities of Maqin and Haiyuan anomalies also appear in the Moho and interface C. The two interfaces are no longer velocity interfaces, but they are complicated transitional layers. Furthermore, there are large offsets of the Moho in these two regions.

As can be readily seen from the record sections and the 2-D velocity model, several distinct anomalies exist in the crustal structure of the Maqin and Haiyuan regions. Two very large strike-slip faults, the Kunlun Fault and the Haiyuan Fault cross these regions respectively. These two faults are closely related to the large thrusts and growing mountain range, and play a very important role in accommodating Indo-Asia convergence (Tapponnier *et al*., 1990; Meyer *et al*., 1998). Their tectonic activity can be seen from the large slip-rates and strong seismicities. The average slip-rates of the Kunlun and Haiyuan faults in Late Pleistocene-Holocene are 11.5 mm/a (Woerd *et al*., 2002) and 11.7-19.2 mm/a (Deng *et al*, 1990) respectively.

As mentioned previously, several models have been proposed to interpret the tectonic evolution of the Tibetan Plateau. In general, these models can be classified into two groups (Tapponnier *et al*., 2001): (1) Continuous thickening and widespread viscous flow of the soft crust and mantle of the entire plateau, (2) Successive oblique subduction of Asian lithosphere mantle, leading to the growth of crustal accretion wedges.

The first model, the viscous Tibetan lithosphere model, ignores the existence of a series of large strike-slip faults within the plateau and at its border. Recent results from surface wave inversion are also not consistent with the soft Tibet paradigm (Griot *et al*., 1998). The phase velocities of Raleigh- and Love-waves show that between the depths of 100 and 300 km, the mantle is faster, and therefore colder, under Tibet than under adjacent regions.

It seems that recent studies of deformation, magnetism and seismic structure beneath the Tibetan plateau support the second model (Tapponnier *et al*., 2001). One important piece of evidence is the existence of magmatic belts becoming younger to the north. This implies that slabs of Asian mantle subducted one after another north of the Zongbo suture. The driving mechanism may be the compression of Indian and Pacific Plates, which results in sufficient stress to reactivate weakly-welded sutures, and thus cause new narrow shears within the Asian lithosphere.

Our 2-D velocity structure appears to support this time-dependent, localized shearing model. This evolution model can easily explain the anomalies of crustal structures in the Haiyuan and Magin Regions. In location, these two regions correspond to two mantle subducted slabs related to the Qilian and Kunlun Sutures. From our results we infer that the detachment zone may be shallower than suspected. One possibility is that the upper crust is decoupled along the top of low velocity layer in the middle crust. Due to subduction, the Moho is no longer a sharp discontinuity, but a very complicated transitional zone. The subduction zones also result in the large offsets of the Moho in these two regions. As the underthrusting action in the Kunlun Region lasted longer than that in the Qilian Region, the crustal structure is more complicated; there are more crustal low velocity layers in the Maqin Region than those in the Haiyuan Region. Furthermore, the crust is thicker and the average velocity is lower in the Maqin Region.

According to the result of Zeng *et al*. (1998) from teleseismic receiver functions and Pn waves, the Moho in the Kunlun and Qilian Blocks dips southward while that in the Qangtang Block dips northward, which is consistent with the evolution model mentioned above. Results from reflection profiling in young (post-Mesozoic) orogens also show that the lower crust usually dips toward the center of the root from both sides and shows seismic laminated structures (Mooney and Meissner, 1992). The long durations of Pc and Pm waves in our Haiyuan and Maqin record sections may therefore reflect a laminated lower crust.

CONCLUSIONS AND RECOMMENDATIONS

The available data from the Kutch, India, region shows the deep-seated effect of the recent seismic activity. We suggest proper imaging of the deep-seated blind thrusts/faults is essential to obtain a meaningful seismicity model for the region.

The Bhuj earthquake has placed the Kutch peninsula and the Little Rann of Kutch west and east of the Bhuj epicenter under increased stress, and it is anticipated that these regions are likely to experience heightened seismicity in the next several decades. Thus, it is imperative that we continue to monitor seismicity and understand the crustal structure so that we will be able to discriminate seismic events. The mapping of potentially active faults with likely increased stress concentration thereby assumes great importance from a monitoring point of view, and seismic surveys are needed to refine the determination of crustal structure in Kutch mainland.

Further experiments are also needed to define the P- and S-wave velocity structure of China. In addition to limited information in other regions of China, we would also seek to verify the step-wise underthrusting evolution model of the Tibetan Plateau. We need better definition of deeper structures, especially within the lithospheric mantle in the northeastern corner of the Tibetan Plateau. Due to the limited observational distance in our refraction profile, we could not image the structures below the Moho. Therefore, further experiments based on teleseismic methods are needed. One possible way is to deploy dense seismic stations in this region for teleseismic observation. By seismic tomography, a 3-D velocity model to a sufficient depth can be obtained which will permit us to refine geologic models of the evolution of this region.

REFERENCES

Antolik, M. and D.S. Dreger, 2001 Source Rupture Process of the 26 January 2001 Bhuj, India, Earthquake (M 7.6), *Eos Trans. AGU, 82*(47), Fall Meet. Suppl., Abstract: S52G-03.

Argand,E., 1924, La tectonique de I'Asie, *Int. Geol. Cong. Rep. Sess*. **13** (1), 170-372.

Barazangi, M., 1989, Continental collision zones: seismotectonics and crustal structure. In James, D. H. (Ed.), *The Encyclopedia of the Solid Earth Geophysics*, Van Nostrand Reinhold, New York, 58-75.

Beghoul, N., M. Barazangi, and B. L. Isacks, 1993, Lithospheric structure of Tibet and western North America: Mechanism of uplift and a comparative study, *J. Geophys. Res.*, **98**, 1997-2016.

Bilham, R., 1998. Slip parameters for the Rann of Kachchh, India, 16 June 1819 earthquake quantified from contemporary accounts. In: *Coastal Tectonics* (Eds: Stewart, L.S. and Vita-Finzi, C.), Geol. Soc. London, Spl. Pub.,146, 295-319.

Bilham, R., K. Wallace, and R. Bendick, 2001. Seismicity Following Deep Reverse-Faulting in the Indian Plate: Implications for Gujarat, *Eos Trans. AGU*, **82** (47), Fall Meet. Suppl., Abstract : S52G-09
Biswas, S.K., 1987.Regional tectonic framework, structure, and evolution of the western marginal basins of India, *Tectonophysics*, 135, 307-327.

Chung, W.P. and H. Gao, 1995. Source parameters of the Anjar earthquake of July 21, 1956, India and its seismotectonic implications for the Kutch rift basin. *Tectonophysics*, **242**, 281-292.

Dewey, J. F. and K. C. A.. Burke, 1973, Tibetan, Variscan and Precambrian reactivation: Products of continental collision, *J. Geol.*, **81**, 683-692.

Deng, Q. and W. Zhang (editors in chief), 1990, *Haiyuan Active Fault*, Seismological Press, Beijing, China, 286 p. (in Chinese).

England, P. and G. Houseman, 1986, Finite strain calculation of continental deformation, 2. Comparison with the India-Asia collision zone, *J. Geophys. Res*., **91**, 3664-3676.

Griot, D., J. P. Montagner, and P. Tapponnier, 1998, Phase velocity structure from Rayleigh and Love waves in the Tibet and its neighboring regions, *J. Geophys. Res*., **103**, 21 215-21 232.

Gupta, H.K., N. Purnachandra Rao, B.K. Rastogi, and D. Sarkar, 2001. The deadliest intra-plate earthquake, *Science*, **291**, 2101-2102.

Kaila, K.L., V.K. Gaur, and H. Narain, 1972. Quantitative seismicity maps of India, *Bull. Seism. Soc. Am*., **62**, 1119-1132.

Karanth, R.V., P.S. Sohoni, G. Mathew, and A.S. Kadkikar, 2001. Geological observations of the 26 January 2001 Bhuj earthquake, *J. Geol. Soc. Ind..*, **58**, 193-202.

Ma, X. Y., 1989, *Lithospheric Dynamic Atlas of China*, Beijing: China Cartographic publishing House.

Malik, J.N., P.S. Sohoni, S.S. Merh, and R.V. Karanth, 2000. Paleoseismology and neotectonism of Kachchh, western India. In: *Active Fault Research for the New Millennium*, Proceedings of the Hokudan International Symposium and School on Active Faulting (Eds. Okumura, K., Goto, H., and Takada, K.).

Mereu, R. F., 1990, The complexity of the crust from refraction/wide angle reflection data, *Pure Appl. Geophys*., **132** (1/2), 269-288.

Meyer, B., P. Tapponnier, L. Bourjot, F. Metivier, Y. Gaudemer, G. Peltzer, G. Shunmin, and C. Zhitai, 1998, Crustal thickening in Gansu-Qinghai, Lithospheric mantle, and oblique, strike-slip controlled growth of the Tibet plateau, *Geophys. J. Int.*, **135**, 1-47.

Molnar, P. and P. Tapponnier, 1975, Cenozoic tectonics of Asia: effects of a continental collision, Science, **189**, 419-426.

Mooney, W. D., 1989, Seismic methods for the determination of earthquake source parameters and lithospheric structure, in Geophysical Framework of the Continental United States, edited by L. C. Pakiser and W. D. Mooney, Geol. Soc. Am. Mem., **172**, 11-34.

Mooney, W. D. and R. Meissner, 1992, Multi-genetic origin of crustal reflectivity: a review of seismic reflection profiling of the continental lower crust and Moho, in: Continental Lower Crust, edited by D. M. Fountain, R. Arculus and R. W. Kay, Elsevier, Amsterdam, 45-79.

Mori, J., T. Sato, and H. Negishi, 2001. Slip Distribution of the 2001 West India Earthquake, *Eos Trans. AGU,* **82** (47), Fall Meet. Suppl., Abstract S51B-0604.

Rajendran, K., C.P. Rajendran, M. Thakkar, and M.P. Tuttle, 2001. The 2001 Kutch (Bhuj) earthquake: Coseismic surface features and their significance, *Current Science*, **80**, 1397-1405.

Rajendran, C.P. and K. Rajendran, 2001. Characteristics of deformation and past seismicity associated with the 1819 Kutch earthquake, northwestern India, *Bull. Seism. Soc. Am*., **91**, 407-426.

Raphael, A., P. Bodin, S. Horton,, and J. Gomberg, 2001. Preliminary Double-Difference Relocations of Bhuj Aftershocks *Eos Trans. AGU*, **82** (47), Fall Meet. Suppl., Abstract : S51B-0605.

Rastogi, B.K., 2001. Personal communication

Seeber, N., B. Senthil, R. Briggs, and S.G. Wesnousky, 2001. Field observations bearing on the genesis of the January 26, 2001 Republic Day Earthquake of India resulting from a field survey of the epicentral region. http://neotectonics.seismo.unr.edu/Bhuj/Report.html

Talwani, P. and A. Gangopadhyay, 2001. Tectonic framework of the Kachchh earthquake of 26 January 2001, *Seism. Res. Lett*., **72**, 338 –341.

Tapponnier, P., 1990, The Ailao Shan-Red River metamorphic belt: Tertiary left-lateral shear between Indochina and south China, *Nature*, **343**, 431-437.

Tapponnier, P., B. Meyer, J. P. Avouac, G. Peltzer, Y. Gaudemer, S. Guo, H. Xiang, K. Yin, Z. Chen, S. Cai, and H. Dai, 1990, Active thrusting and folding in the Qilian Shan, and decoupling between upper crust and mantle in northeastern Tibet, *Earth Planet. Sci. Lett*., **97**, 382-403.

Tapponnier, P., Z. Xu, F. Roger, B. Meyer, N. Arnaud, G. Wittinger, and J. Yang, 2001, Oblique stepwise rise and growth of the Tibet Plateau, *Science*, 294, **23**, 1671-1677.

Westaway, R., 1995, Crustal volume balance during the India-Eurasia collision and altitude of the Tibetan plateau: a working hypothesis, *J. Geophys. Res*., **100**, 15 173-15 192.

Woerd, J. V. D., P. Tapponnier, F. J. Ryerson, A. S. Meriaux, B. Meyer, Y. Gaudemer, R. C. Finkel, M. W. Caffee, G. G. Zhao and Zh. Q. Xu, 2002, Uniform postglacial slip-rate along the central 600 km of the Kunlun Fault (Tibet), from 26Al, 10Be and 14C dating of riser offsets, and climatic origin of the regional morphology, *Geophys. J. Int*., **148**, 356-388.

Wu, G., X. Xu,, and T. Li, 1990, The Yadong-Golmud geoscience transect in the Qinghai-Tibet plateau, *Acta Geol. Sin*., **3,** 115-127.

Zhao, W. J. and W. J. Morgan, 1985, Uplift of Tibetan Plateau, *Tectonics*, **4**, 359-369.

Zhao, W. J. and W. J. Morgan, 1987, Injection of Indian crust into Tibetan lower crust: a two-dimensional finite element model study, *Tectonics*, **6**, 489-504.

Zelt, C. A. and R. B. Smith, 1992, Seismic traveling inversion for 2-D crustal velocity structure, *Geophys. J. Int.*, **108**, 16-34.

Zeng, R. S., Z. F. Ding, and Q. J. Wu, 1998, The crustal structures from Himalaya to Qilian and its implications for continent collision process, Chinese Journal of Geophysics *Acta Geophys. Sin.*, **41**, 49-60 (in Chinese).

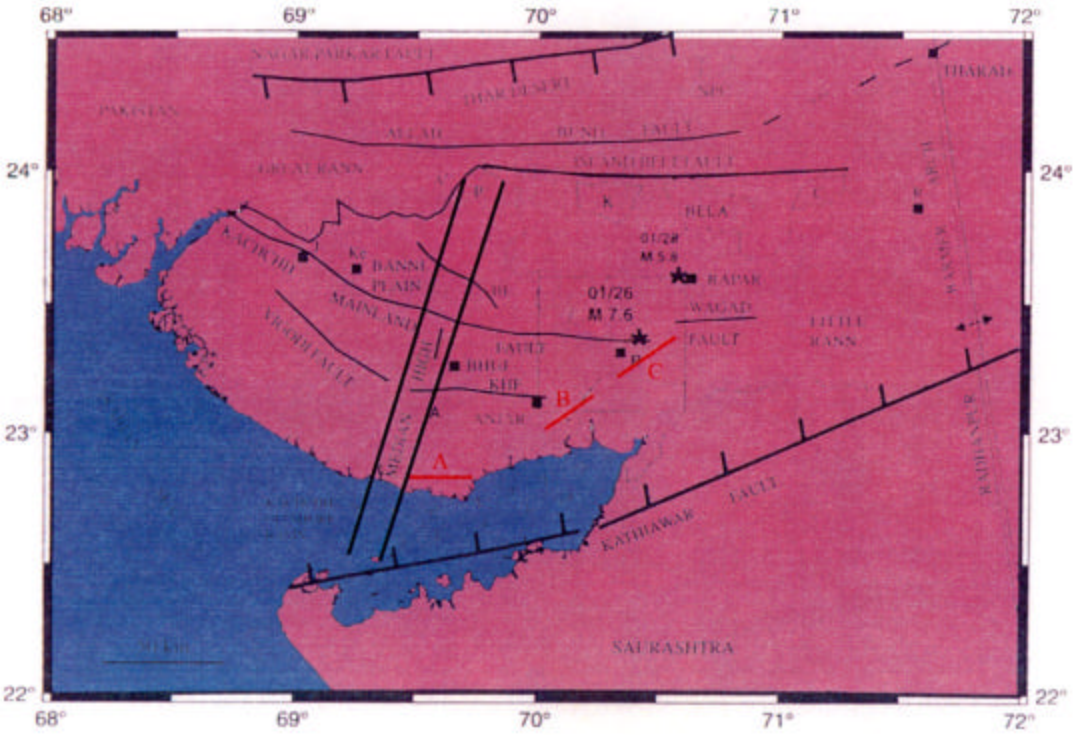

Figure 1. Structural elements in the Kutch basin. Asterisks show the USGS location of the 2001 main and one aftershock events (after Talwani and Gandopadhyay, 2001). Three seismic refraction segments (A, B, and C) are shown in red.

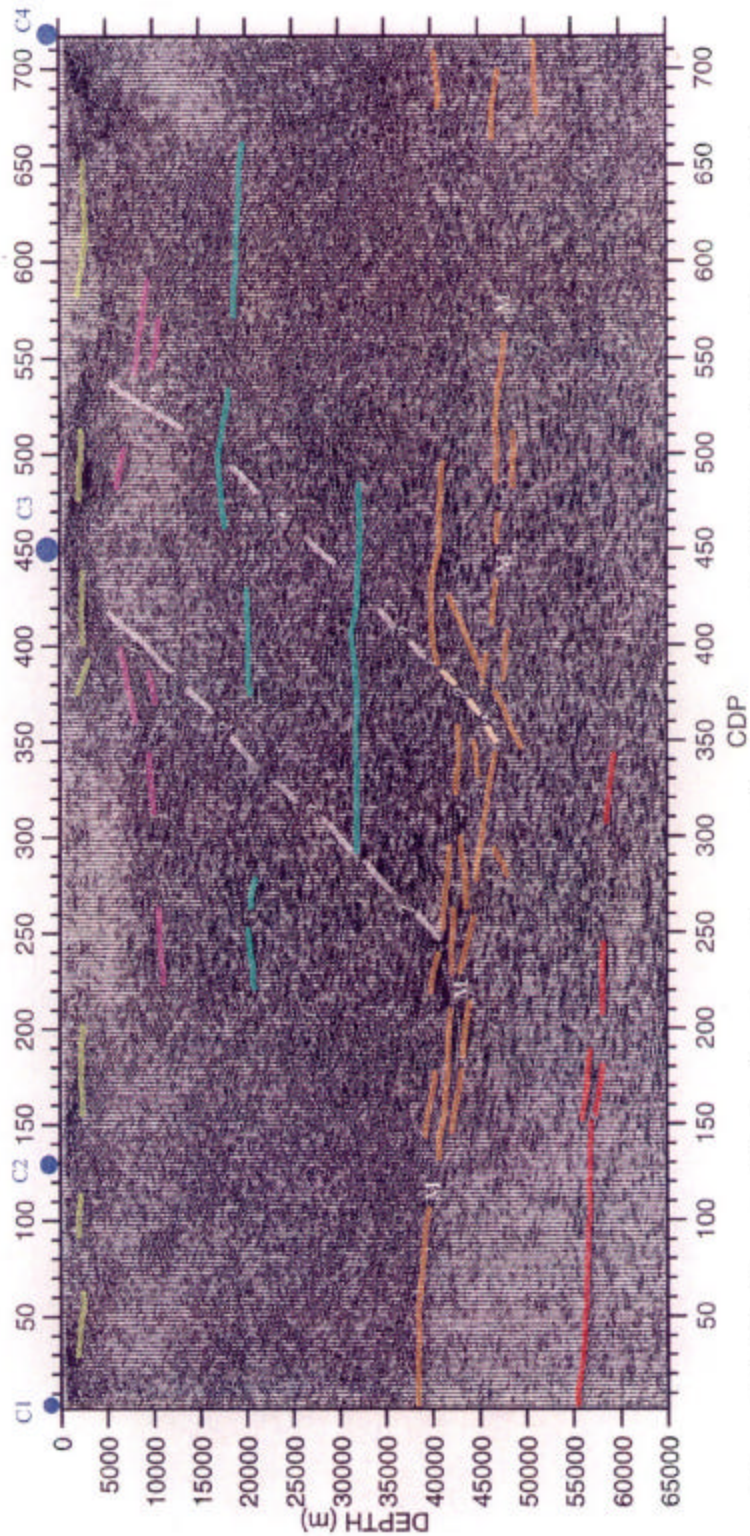

Figure 2. Kirchhoff pre-stack depth migrated crustal cross-section along segment C. CDP interval is 50 m. Interpreted horizonas are superimposed. Dots above represent shot point locations.

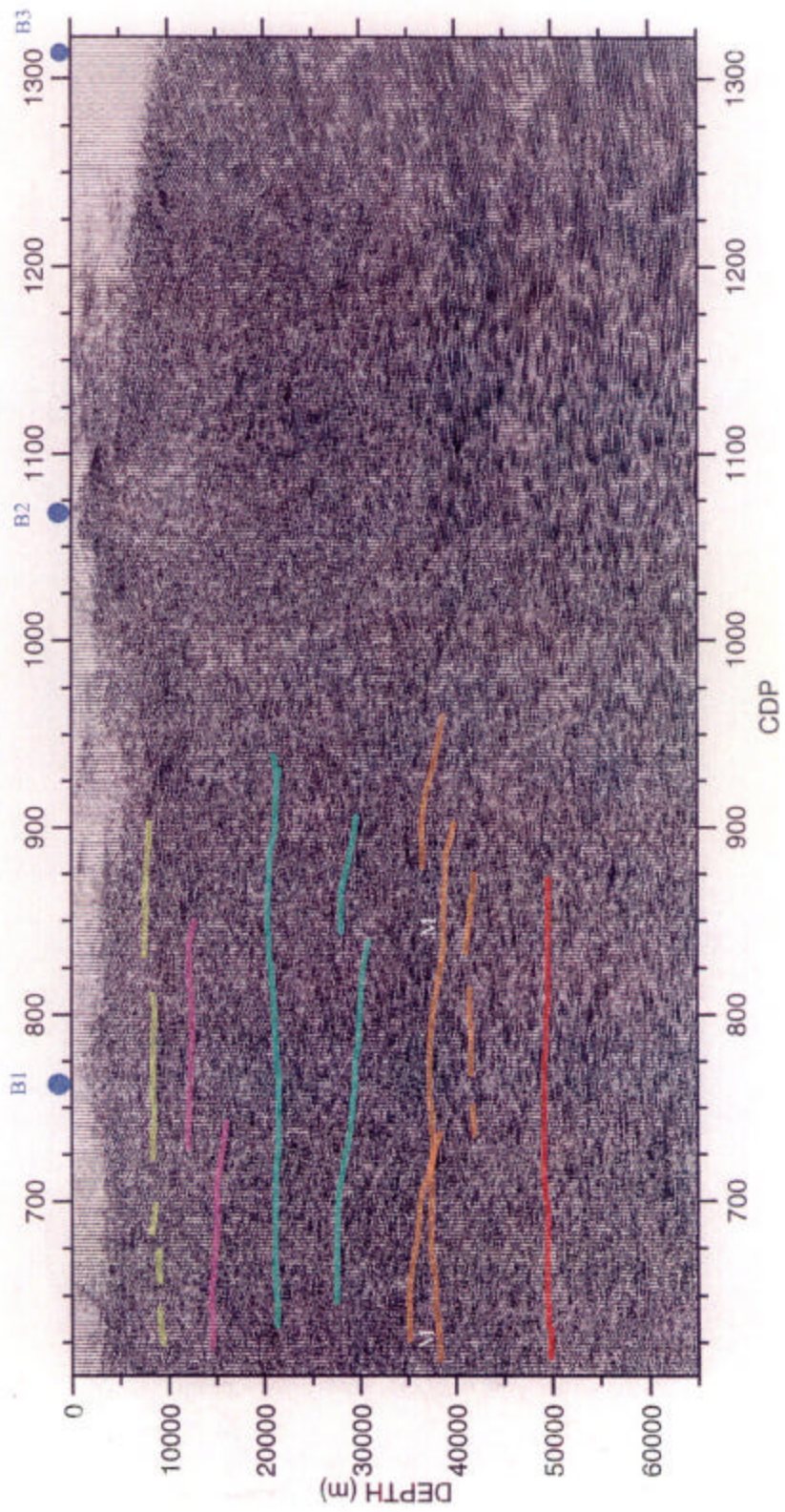

Figure 3. Kirchhoff pre-stack depth migrated crustal cross-section along segment B. CDP interval is 50 m. Interpreted horizons are superimposed. Dots above represent shot point locations.

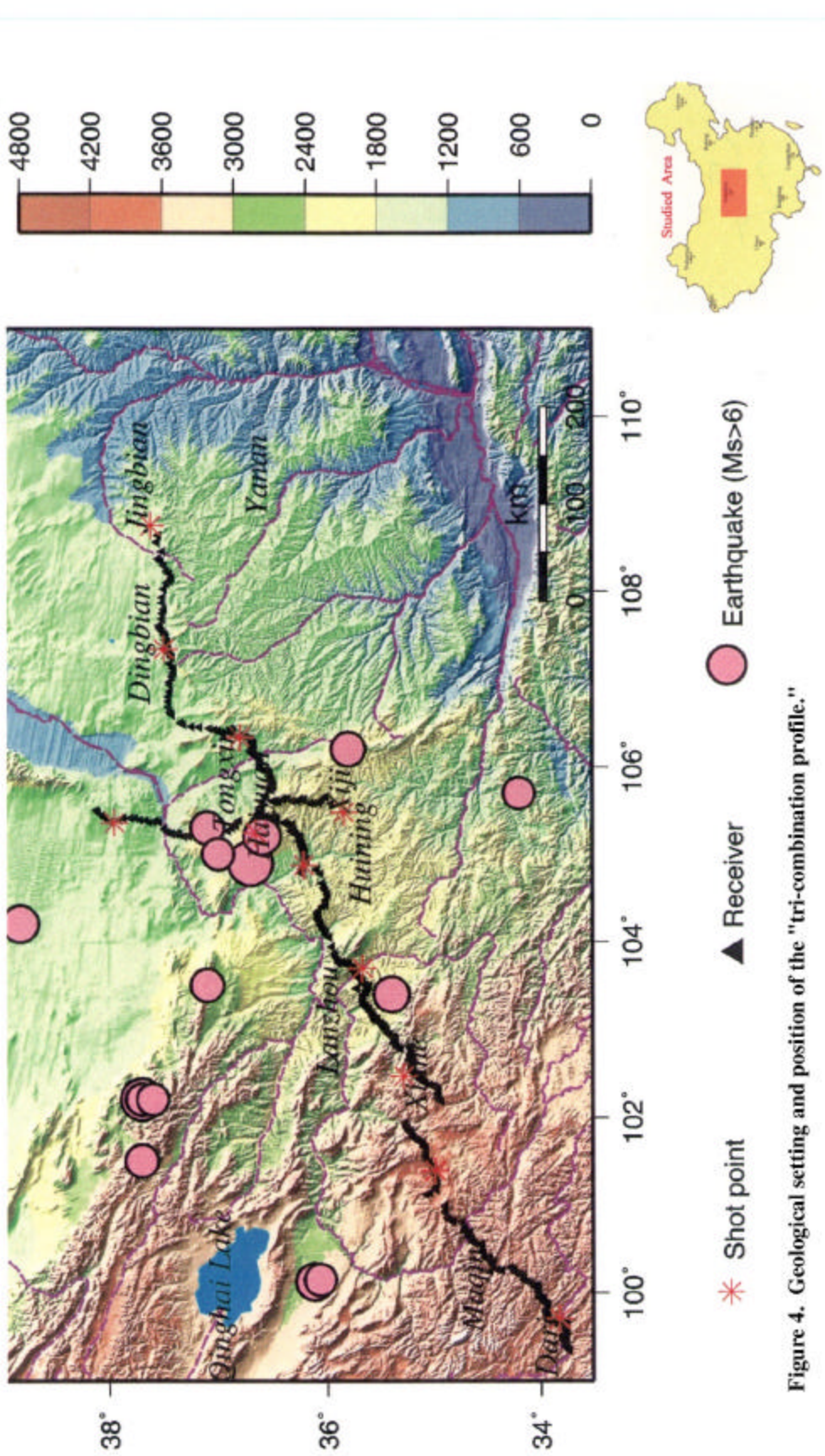

Figure 4. Geological setting and position of the "tri-combination profile."

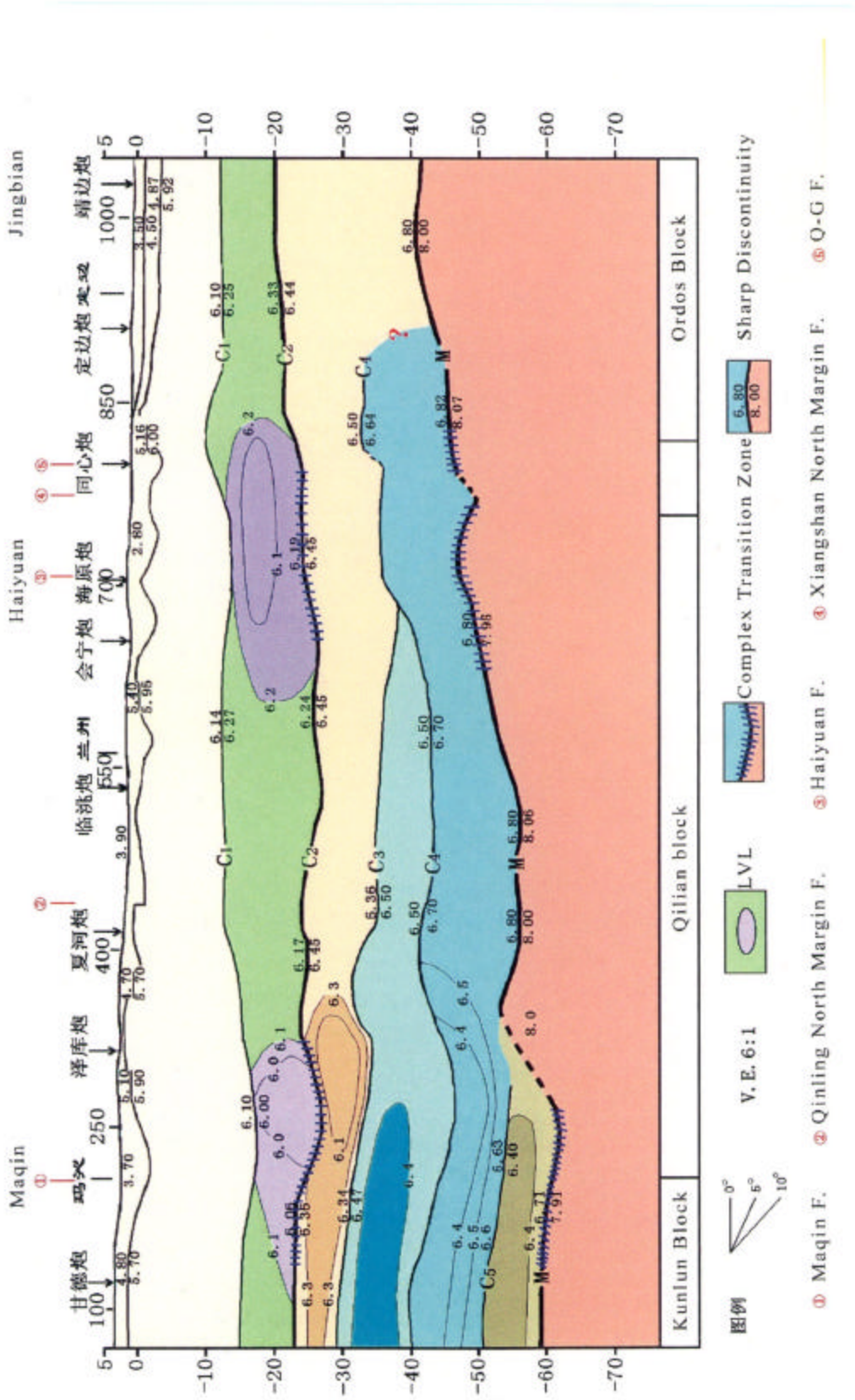

Figure 5. 2-D crustal seismic velocity structure of the Maqin-Jingbian DSS profile.

EFFICIENT INTEGRATION OF OLD AND NEW RESEARCH TOOLS FOR AUTOMATING THE IDENTIFICATION AND ANALYSIS OF SEISMIC REFERENCE EVENTS

D. Wilmer Rivers,[1] Craig A. Schultz,[2] and Douglas A. Dodge[2]

Multimax, Inc.,[1] Lawrence Livermore National Laboratory[2]

Sponsored by National Nuclear Security Administration
Office of Nonproliferation Research and Engineering
Office of Defense Nuclear Nonproliferation

Contract No. DE-FG02-01ER83218[1] and W-7405-ENG-48[2]

ABSTRACT

The selection and study of reference events for inclusion in the National Nuclear Security Administration (NNSA) Knowledge Base requires the application of a much broader suite of seismic analysis software than does either the routine production of a seismic bulletin or the subsequent preliminary screening of those bulletin events to conduct nuclear explosion monitoring. For either of those latter applications, a large program designed explicitly for that single purpose can be applied in a set analysis procedure for every one of the many events that will be processed daily, but to study the much smaller number of reference events in adequate detail, it is necessary to use many separate specialized programs, including new routines that may still be in the testing phase or even some that were developed or modified specifically to study the particular event at hand. In order to make the most effective use of this software suite, the individual programs must communicate with one another in an efficient and flexible manner, so that a scientist can select which programs to run and in what order, thereby improvising a data-processing pipeline of programs passing their results from one to the next.

We have explored the technical feasibility of constructing such a reference event analysis system by using the Common Object Request Broker Architecture (CORBA) as the data communications tool for passing data among programs and for allowing them to make Remote Procedure Calls (RPCs) to invoke one another's services. We have extended the standard seismic analysis program *geotool* to incorporate a CORBA interface, and through it, we can send data and RPC messages to other programs for processing, and then back again to *geotool* for interactive graphics display of the results. The communications take place through separate Object Request Brokers (ORBs) for *geotool* and for the analysis programs. We demonstrate this procedure by using the C-language program *geotool* as server software on Linux and a Java application for waveform filtering as client software in MS Windows. The two programs on the separate platforms are able to function together just as if the remote Java application were actually a local C-language routine within *geotool* called via a pull-down menu. All data communications take place within memory, and no new disk files or database records need be generated as output from one program and then read as input to the other. It is this type of seamless data communications that should form the infrastructure for integrating the many separate programs that will be needed to analyze seismic reference events thoroughly.

Although the work performed to date has used CORBA as the mechanism for inter-process communications, we have monitored the software industry's increasing acceptance within the last year of "Web services" as an alternative approach to the integration of distributed software components. Web services technology is based on Simple Object Access Protocol (SOAP) invocations of remote procedures, and the SOAP calls are transmitted through XML-formatted text messages sent via HTTP. Since the messages are text-based, and since they are handled by a SOAP-enabled Web server rather than by an ORB, inter-platform data communications are simpler (but more bandwidth intensive) through Web services than through CORBA. The potential for integrating native Windows applications with UNIX applications through Web services is particularly appealing, so in our future work, we intend to investigate the use of Web services as an alternative to CORBA for transmitting data and RPCs among the programs that will be used to analyze reference events. In particular, the XML messages invoking the remote processing offer a means for creating a metadata tracking system that can be used to record the data-processing history of each parameter measurement made by the distributed system of independent software components, so the metadata for the entire suite of data analysis procedures for each waveform can be archived for repeating (or undoing) any or all of the measurements.

OBJECTIVE

Scientists use a variety of stand-alone computer programs to analyze and identify seismic events for nuclear explosion and treaty monitoring, and an especially wide selection of software tools is needed for the detection and intensive study of reference events that will be included in the NNSA Knowledge Base for use in future event comparisons. Some of these stand-alone programs are large software packages that offer many tools for routine seismic analysis, but they are difficult to modify to include additional tools for specialized tasks. Others of these stand-alone programs offer the capability of performing only specific operations, and they must be used in conjunction with other programs such as interactive waveform graphics displays that offer more general analysis capabilities. In most cases neither the large software packages nor the specialized analysis programs can communicate adequately from one to another without the tedious creation and input of temporary data files and other awkward techniques. Since the stand-alone programs cannot exchange data easily, it is difficult to use them in a data-processing pipeline that could add new capabilities to those offered by the large software packages or that could allow the specialized analysis programs to rely on other software for tasks such as graphics displays.

A reference event analysis system should therefore be built by using a system architecture that facilitates data flow among these stand-alone programs, including any new programs that will be developed in the course of future research and that may be especially valuable for the identification and characterization of reference events. This new architecture should allow the results of one program to be sent easily to another one, as chosen on a case-by-case basis by the seismic analyst, without the creation of temporary files and database tables. Because many of the stand-alone seismic analysis programs that need to communicate with one another are written in different computer languages, and many are written for use under different operating systems, it will be important for this architecture to be as nearly platform-independent as possible. Furthermore, the communications among the separate programs should allow access to remote resources for data retrieval or specialized computations. The reference event analysis system should therefore be constructed as a distributed system of individual software components rather than as a single large software package. The first objective of our study is to examine software architectures and communications protocols that will allow existing and newly developed programs to be used as the components in this distributed system. Our next objective is to select and modify those programs so that they can be integrated into a reference event analysis system using that distributed system architecture.

RESEARCH ACCOMPLISHED

This project is divided into two phases: a six-month proof-of-concept phase, which has recently been completed, and a two-year implementation phase, which has now begun. The proof of concept was intended to explore the architectural underpinnings of a software system for analyzing seismic reference events, and it was not intended in this first stage to design and construct any of the graphics, signal processing, geophysical, communications and other modules that would be the constituent parts of such a system. Our study has not focused so much on the construction of a new seismic analysis package that is intended to replace the ones currently in use as it has focused on the integration of separate modules, including both existing code and newly developed routines, into a flexible software system. We shall select the individual modules to use for analyzing reference events, and we shall build certain new data processing tools as required, during the two-year implementation phase that is now underway.

In examining possible architectures for a reference event analysis system, our choices have been guided strongly by the differences between routine seismic analysis performed for constructing event bulletins and the more nearly *ad hoc* analysis that is required to identify and characterize reference events for inclusion in the Knowledge Base. Software packages for routine seismic analysis are designed to facilitate the repetitive performance of a pre-determined series of tasks. Although a data analyst engaged in constructing an event bulletin will have some flexibility in choosing to perform certain ones of those analysis tasks for every waveform under consideration while reserving other analysis tasks for use only in unusual circumstances (such as using a polarization filter to help separate the sources of mixed signal arrivals), by and large the processing of every new event will conform to set procedures. In particular, if the analyst makes any choice of data processing tools at all, the selection of those tools will be limited to only those modules that are included within the seismic analysis software package, so the designer of that package must therefore foresee all the tasks that the analyst may need to perform. For screening all seismograms recorded by a network and pre-processed by an automated system, and especially for making a specified set of measurements that are agreed upon for international data exchange, this approach is, in fact, a suitable one. A number of software packages such as Seismic Analysis Code (SAC2000; *viz.* Goldstein, 1998),

Analyst Review Station (ARS; *viz.* Wang, 1996), *geotool* (Henson, 1993), and MatSeis (Young, 2001), among others, are commonly used for these analysis tasks. These same packages can also be used satisfactorily for the analysis of reference events, but we feel that the use of any one of these packages, or for that matter the use of any other single large program that we could design and build *ab initio* as a product of our current study, may not be the best possible approach for this purpose. We shall now discuss some shortcomings of that approach and describe alternatives to it.

For identifying and characterizing possible reference events for use within the Knowledge Base, it is critical that the scientist have maximum flexibility in choosing what algorithms and data processing routines should be used in any particular case. The purpose of a reference event is to exemplify the seismograms that are to be expected from a particular type of event, in a particular region, as recorded at particular stations, and the tools needed to characterize those seismograms will be as varied as the waveforms themselves. A wavetrain from a small strike-slip earthquake in the upper mantle in a region of low anelastic attenuation will, of course, be markedly different from the waveform of a large thrust-fault earthquake at shallow depth in a tectonically active region, and a scientist may wish to choose to apply a different suite of tools depending on certain features that are exhibited by one of these events but not by the other. In fact, highlighting these differences in order to categorize patterns that can be used to distinguish one type of event from another is one of the goals of reference event analysis. Even for conventional applications such as picking arrival times, determining epicenters and confidence regions, measuring signal amplitudes and periods, etc., when studying a reference event, a scientist may well wish to apply unusual tools that would not conventionally be applied during routine event screening. For instance, elaborate de-ghosting algorithms may be used to identify multiple small echoes within reference signals propagating along paths characterized by strong multipath arrivals, a procedure that is unlikely to be applied to signals not intended for inclusion in the Knowledge Base. It is even possible that a scientist may wish to develop special software for application to a particular signal, if no tool that is available seems appropriate for the purpose. Applying specialized tools would require making modifications or extensions to the seismic analysis software packages. Another reason that these packages could need to be modified for reference event analysis is that it can be the software itself, rather than the seismogram, that is the subject of the analysis. This would happen because a scientist who is developing a new analysis routine will likely want to test it by applying it to reference signals in conjunction with the existing tools that already exist in those packages. For instance, a scientist who has developed some variant on the conventional computation of the complex signal cepstrum will want to test only that algorithm and not have to write new graphics code for the display of the waveforms, spectra, cepstra, etc., capabilities that are already offered by the existing seismic analysis packages. For processing reference events, then, it will be necessary for a scientist to make modifications to SAC, ARS, *geotool*, etc., by incorporating unusual or newly developed analysis tools into the software package.

Although most of these seismic analysis software packages can be modified to some extent, the process is usually not an easy one. In some cases modifications can be made to the software through the resource files it processes as data, and in other cases new libraries can be linked in and operated from existing callbacks, but often it is necessary to modify (and thus have access to) the source code to make some desired changes. Even when it is possible to do this, it is dangerous to do so, since modifying code in the huge single programs that form the basis of most of these packages is liable to result in unanticipated "side effects" that cause existing functionality in the program to break or to behave in a different manner than before. Another major problem is that often a scientist who is working with a large seismic analysis program written in the C programming language, for example, will want to implement a processing routine that is written in Java or some other language. Although software programs can be constructed to invoke routines written in one language from main programs written in another, the process is not so straightforward that a scientist or data analyst could rig it together in short order as an improvised addition to the analysis of a specific event. Scientists who are running a program like *geotool* that is intrinsically hard coded with calls to a particular graphics platform (in this case, Motif) are furthermore constrained to work within a particular operating system such as UNIX and therefore cannot take advantage of seismic analysis codes written to run on another platform such as Windows. To overcome these problems associated with adding functionality to large software systems for seismic analysis, we have decided to take a different approach to constructing the reference event analysis system. Instead of augmenting an existing large program, or writing a new one that would be more nearly comprehensive but that would itself eventually become inadequate when future research results in new analysis algorithms and new software tools, we have chosen to implement a distributed architecture that will permit existing code as well as new code to be invoked remotely from the large programs currently used for seismic analysis.

The distributed system architecture that we have investigated during the recently concluded proof-of-concept phase is based on CORBA, a technology that was developed in the mid-1990s for client/server data communications between desktop computers and corporate mainframes. Our scheme for implementing CORBA as the backbone for a distributed seismic analysis software system is illustrated in Figure 1. We are using the C-language program *geotool* as the server software, running under the Linux operating system, and for the proof of concept, we have used a simple Java program called "WaveformViewer" as a client application, running under the Windows 2000 operating system on a separate computer within the same local area network (LAN). As its name implies, WaveformViewer does little more than display waveforms using Java graphics, but it does offer a limited functionality, such as digital filtering, that will suffice to demonstrate how the reference event analysis system should work. WaveformViewer is, in fact, assembled from only a few of the many Java classes that make up a much more comprehensive seismic analysis system (Henson *et al.*, 2000), but rather than use that full system, thereby linking together two large programs that offer many duplicate capabilities, we wish to show how a single server can drive data analysis by communicating with a number of small client programs, each of which perform only a small number of particular tasks, perhaps only a single function. This is the system design that we intend to implement in the reference event analysis system.

As is shown in the diagram in Figure 1, we have modified *geotool* by adding new callback functions that allow it to communicate with an ORB. (Since *geotool* is running under Red Hat's distribution of Linux, we can make use of the open-source ORB known as "ORBit" that is bundled as a part of the distribution. For a *geotool* server running instead under Solaris, we could use one of a number of commercial ORBs for UNIX.) Using the X Resources file for *geotool*, we can then add a new pull-down menu item that will allow the user to send data to our client program, WaveformViewer. To expedite the process (external to *geotoo*l) of setting up the data connection, we have written a utility called "CORBA Center" that effectively acts as a switchboard for choosing a server side and a client side of the data flow. This utility registers the IP addresses with the CORBA Naming Service (to associate object references with symbolic names) so that the two programs can exchange data across the LAN as easily as if they were both running on the same computer. CORBA's data communication across the LAN takes place using the Internet Inter-ORB Protocol (IIOP). This is an official internet protocol (like FTP and HTTP) that allows an ORB on one platform to communicate with one on another platform. Note that it is irrelevant that the server-side software is in C and the client-side software is in Java, since IIOP is platform independent. We have modified the WaveformViewer client application by adding callback functions that allow it to communicate with a new "Agent" Java class, which, in turn, handles the communication with the ORB that is included within the Java platform under release JDK 1.2. The data messages that are exchanged through this client/server communication consist of seismograms and the metadata that describe them, in conformance with the standard CSS data schema (Carter *et al.*, 2001). To allow this communication, we have translated the CSS-schema data structures such as *.wfdisc*, *.arrival*, *.origin*, etc., into CORBA's Interface Definition Language (IDL). An IDL routine does not know whether the application with which it is communicating is written in C or Java (or one of several other languages). All it knows is that the application on the other side of the data stream expects to receive a message conforming to a particular IDL argument list, and we have therefore translated all the standard CSS data tables into a single IDL interface so that we can re-use that same interface for as many different *geotool* client/server applications as possible.

Figure 2 shows a server-side view of how this system can be used in practice. Once the program "CORBA Center" has been run to specify that *geotool* on the Linux computer will be a server and that WaveformViewer on the Windows computer will be a client, the data analyst starts up *geotool* in the normal manner. To make it readily apparent on the screen what is happening within the client/server data flow, in Figure 1 the analyst has used *geotool*'s own data-processing functionality to apply a high-pass filter to two seismograms. Those two seismograms are thus now different within *geotool* from the versions that were read in from the disk file, and (depending on what processing was applied) perhaps they are no longer correctly described by the CSS-schema tables residing in the database. The analyst will now use a new menu item that we have added to *geotool* to send to the client whichever seismograms are selected on the screen. In this case we shall send to WaveformViewer five seismograms, including the two that we have changed within *geotool*. These waveforms will be sent to the client directly from memory, so the analyst will not have to write the new waveforms to disk, then store new CSS-schema tables in the database, and then send those new disk-resident data to the Windows computer via FTP, where they would next have to be written to that computer's disk and finally read in by WaveformViewer. Instead, the data are sent directly between the programs through the IDL interfaces. This is in effect a client/server RPC, but it is considerably easier to implement using the high-level CORBA architecture than it would be by using a low-level interface such as code for sockets.

Figure 3 is a screen shot from the Java program WaveformViewer running on the Windows platform, showing a callback we have added that displays the *.wfdisc* description of the waveforms received through the IDL interface, just as if they had been read from the disk. The analyst can select which seismograms to display within the Java-graphics WaveformViewer display (which mimics the Motif waveform display used by *geotool*), and in this case we choose to display all five waveforms. In Figure 5 the analyst has applied WaveformViewer's own filtering routine to apply a different high-pass filter to two of the seismograms that were received from geotool as unfiltered waveforms. The analyst will then use a menu item we have added to WaveformViewer to send data back to the server program. Figure 5 shows that the waveforms newly modified by WaveformViewer are indeed now present within *geotool*. The whole process is as simple for the analyst to use as it would be if all the digital filtering had been performed within *geotool* itself. All that is required is to make a few mouse clicks, just as if WaveformViewer were simply a function that is part of *geotool* instead of its being in fact a separate program, written in a different language, running on a different computer and under a different operating system.

This proof of concept demonstrates that a distributed software architecture built using CORBA can form the basis of a reference event analysis system. Instead of having a single huge program, which is hard and/or dangerous to modify, as the tool to use for identifying and characterizing reference events, it is possible to modify *geotool* (or ARS, or SAC, etc.) to be used as a data server and then to perform the actual seismic analysis externally to *geotool* by using a host of separate applications, including both existing code and programs yet to be written, running on whatever platform is most appropriate. In particular, the analyst should be able to use seismic data centers and supercomputers located at remote facilities accessible via the Internet, just as if those capabilities were offered by the server platform itself. The data communications should be performed as easily as possible without requiring the analyst to go through intermediate steps of creating, exporting, and importing temporary files and database records. This flexibility will be required for the intensive study of reference events, where new algorithms not ordinarily used for routine seismic analysis may be required in order to perform specialized investigations in individual cases. The analyst should be able to select which programs to run, and in what order to run them, and in many cases it may well be necessary to construct new programs. The analysis programs that run as client applications should perform only one or two specific tasks, and they can be written to perform only those particular functions without reproducing all the overhead capabilities for data management that are required by the server program.

The example that is illustrated in Figures 2 – 5 should serve to demonstrate the need for certain features in a distributed processing architecture that are not conventionally part of a software system like *geotool* that runs as a single program on one computer (albeit within multiple windows). In Figure 2 data channels 6 and 8 are unfiltered, in Figure 4 they have been filtered by the client application, and in Figure 6 they have been returned to the *geotool* server in their filtered form. What, then, should the *geotool* server program do with the unfiltered versions of these channels, which, of course, are still resident in the program's RAM, and are still displayed on the Linux computer screen, once the client program is ready to send the filtered versions back to the server? Should the process of returning the filtered data from the client automatically cause the server to delete the unfiltered data? Should the *geotool* window instead now display the presence of two different versions of these waveforms, and if so, should it change the waveform identification label *.wfid* to reflect that there are now two different waveforms for the same time windows on these particular data channels? Should the return of the filtered data from the server be blocked until the analyst has hit a "receive" button in *geotool* indicating that the original data should now be overwritten? (Blocking the transmission of a data message from the client until the server specifies that it is ready to receive it makes the data stream function in many ways like an Instant Messenger service such as AOL IM or ICQ.) What happens if the data analyst sends the unfiltered data to one client application for filtering and then chooses to send those same data to a different client program for some other processing, such as polarity reversal, *before* the first client program has returned its results? Clearly, the distributed processing architecture presents a number of issues related to the data's referential integrity, versioning, and configuration management. Establishing and enforcing policies for handling these issues will be an important part of the design of the reference event analysis system.

It is also clear that the system must use some sort of metadata audit trail for tracking the distributed processing. Regardless of whether the unfiltered data are deleted from the server's memory and screen display when the filtered data are returned from the client, how will the system distinguish between the filtered waveforms and the original ones that reside on the disk? In the particular case of the interactive WaveformViewer client application, the analyst was required to input the filter parameters by using a GUI, so it is known (at least by the analyst, if not by *geotool*) what sort of filter was applied. In general, however, it is far more likely that the client code will run automatically, and the analyst will have no knowledge of the exact parameters that govern the algorithm implemented by the client

program, which, after all, is likely to be running on a different computer, perhaps even at a different facility. The client must therefore return not only the processed data but also a metadata message describing just what operations it performed and the parameters it used. The server must construct a database archive of these metadata records as a tool to use for the data versioning and configuration management so that any one or all of the data processing routines executed by the distributed client applications can later be repeated or undone.

Finally, although our work has shown that CORBA can be used as the backbone for the reference event analysis system, we have now begun an investigation into the use of an alternative technology. Within the last year the software industry has begun to move from using CORBA for client/server applications to an Internet- or Intranet-hosted approach based on Web services. This technology relies on Web servers, rather than ORBs, for data communications, and the data (including SOAP's RPC invocations to process the data) are sent as XML messages via HTTP rather than as binary data sent via IIOP. There are a number of advantages to this approach. Because XML messages are alphanumeric data, they can be sent through firewalls more easily than can binary data (although more bandwidth is required). XML and SOAP are easier to use than CORBA (even though we have made that process easier by the construction of the "CORBA Center" program that facilitated the *geotool*-to-WaveformViewer connection). Because XML is just alphanumeric data, it is truly platform independent. In particular, it is quite difficult to use CORBA to communicate with applications that are running under Windows as native code (as opposed to applications like WaveformViewer that run under Windows but within Java's own platform), since the standard Windows platform uses the Component Object Model (COM), which is incompatible with the CORBA object model. Software bridges can be constructed, but the process is difficult. XML bypasses this problem, and so Web services that are developed for UNIX work perfectly with those that are developed for Windows. Microsoft has made the construction of Web services especially easy by now replacing COM with a new platform called ".NET" that automates much of the use of SOAP. We feel that this platform will be an important one, and the reference event analysis system should be able to make use of it. Using XML as the basis for data communications has further advantages, including the fact that in a real sense, XML is itself metadata. Database vendors are therefore making sure that new releases of their software can store and transmit XML. We feel that this would be a good approach for constructing the metadata archive that will be an important component of the planned system.

CONCLUSIONS AND RECOMMENDATIONS

We conclude that the best system architecture for a reference event analysis system is likely to be one that is based on distributed stand-alone software components (which can all be on the same computer or distributed across a network) rather than on a single large program. Our proof of concept study has shown that CORBA technology can be used to connect a server program for seismic analysis (like *geotool*) to client programs developed for specialized applications, even if they are written in other languages and run under different operating systems. We recommend, however, that Web services technology be investigated thoroughly as an alternative to the use of CORBA as the backbone for the distributed processing. We shall implement that recommendation during the next phase of work, and then we shall begin incorporating both existing and new programs into that distributed processing system

REFERENCES

Carter, J., R. Bowman, K. Biegalski, J. Bohlin, M. Fisk, R. Carlson, W. Farrell, B. MacRitchie, and H. Magyar (2001), IDC Documentation Database Schema Revision 3, Center for Monitoring Research User Guide on-line document (available at http://www.pidc.org/librarybox/idcdocs/downloads/511r3ab.pdf).

Goldstein, P. (1998), SAC Tutorial Guide for New Users, Lawrence Livermore National Laboratory report UCRL-MA-112836 (available at http://www.llnl.gov/sac/).

Henson, I. (1993), The *geotool* Seismic Analysis System, in: Proceedings of the 15th Annual Seismic Research Symposium 8-10 September 1993, Phillips Laboratory report PL-TR-93-2160.

Henson, I., R. Wagner, and W. Rivers (2000), Automated Seismic Event Monitoring System, U.S. Nuclear Regulatory Commission report NUREG/CR-6625.

Wang, J. (1996), Analyst Review Station's User Manual, Science Applications International Corporation report SAIC-96/1100.

Young, C. (2001), MatSeis User's Manual, Version 1.3, Sandia National Laboratories on-line document (available at http://www.nemre.nn.doe.gov/nemre/data/matseis/matseis_manual.pdf).

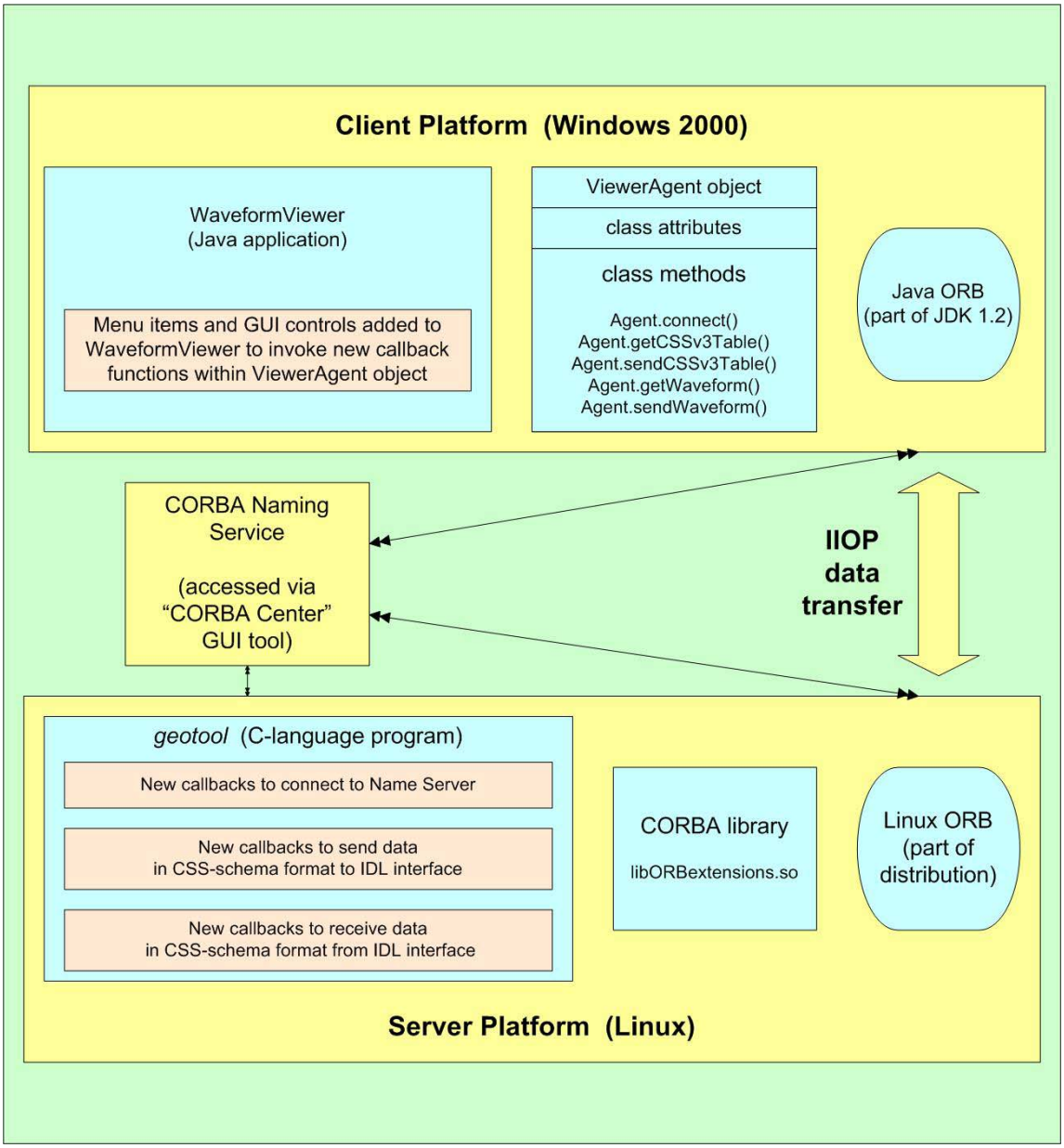

Figure 1. Using CORBA to enable client/server data communications between the C-language program *geotool*, running as a server on a Linux platform, and the Java program WaveformViewer, running as a client application on a Windows 2000 platform. The data communication takes place between the Object Request Brokers on each platform via the Internet Inter-ORB Protocol, which is an internet standard. We have modified the client code and the server code so that they link to CORBA, and that link can now be used to permit data communications between the sever and additional client applications that are invoked by the user through items added to the *geotool* pull-down menus. The data that are exchanged between the client and server programs are translated from the standard CSS database table schema to CORBA Interface Definition Language. We have written a utility called "CORBA Center" that makes it easier for the user to set up the client/server link (which requires the *geotoo*l server to register itself with the CORBA Name Server).

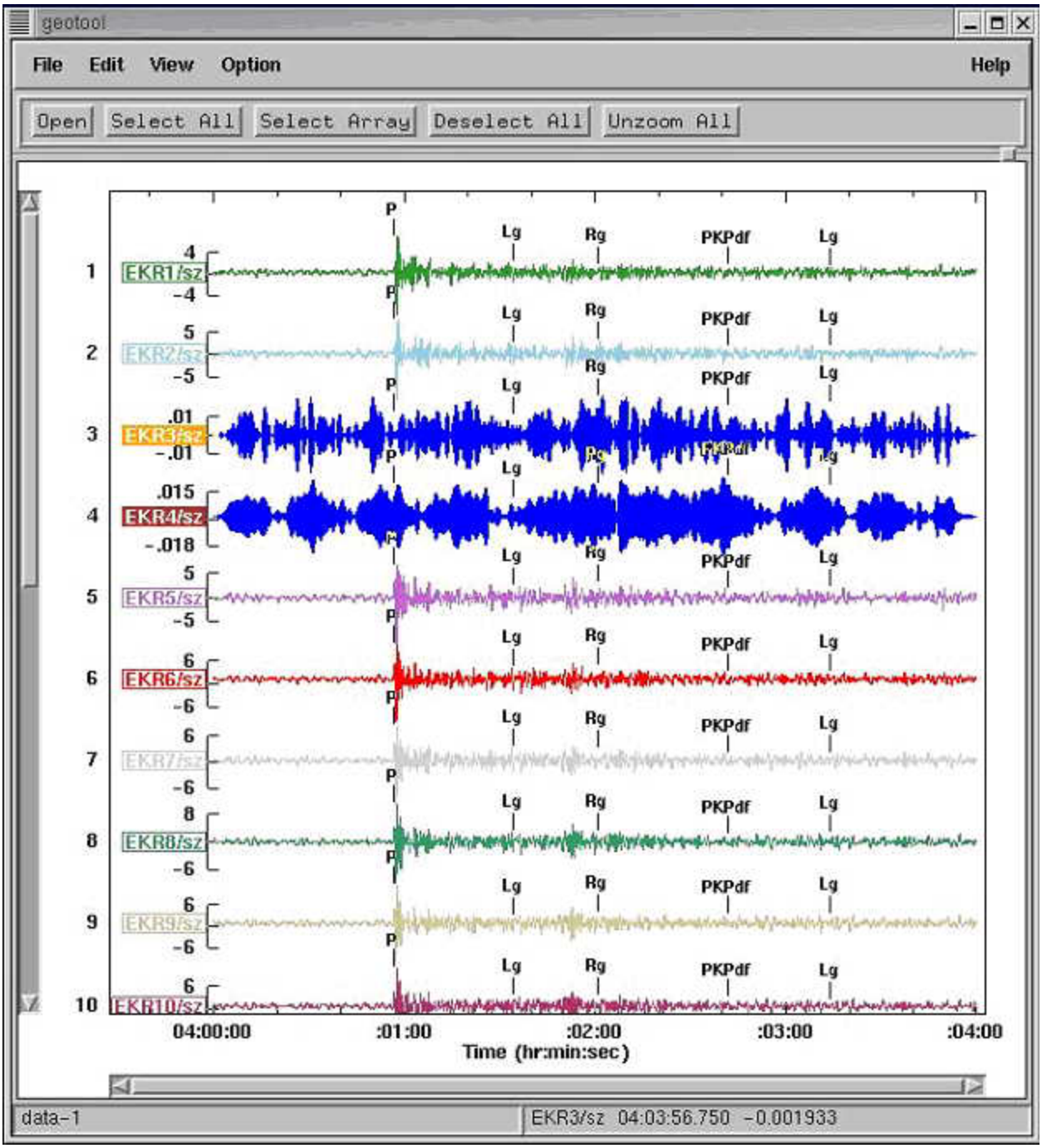

Figure 2. Screen shot of the C-language program *geotool* running on a Linux computer and displaying ten short-period vertical channels recorded by the seismic array EKA. The waveforms on channels 3 and 4 have been passed through a very high-pass filter by a Butterworth-filtering function in *geotool*. These two seismograms are therefore different in this screen image, and in the Linux computer's active memory, from the original versions that still reside on the hard disk. These two altered seismograms and the unaltered ones on channels 1, 6, and 8, along with the *.wfdisc* data structures that describe the seismograms, will be transmitted via CORBA to the Java-language program WaveformViewer running on a Windows 2000 computer. Rather than the disk-resident version of these waveforms, it is the memory-resident version, including the changes made within *geotool* by applying the high-pass filter, which will be transmitted from *geotool* to WaveformViewer.

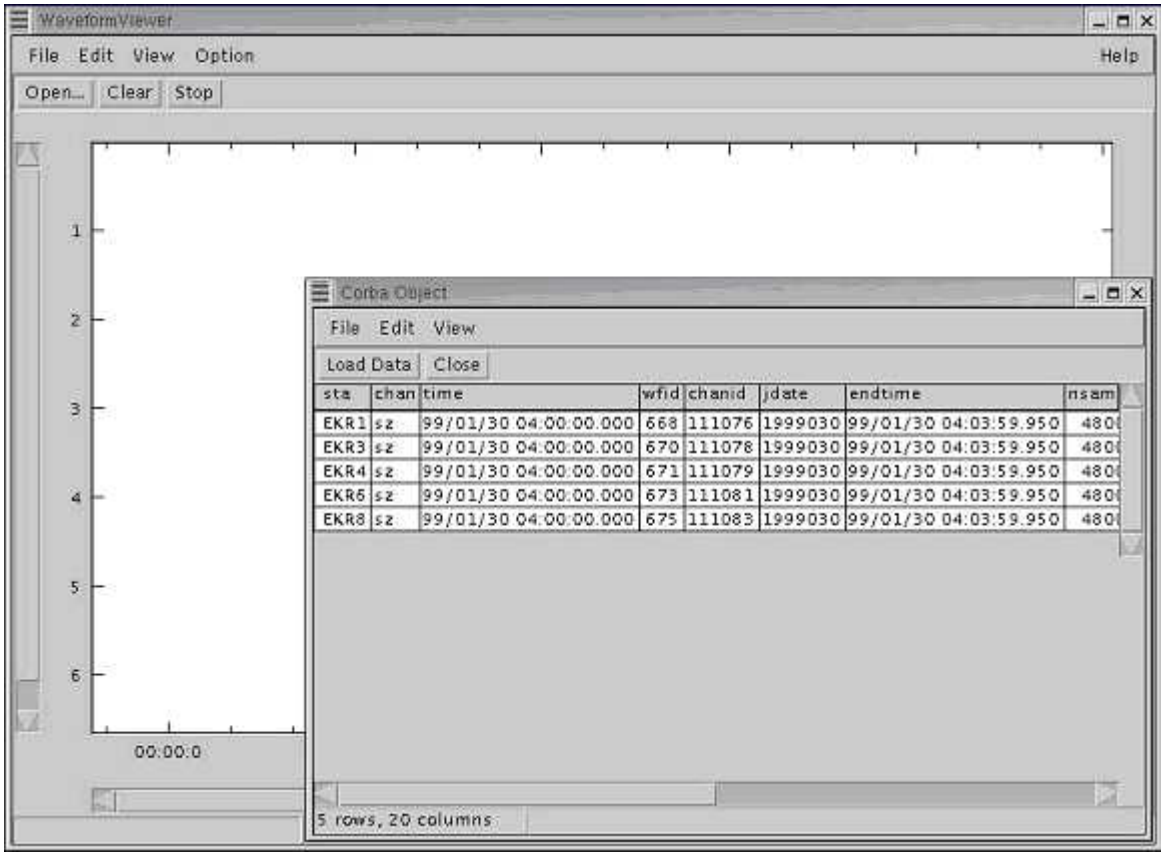

Figure 3. On the Windows 2000 computer running the Java-language program WaveformViewer, the CORBA connection causes a window to pop up that displays the *.wfdisc* record that was sent across from *geotool* on the Linux computer. From that pop-up window, the user selects which waveforms to display. We shall choose to display all five channels that were exported from *geotool*.

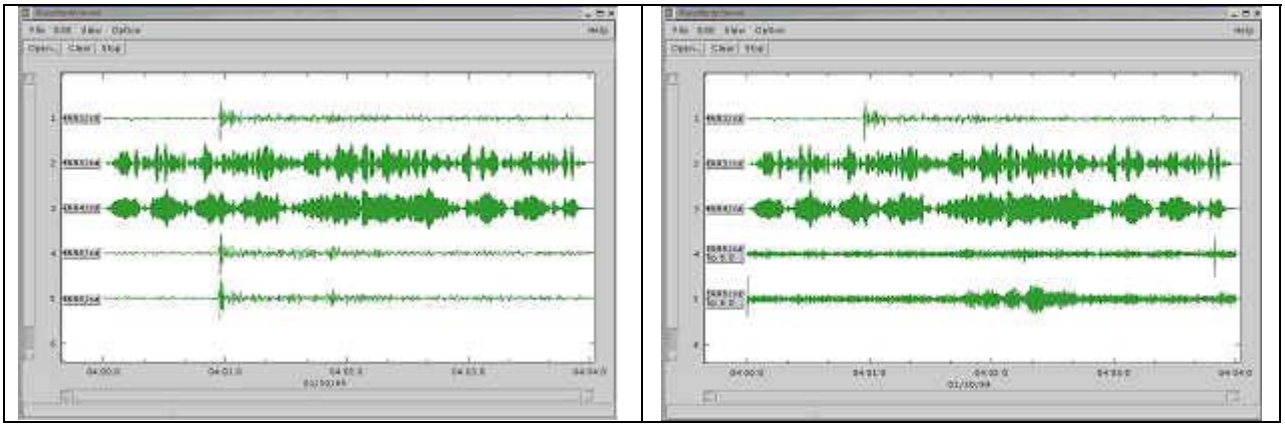

Figure 4. (a) Waveforms imported into WaveformViewer from *geotool*. Note that two of the waveforms reflect the filtering applied by *geotool* and thus show that they have been sent to the Windows computer directly from memory on the Linux computer and not from the disk files. (b) The bottom two waveforms in the display (channels 6 and 8) have now been filtered with WaveformViewer's own Butterworth high-pass filtering routine. A different bandpass was selected in WaveformViewer than in *geotool*, so we can recognize which waveforms were filtered by which program. The waveforms filtered by the WaveformViewer client program will now be sent back from Windows to Linux via the CORBA connection so that they can be displayed within the *geotool* server program.

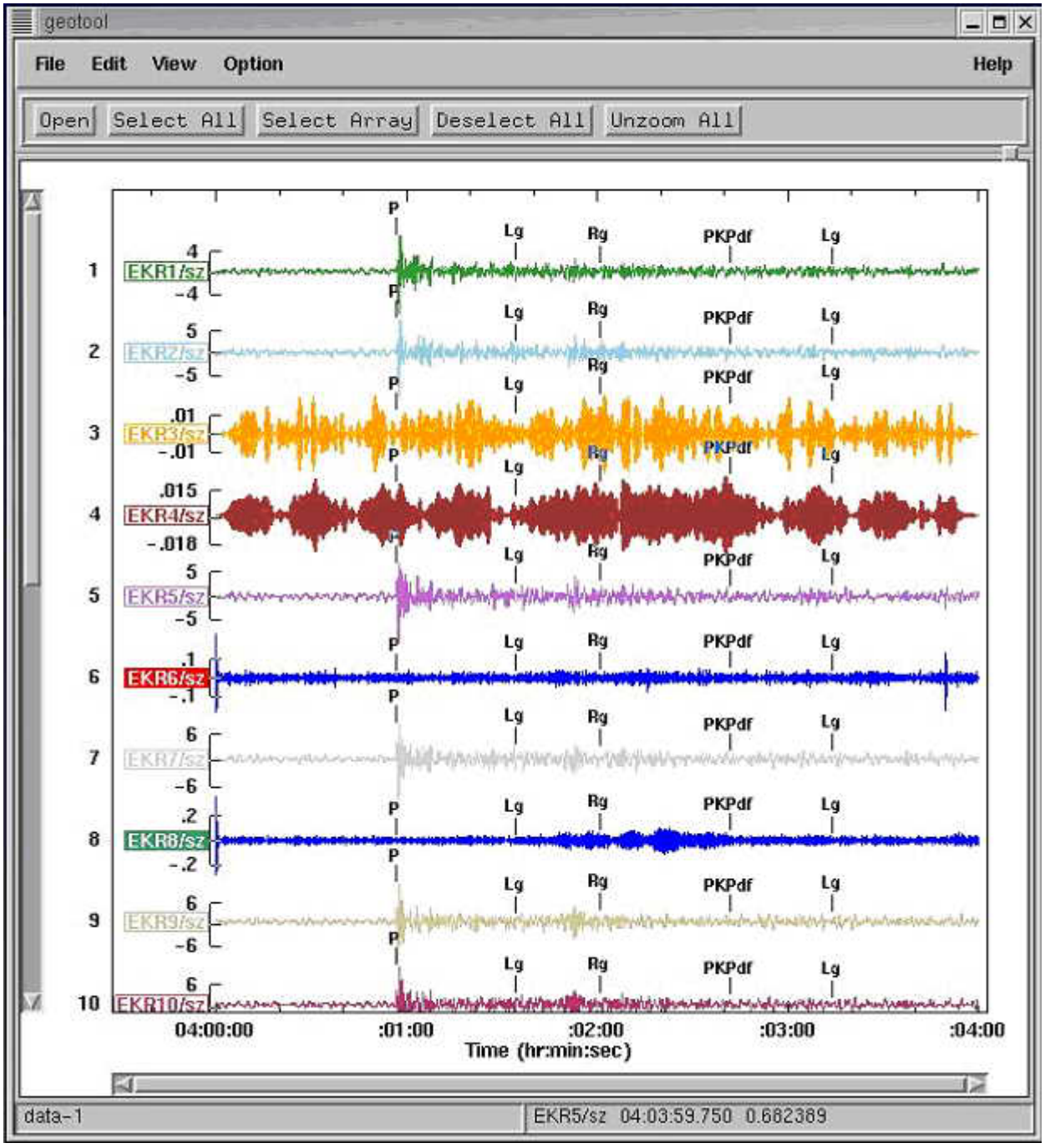

Figure 5. The waveform display that has been running within the *geotool* server program running under Linux is now updated with the seismograms for channels 6 and 8 that were filtered by the WaveformViewer client program running under Windows 2000. Just as with the data transmission from the server to the client, the data that were transmitted back were sent dynamically from the computer's memory rather than being written out as disk files. The whole process shows how a filter could be applied in the reference event analysis system: the data analyst can apply either a filter using a routine that is part of *geotool* or a filter that is part of a separate application (in this case, one written in Java and running on a different computer under a different operating system). This demonstrates the technical feasibility of constructing a reference event analysis system by using CORBA to link stand-alone seismic data analysis programs that are distributed across a network.

IMAGERY ASSETS FOR SUPPORTING NUCLEAR EXPLOSION MONITORING RESEARCH AND DEVELOPMENT

Michael Skov, Benjamin Kohl, and Robert L. Woodward

Science Applications International Corporation

Sponsored by Defense Threat Reduction Agency

Contract No. DTRA01-99-C-0025

ABSTRACT

The Defense Threat Reduction Agency's (DTRA) Center for Monitoring Research (CMR) maintains a wide range of technical capabilities to support nuclear explosion monitoring research and development. Within the CMR the Research and Development Support System (RDSS) operates as the vehicle to both digest and distribute data and research results of value to both DTRA authorized researchers and the general research community, in particular providing access to processed commercial imagery.

In recent years, commercial products, such as the 1-m-resolution panchromatic products of IKONOS, have enabled the nuclear explosion monitoring research community to benefit from satellite-based imagery acquisition systems. CMR maintains a library of imagery products ranging from the recently acquired, freely available (www.visibleearth.nasa.gov) low-resolution (1-km) composite images of the entire Earth, to 4-m multispectral and 1-m panchromatic (IKONOS) images of selected regions. Supplementing the high-resolution imagery products are 10-m panchromatic (SPOT) and 30-m multispectral (Landsat) images. Even higher resolution (0.7-m) commercial services (Digital Globe) are becoming available and high-resolution images will be acquired by the CMR to extend current holdings.

Within the CMR, research is conducted to determine methodologies for integrating enhanced event location and characterization techniques for nuclear explosion monitoring systems. One aspect of this effort is the utilization of imagery products to provide geographic context for event solutions, and, in some cases, to validate event location hypotheses.

The RDSS makes available selected imagery holdings via http://www.cmr.gov/rdss . Assets include interactive Portable Document Format (PDF) files of annotated images of Novaya Zemlya, Russia; Lop Nor, China; Pakistan; and India. Other imagery assets may be made available to the research community subject to the license agreement of the imagery vendor.

OBJECTIVE

The Defense Threat Reduction Agency (DTRA) sponsors the Center for Monitoring Research's (CMR) effort to improve nuclear explosion monitoring. Within the CMR, the Research and Development Support System (RDSS) (Woodward and North, 2002) supports the DTRA PRDA and general R&D communities with assistance ranging from data and research product dissemination to integration and testing of research and development results. Also within the CMR, the Technical Verification and Analysis Support project provides an environment to demonstrate nuclear explosion monitoring advances applied to generalized conditions. More focused efforts, such as the Lop Nor Advanced Concept Demonstration (Kohl *et al*, 2002), provide environments to develop, integrate and demonstrate advanced techniques applied to specific nuclear explosion monitoring regimes. Despite the broad scope of CMR activities, one common component is the application of imagery assets to the nuclear explosion monitoring research and development effort.

RESEARCH ACCOMPLISHED

The CMR maintains an assortment of imagery products to support research and development. Products range in scale and scope from high-resolution (1-m) geographically registered images (IKONOS) of small regions (~100 sq. km per scene) to low-resolution (1-km) composite images covering the entire Earth. The CMR employs these assets in a variety of ways, including validation and refinement of ground truth locations, event analysis and context visualization, and site identification. Additionally a selection of the imagery assets has been annotated and packaged as interactive Portable Document Format (PDF) documents for use by the general R&D community. In the sections below, each of these areas will be described, and we will close with a summary of planned imagery acquisitions.

Imagery to support ground truth

Many R&D efforts rely on the existence of well-located reference events. Such events, categorized by their absolute location uncertainty in kilometers as GT1 (ground truth, 1 km), GT2, GT5 and so on, are highly valuable for the establishment of regional travel-time corrections and for use as master events when applying Joint Hypocentral Determination (JHD) and Master Event Location techniques. Fisk (2002) demonstrates the advantage of applying high-resolution imagery to the task of establishing ground truth for nuclear explosions at the Lop Nor, China nuclear weapons testing facility.

CMR imagery assets covering the tunnel (western) and vertical-borehole (eastern) areas of the Lop Nor facility were analyzed for surface features associated with nuclear explosions. Features such as adits, boreholes, roads, and structures were identified. Subtler features, such as erosional characteristics, were utilized to establish the relative age of the surface features. Using these features, Fisk (2002) determined precise locations for three nuclear explosions. Using these three events as master events, eight other explosions were relocated. Semi-major axis error estimates for these events were less than about 0.65km. Event locations could be associated with observed features to provide an absolute accuracy of 300 m or less – the registration accuracy of the satellite imagery.

Figure 1 demonstrates the clarity of surface features visible in the tunnel region of the Lop Nor facility. The image is a panchromatic (1-m) sharpened, multispectral (4-m) image producing an approximately 1-m-resolution natural color image. This image, covering approximately ¼ of a square kilometer, highlights two (areas 'A' and 'B') of the four tunnel adits described by Fisk (2002). Also visible in the scene are numerous road and support structures. Figure 2 similarly displays the anthropogenic features associated with a portion of the vertical borehole region of the Lop Nor facility.

Using imagery to support the determination of ground truth locations, 11 nuclear explosions, detonated between May 1990 and July 1996 have been relocated and established as GT1 events. These events were utilized during the Lop Nor Advanced Concept Demonstration (Kohl *et al*, 2002) to illustrate the advantage of employing Master Event Location techniques to locate small (mb 2.5-3.5) events.

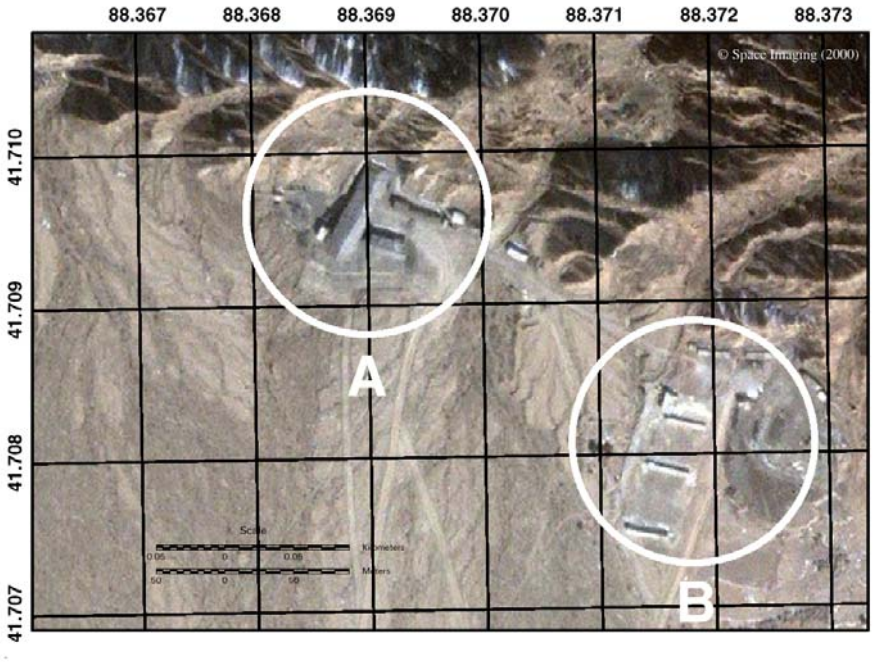

Figure 1. IKONOS imagery from CMR's collection showing two tunnel adits in the Lop Nor complex. The regions labeled 'A' and 'B' correspond to tunnel adits 'A' and 'B' as described by Fisk (2002).

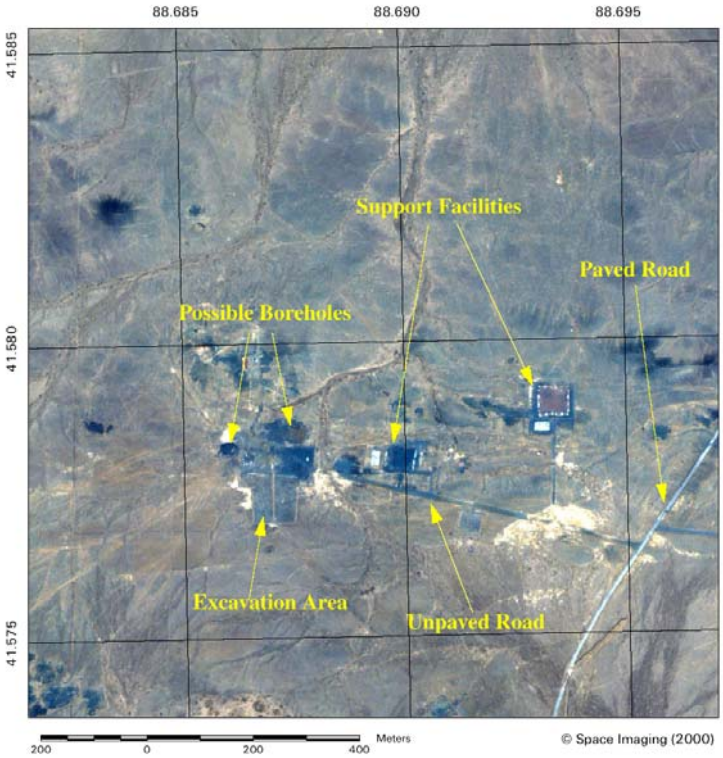

Figure 2. Surface features associated with vertical borehole emplacements in the Lop Nor complex. The IKONOS imagery was acquired, processed and archived by CMR analysts; the annotations are from Fisk (2002).

Imagery to support event analysis and context visualization

Satellite imagery can provide a rich backdrop for conveying information relevant to event analysis or to an event location. High-resolution images such as those shown in Figures 1 and 2 are often required to identify small-scale surface features associated with an event. In some situations, however, broader coverage is desired. Figure 3 shows the Novaya Zemlya, Russia region including several hypothesized locations for a February 23, 2002, seismic event. Also shown, for additional context, are the locations of several historical events of interest (blue triangles) and of underground nuclear explosions (red stars). The larger coverage area provides better visual clues as to the separation of this event from known nuclear tests and places the event in the overall geographic context. Displaying larger coverage areas is neither technically practical nor financially feasible using high-resolution products such as IKONOS. Figure 3 is based on lower resolution (~40 m) MODIS imagery freely available from NASA's Earth images web site (http://visibleearth.nasa.gov).

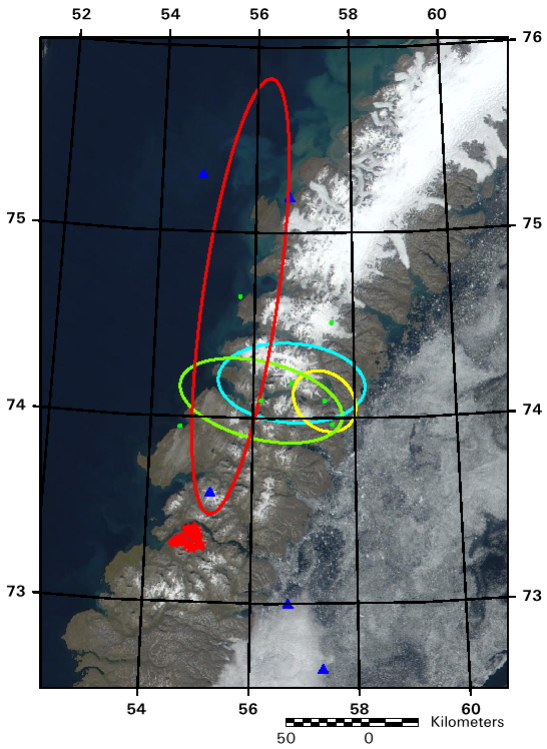

Figure 3. NASA MODIS imagery of Novaya Zemlya, Russia (http://visibleearth.nasa.gov).

NASA maintains a substantial catalog that CMR staff utilize to identify images of potential value to nuclear explosion monitoring research and development. Also available from NASA (http://visibleearth.nasa.gov) are low-resolution (1-km) composite images covering the entire Earth. CMR has acquired this collection of images and is currently assembling relevant regional composite images.

CMR's usage of imagery also includes sophisticated visualization techniques such as imagery draping. Figure 4 illustrates the technique. The region shown in Figure 1 is draped over digital terrain elevation data to produce a three-dimensional (3-D) transformation of IKONOS imagery. This specific example shows non-exaggerated surface elevation features associated with two of the adits in the western portion of the Lop Nor, China, nuclear weapons testing facility. Of particular note is the extent of the overburden provided by the ridge. The extent and relative isolation of the overburden is further illustrated through the creation of "flyby" animations. Two such animations were constructed to support the Lop Nor Advanced Concept Demonstration (Kohl *et al*, 2002). One such animation toured the western tunnel region; the second illustrated the features around the vertical borehole complex in the eastern portion of the Lop Nor facility.

Figure 4. IKONOS imagery of the region shown in Figure 1 draped over terrain data.

Imagery for site identification

Supporting the efforts of ground truth determination and event context visualization is an effort to maintain imagery holdings for regions of particular interest. Recent imagery acquisitions can obviously aid research and development by providing the most up-to-date view possible of surface features in a region of interest. However, other benefits, such as resolving surface features obscured by clouds or shadows, can also be realized through routine acquisition of imagery.

Most sites of interest are best imaged by acquisitions in mid to late summer. These times provide high sun angles and minimize cloud and snow cover. For this reason, most images commissioned by CMR have acquisition dates of July, August, and September (images of sites in the northern hemisphere dominate current holdings). The subtle changes in acquisition date and time can be beneficial for altering sun angles, but often the more overt changes seen year-to-year are the most interesting.

Identification of changes can be highly valuable for tasks such as establishment of ground truth. Fisk (2002) used substantially more subtle features, such as relative erosional characteristics, to establish the relative age of various components of the Lop Nor, China, facility. Clear changes observed in sequential images, such as those illustrated in Figure 5, can provide substantially better temporal information than can be inferred by interpretation of erosional features. The region highlighted with the white box in Figure 5 illustrates the substantial development that occurred in the 14 months between the acquisition dates of July 2000 and September 2001 of high-resolution (~1 m) IKONOS imagery and illustrate the advantage of maintaining and refreshing imagery holdings.

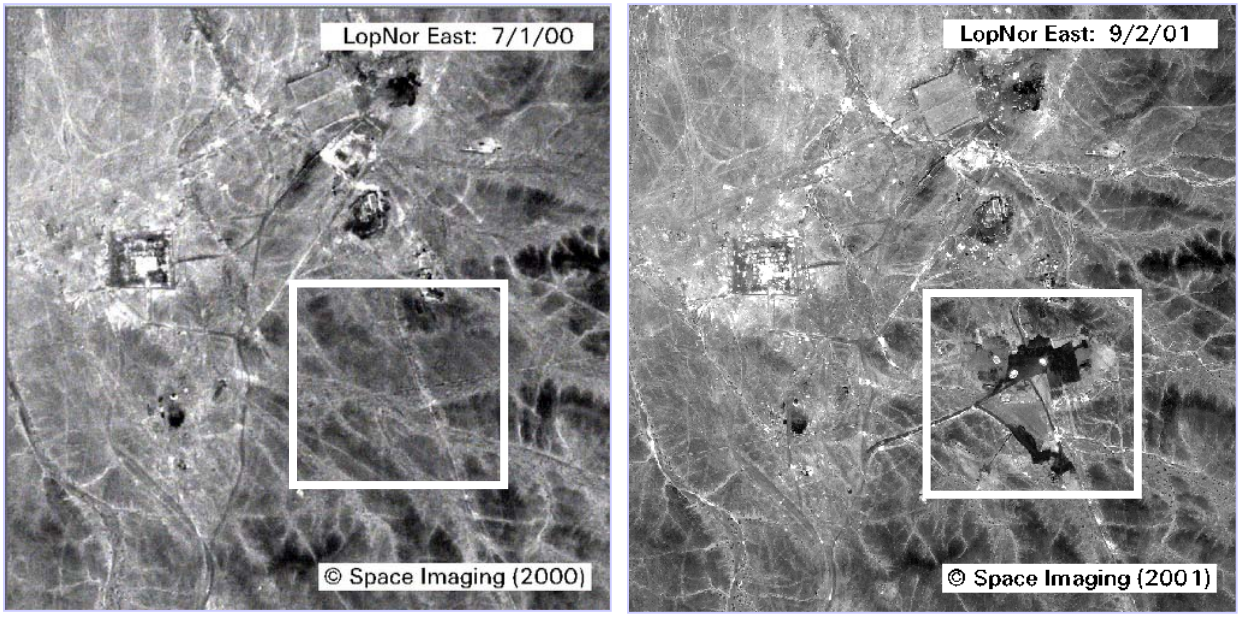

Figure 5. Two IKONOS images of Lop Nor, China taken approximately 14 months apart illustrating the substantial observable changes occurring at the site.

Detailed analysis of the changes has not been conducted; however, current plans include the acquisition of higher-resolution (~0. 7-m) Digital Globe imagery for this site in 2002. A more detailed study may be initiated pending the initial analysis of new imagery and a determination of need.

Imagery for the research community

CMR provides annotated satellite imagery products for use by the research community. Subject to the end user license agreement of the image provider, selected imagery is packaged in PDF format and made available from the RDSS portion of the CMR web site at http://www.cmr.gov/rdss . The PDF documents provide mechanisms to zoom on features of interest and navigate the region. Figure 6 shows a snapshot of the portion of the RDSS web content that provides a high-level view of the Novaya Zemlya, Russia, region. Annotations include structures, roads and rivers, as well as features more directly related to nuclear weapons testing, such as tailings and subsidence craters. The images viewable directly on the web site are reduced resolution; however, the PDF format documents available for download provide full resolution versions of the imagery.

Currently available imagery includes a mosaic of three images of Novaya Zemlya, Russia, (Figure 6), two images of Lop Nor, China, showing both the tunnel and vertical borehole regions, one image of the site of the May 5, 1974, and May 11, 1998, underground nuclear tests in India, and two images of the test facility in Pakistan, including the site of the May 28, 1998, underground nuclear test. Each of these is available via the CMR web site. Also available are examples of typical features associated with nuclear weapons testing, such as support infrastructure and collapse features. The main entry point for the CMR web site may be accessed at http://www.cmr.gov .

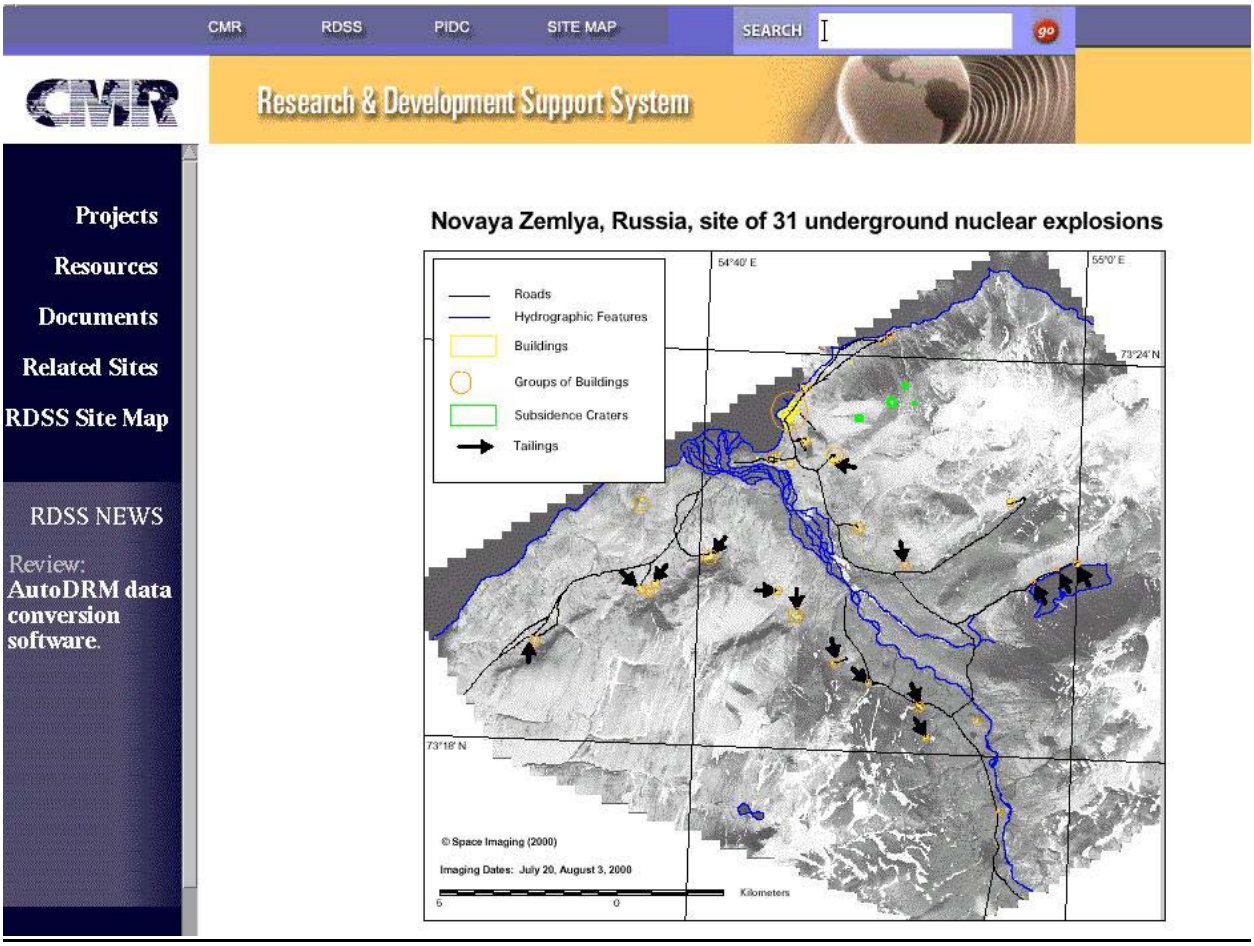

Figure 6. Screenshot of a portion of the CMR web site showing one of the images (Novaya Zemlya, Russia) available from the RDSS.

Planned 2002 acquisitions

As of this writing, the Technical Verification and Analysis Support component of CMR has initiated imagery acquisitions for 2002. Pending the outcome of the price quote process, CMR is considering new acquisitions for four regions of interest. For all sites, CMR is considering the acquisition of higher-resolution panchromatic (0.7-m) Digital Globe products. Multispectral images may be acquired for selected sites. Two images covering the Novaya Zemlya, Russia, test facility are being considered. Three new images of the Lop Nor, China, region are being considering, including one of the western (tunnel) area, one of the eastern (vertical borehole) area including the altered region identified in Figure 5, and possibly an image of the region southwest of this complex where two tests are reported to have been conducted many years ago. Also under consideration are updates to the imagery holdings for India and Pakistan.

CONCLUSIONS AND RECOMMENDATIONS

CMR's imagery acquisition program has proven a valuable aid to efforts such as the establishment of ground truth locations and for the visualization of research and development results. Additional, commercial, high-resolution imagery will be acquired on a periodic basis to ensure CMR's imagery holdings remain current. These commercial products will be supplemented with freely available products whenever possible.

ACKNOWLEDGEMENTS

The authors would like to thank Mark Fisk for providing a pre-publication version of his upcoming paper describing the use of satellite imagery to establish ground truth locations. Many thanks to Brenda Zuzolo for her continuing work to acquire, register, catalog, and interpret imagery products for CMR. Special thanks to Elizabeth Eaton of SAIC's Imagery Central (http://www.imagery-central.com), who provides continuing logistical support for CMR's commercial imagery acquisition program. Finally, the authors would like to recognize the effort and support of the Defense Threat Reduction Agency and of the Nuclear Treaty Program Office.

REFERENCES

Fisk, M. D. (2002), Accurate Locations of Nuclear Explosions at the Lop Nor Test Site Using Alignment of Seismograms and IKONOS Satellite Imagery, in press, *Bull. Seism. Soc. Am.*

Kohl, B., R. North, J. R. Murphy, M. Fisk, and G. Beall (2002), Demonstration of Advanced Concepts for Nuclear Test Monitoring Applied to the Nuclear Test Site at Lop Nor, China, *24th Seismic Research Review*, September 17-19.

Woodward, R. L. and R. G. North (2002), A Support System for Nuclear Explosion Monitoring Research and Development, *24th Seismic Research Review,* September 17-19.

THE GNEM R&E SPATIAL DATA INTERFACE

Lisa K. Wilkening, Matthew N. Chown, and Bion J. Merchant

Sandia National Laboratories

Sponsored by National Nuclear Security Administration
Office of Nonproliferation Research and Engineering
Office of Defense Nuclear Nonproliferation

Contract No. DE-AC04-94AL85000

ABSTRACT

In the course of developing contextual data products for the Ground-based Nuclear Explosion Monitoring Research & Engineering (GNEMR&E) program, a need for rapid spatial analysis of seismic events has been realized. To this end, Sandia National Laboratories is working to develop a Spatial Data Interface (SDI) application, which will assist in the identification of these events. The SDI is supported by contextual data and reference seismic information produced by the GNEM R&E program.

The Spatial Data Interface is designed to be a generic application, which can be accessed from any of the GNEM monitoring tools (ArcView, the MatSeis package and associated regional seismic analysis tools, etc.), and which could be accessed by processes within an automated event monitoring pipeline. Contextual data is stored in a relational database, Oracle, and is accessed via an Environmental Systems Research Institute (ESRI) software package, ArcSDE. A suspicious seismic event may be submitted to the SDI, which in turn evaluates the event against a set of criteria using reference contextual data. These criteria consist of a set of spatial queries, which are the basis upon which an event may be tagged for further analysis or dismissed.

OBJECTIVE

The objective of the Sandia National Laboratories (SNL) Spatial Data Interface (SDI) is to provide a generic interface designed to enhance the processing of seismic events, which can be used either in automated or interactive processing pipelines for treaty monitoring. An application using SDI will process these events through a series of spatial queries, specifically formulated to assist in their identification and analysis. SDI will be developed using an existing programming interface for ArcSDE, an Environmental Systems Research Institute (ESRI) product. This product facilitates rapid access and query functions for spatial data stored in an Oracle database. It can take advantage of the availability of contextual and reference information properly stored within a database, and complement the capabilities of existing tools, data sets, and infrastructure.

RESEARCH ACCOMPLISHED

Introduction

Meeting the GNEM R&E program monitoring goals implies the detection, location, identification, and characterization of possibly hundreds of seismic events daily. Automated processing procedures are in place to perform this duty. As an event moves through the automated system, various software applications are accessed, which draw upon reference information stored in Oracle databases and flat files on the operating system.

Occasionally, a suspicious event is detected. An automated monitoring system may have embedded logic with which it can determine the priority of this event. This logic is based on select criteria, coupled with existing reference data sets. An event may then be dismissed as irrelevant to the monitoring mission, or tagged for further seismic analysis.

Development of the SDI is intended to enhance the automated system processing of questionable events by referring to spatially referenced datasets. Most applications support special event identification, but are somewhat limited. By incorporating access to additional detailed spatial data and enhanced query logic, monitoring analysis may be more efficiently accomplished, providing robust results for event prioritization and reporting efforts.

Spatial Data Interface Application Development

The Spatial Data Interface will be prototyped using ArcSDE 8.2 (formerly SDE, Spatial Database Engine) from ESRI. ArcSDE is an interface, which resides on top of any supported relational database (in this case Oracle), and is capable of serving spatial data to different applications. Via ArcSDE, spatial data is loaded into Oracle where it is stored and managed as tables. This application will also take advantage of the Oracle Spatial extension for spatial data types. ArcSDE can either use these data types or provide its own mechanisms for managing the feature geometry (West, 2001). In addition, ArcSDE provides fast, flexible querying capabilities by spatially indexing the data features. These indexes can be fine-tuned for maximum performance in concert with the Oracle Spatial tuning guidelines.

The SDI application itself will be designed and implemented using ArcSDE's open, high-level C programming language API. The C API allows a developer to build a custom application for ArcSDE, incorporating many advanced geographic information system (GIS) functions for spatial querying (West, 2001). The C API is also the means by which all applicable ESRI software products access ArcSDE. This flexibility would allow the SDI application to be coupled with other customized GIS applications along the monitoring pipeline, such as ArcView GIS for graphic display of SDI results. The ArcView GIS application is customized using its own object-oriented programming language, Avenue, which also allows access to ArcSDE's functionality.

The SDI interface is intended to be generic and independent. Therefore, it could theoretically reside anywhere on the system and be called from any application providing that a valid interprocess communication interface is in place. The SDI will operate with minimal input from the user beyond some key information to initiate processing. This information can either be provided by the user via a GUI or can be contained in a message delivered to the SDI from another application. This information can include the error ellipse information for the event, point location information for the event, and a dataset of interest against which the spatial analysis will be made. A set of canned queries will be accessible for processing. The user will also have the ability to customize the query set or iterate the

process as necessary. A user may also elect to perform spatial analysis between any of the contextual datasets available, or against a spatial feature stored in seismic database holdings (such as stations, arrival paths, etc.).

The output of the SDI will be passed back to the calling application, which can be archived, displayed (Figure 1) or used to trigger further processing. For example, a message may be passed to ArcView for viewing the selected event on a map, or to MatSeis to view associated waveform information, or to a web-based bulletin generation tool for event reporting. The goal is to provide an output format that can be easily incorporated into any monitoring task.

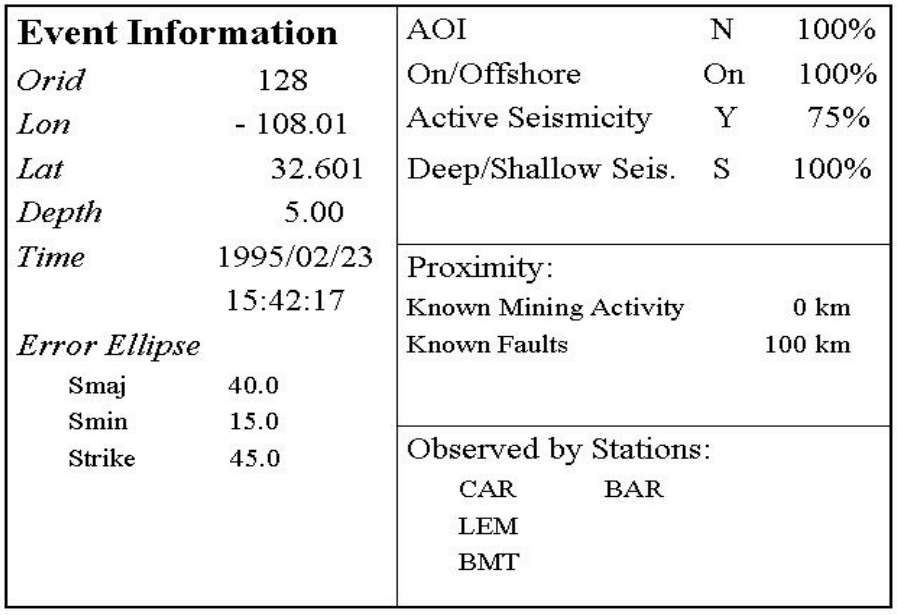

Figure 1. Example of an event identification application, which has used SDI to characterize an event.

Data Sets

A given monitoring system architecture will generally incorporate software and interfaces to perform seismic analysis and data visualization, either for automated or interactive processing components. Depending on the sources, the architecture will likely manage data as a mix of relational databases and flat files stored on the operating system. Therefore, the calling application must be able to access and incorporate either data storage method, or have an interface, which formats the data accordingly.

As noted above, the customized SDI interface utilizes data stored in Oracle tables. Seismic database holdings include event data and associated attribute information. Generally speaking, events have an implied spatial attribute associated with them (a latitude and a longitude), which will form the basis for many of the spatial queries. However, the remainder of contextual data holdings is stored in flat file format at present, and must be loaded into Oracle.

A wide variety of reference information may be used in order to analyze a seismic event. In order to account for the nature and location of an event anywhere across the globe, the contextual data holdings must be diverse. Spatial contextual information may include:

- Political Boundaries
- Coastlines
- Continental shelf
- Roads/railroads
- Topography/bathymetry contours
- Mines

- Seismic stations
- Regions of seismicity
- Faults
- Volcanoes

The ArcSDE software also allows spatial data to be stored with internal behaviors or relationships. The SDI can take advantage of these relationships, and other non-spatial information submitted to it, when evaluating a spatial query against these data.

Spatial Queries

Spatial data is generally stored in one of two models, raster and vector. Raster data are represented as cells of a uniform size, each containing a single numeric value. They are often used for modeling surfaces, such as elevation or depth to basement. For the purposes of this prototype, raster data are not utilized, but may be incorporated in future iterations of this application.

The contextual data sets listed previously are stored as vector data in the SDI's prototype monitoring system. Vector data is made up of a series of features with explicit geometry. Attributes, behavioral, and relationship information may also be stored for each feature. Queries can be based on the spatial relationship of features' geometries as easily as on specific attributes or behaviors. For example, a query may select for a political boundary, which contains features of a global seismic activity data set. The query can then be modified to subselect a particular political boundary that contains only shallow seismic activity and return the results (see Figure 2).

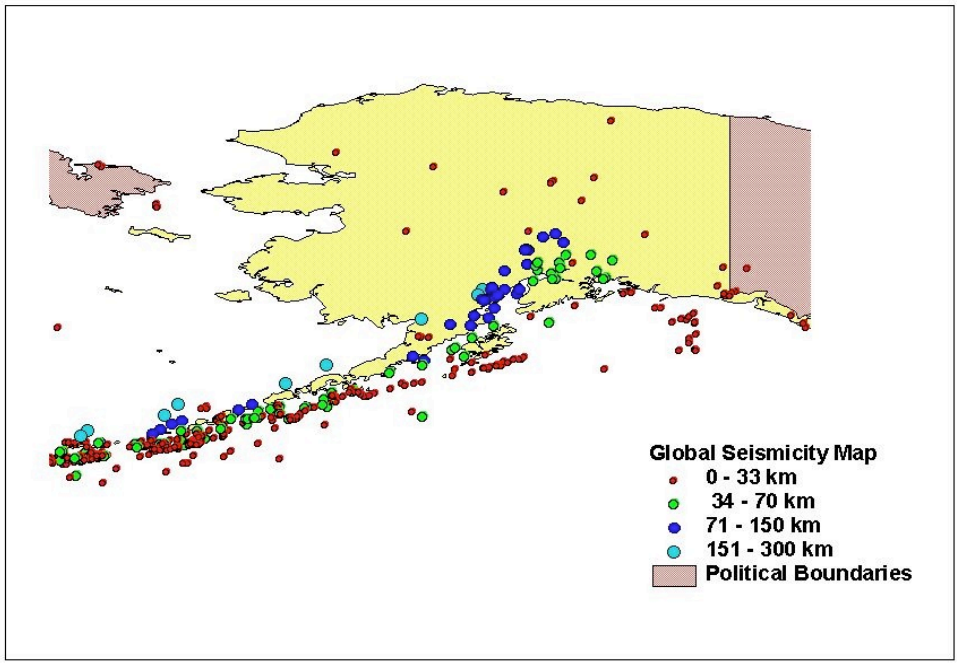

Figure 2. Graphic display of a query depicting a shallow depth seismic activity features within a political boundary.

The SDI application must be able to analyze spatial relationships between a target feature and any feature of a comparison data set. It may do this by performing any one of a basic set of built-in spatial querying capabilities that test a spatial relationship (see Figure 3), using the C API functions. SDI will also take advantage of basic GIS functions such as finding the distance and bearing between features, buffering features or generating new data sets from query results.

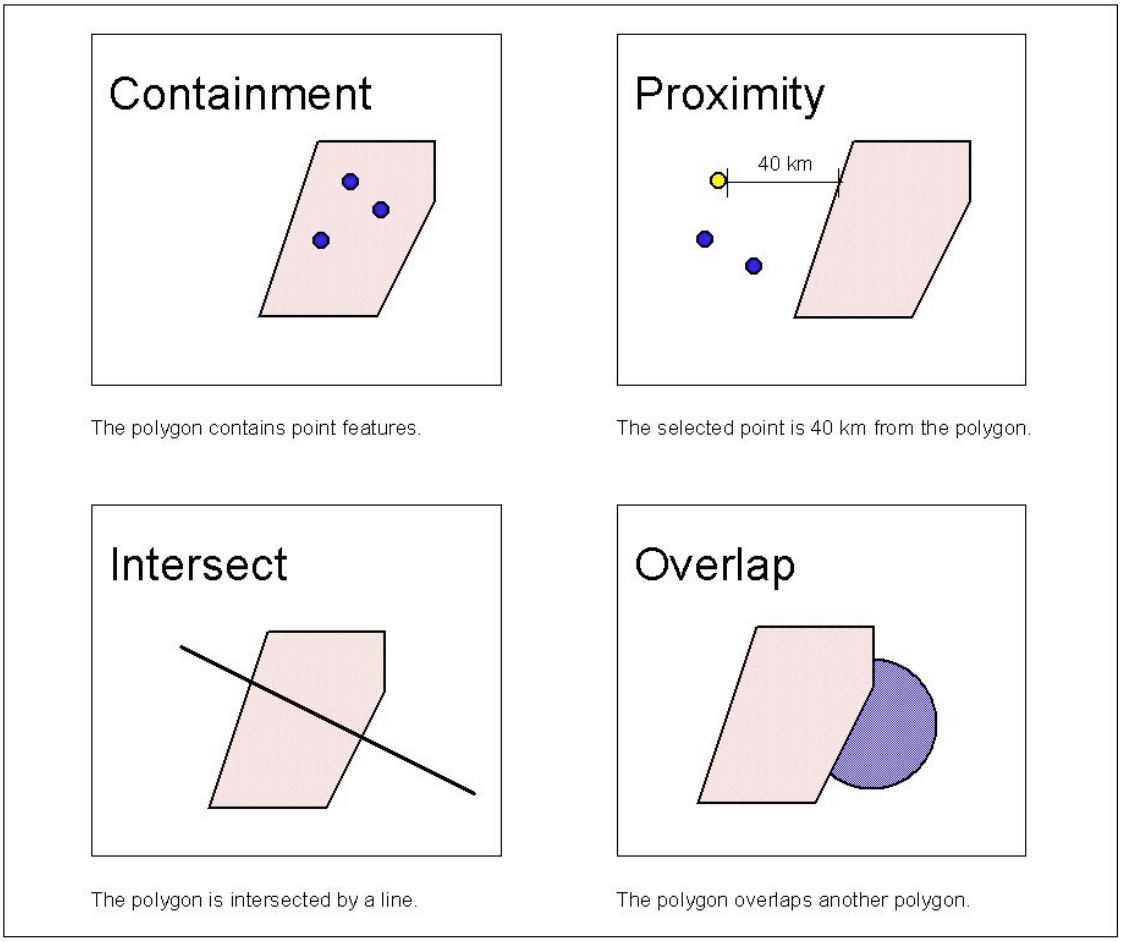

Figure 3. Examples of common spatial relationships between features.

While an automated procedure may have existing logic for defining priorities of seismic activity monitoring, performing spatial analysis on suspicious events can enhance the process by finding relationships between contextual features. Figure 1 gave an example of simple, first-cut analysis. Many times, this may be all that is required to dismiss an event. However, for those suspicious events, which are not immediately dismissed, the SDI can add another dimension to the process, strengthening confidence in the event analysis. The utility of this application is most apparent when placed in the context of normal event processing. An example is depicted in Figure 4.

Figure 4 models an automated processing system within which decisions are made regarding a suspicious event. In this case, an event, which occurs beyond realistic testing depths, will be dismissed immediately. This decision will have been made outside the SDI application. If the answer is yes, a spatial query is submitted to the SDI, which evaluates the overlap of the event's error ellipse with the predefined area of interest data set. The result is returned to the calling application. The next call may be to check the event's error ellipse against seismic data sets of the region, or its proximity to dams or roadways. Specific contextual data, such as depth values ("Deep" in Figure 4), may be queried repeatedly as the event is more accurately defined and characterized. This process can iterate as necessary through the automated analysis pipeline, querying the event against a series of contextual data sets until either a decision is reached, or the event is kicked out to an interactive processing pipeline for special event analysis. SDI analysis may then be reapplied.

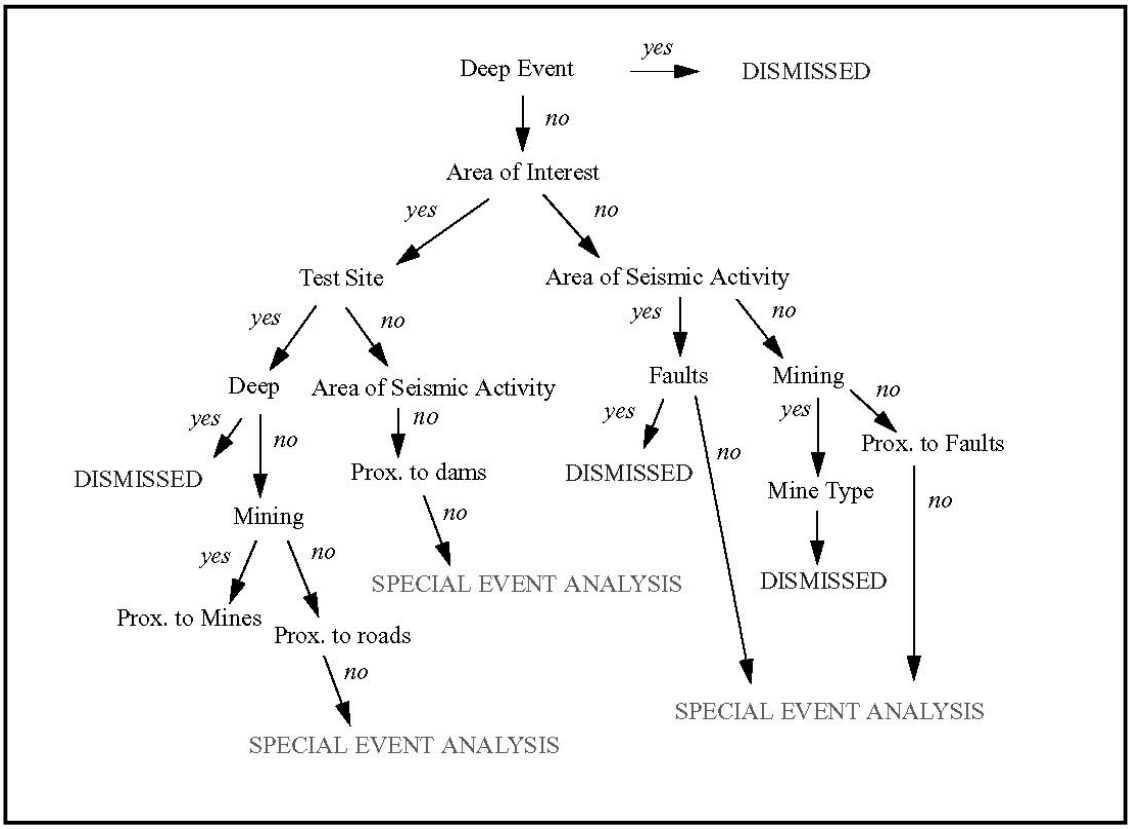

Figure 4. Example of an automated processing decision tree. Event processing moves through the tree, interfacing with SDI for spatial analysis where applicable.

Interactive event processing may require entirely new spatial querying capability. For example, the automated procedure will have established the initial key criteria that an event is shallow, in an area of active deep seismicity, and close to, but not inside, an area of interest. The SDI may then be called upon to answer spatial questions, which provide the analyst with context about the geographic and geophysical attributes of the region. These may include questions about the predominant geologic features in the region, topographic elevations, proximity to faults, types of materials mined in the area, or proximity to human habitation and other man-made features.

CONCLUSIONS AND RECOMMENDATIONS

The application developers recognize that there may be several iterations of the SDI before it is considered a "complete" tool. Future developments will likely focus on creating the "front-end" application to structure the processing rule-set and handle information passing between monitoring system components. As its use grows, new datasets may be developed and new spatial relationships defined. The questions will continue to define the system requirements. Given the availability of and confidence in the spatial contextual data, the SDI should prove to be both an efficient and effective analysis tool, and it should be considered for use as part of an automated event monitoring pipeline.

REFERENCES

West, R. (2001), Understanding ArcSDE, Environmental Systems Research Institute, Inc. (ESRI), Redlands, CA.

A SUPPORT SYSTEM FOR NUCLEAR-EXPLOSION MONITORING RESEARCH AND DEVELOPMENT

Robert L. Woodward and Robert G. North

Science Applications International Corporation

Sponsored by Defense Threat Reduction Agency

Contract No. DTRA01-99-C-0025

ABSTRACT

A comprehensive support system for Research and Development (R&D) efforts funded by the Defense Threat Reduction Agency that address nuclear-explosion monitoring and verification research and development is provided by the Research and Development Support System (RDSS) at the Center for Monitoring Research (CMR). The RDSS provides resources to support ongoing research and development, most importantly through extensive data sets and testing environments at appropriate scales, and identifies important technical issues for achieving improved nuclear monitoring capability.

The RDSS provides researchers with access to a ten terabyte data archive containing current International Monitoring System (IMS) seismic, hydroacoustic, infrasound, and radionuclide data, as well as data archives spanning several years; past and present products of the International Data Centre (IDC) and Prototype IDC, including Reviewed Event Bulletins and various radionuclide reports; test environments; a variety of special purpose data sets and databases, such as the Nuclear Explosion, Ground Truth, and Infrasound databases; and an on-line technical library.

Defense Threat Reduction Agency (DTRA)-sponsored researchers actively deliver results of their research contracts to the RDSS. These results are archived and are available for download from the RDSS web site (see below) to authorized researchers. Recent deliveries include infrasound recordings of atmospheric nuclear explosions, earthquake bulletins for various parts of the world, Geographic Information System databases, and reports on a wide range of seismic, hydroacoustic, and infrasound research topics.

The RDSS supports and collaborates on integration and testing of R&D results. Recent examples include testing of station-specific source corrections (SSSCs) produced by DTRA-sponsored calibration consortia for IMS stations in Eurasia and North Africa. We also highlight a collaborative effort with researchers at the University of California, Berkeley (UCB) to establish a platform with direct access to near-real-time data for testing and developing Automatic Moment Tensor Analysis software.

The RDSS actively develops tools and products to better serve the nuclear-explosion-monitoring R&D community, as well as to provide a gateway to a wide range of CMR resources. A variety of commercial imagery for nuclear test sites is available on the RDSS web site. We have also recently developed a remote user interface to our EvLoc event location software. Authorized members of the nuclear monitoring R&D community can submit any combination of seismic, hydroacoustic, and infrasound arrival and amplitude information and the EvLoc software running at the CMR (the same software as delivered to the IDC) will compute an event location and magnitude. Comprehensive guides to CMR hydroacoustic and infrasound resources are also available. Further information on RDSS resources and services may be found by researchers on the RDSS web sites (http://www.cmr.gov/rdss).

OBJECTIVE

The purpose of the Research and Development Support System (RDSS) at the Defense Threat Reduction Agency's (DTRA) Center for Monitoring Research (CMR) is to improve nuclear-explosion monitoring capability by supporting the R&D community with a broad range of activities and resources.

RDSS activities include providing environments for testing and evaluating promising research results at a range of scales. Such testing provides the US government with quantitative measures of current monitoring capability, identifying obstacles and establishing expectations for achieving improved capability. The RDSS organizes and archives research results produced by the R&D community in a manner that facilitates the access to these results for the entire research community. Finally, a wide range of CMR internal resources is made available to the R&D community via the RDSS.

RESEARCH ACCOMPLISHED

The Center for Monitoring Research (CMR) provides many unique resources to support basic and applied research and development. CMR maintains a large and growing archive of seismic, hydroacoustic, infrasound, and radionuclide data, as well as special tools and functionality built to maximize information available for each data technology. In addition, a wide variety of special data products (both databases and data sets) has been assembled to support monitoring research. These data sets are routinely augmented with new data as they become available.

Researchers may also take advantage of the results of the DTRA PRDA research program that are delivered to the RDSS. These results are reviewed, archived and redistributed by the RDSS. The PRDA results are distributed in their raw (as delivered) form and if appropriate, in value-added form (e.g. added to related data to create a new product).

Finally, researchers may take advantage of the facilities and test capabilities provided by the RDSS. Testing environments can be arranged at any scale, from the full data-load of the IMS network and the full-processing environment of the IDC monitoring system, to highly specific experimental arrangements with historical data sets. Supporting facilities include a large UNIX-based computing environment, databases, and data archives.

In the remainder of this paper, we describe some of the data, data products, and capabilities that are available to the R&D community via the CMR RDSS.

Data Resources

The CMR has been continuously acquiring and archiving time-series and radionuclide data since 1992. Currently, the CMR receives data from a variety of international stations, including stations of the International Monitoring System (IMS) network. The data archive consists of over 10 terabytes of waveform data from seismic, hydroacoustic, and infrasound stations and is growing at a rate of approximately 1.5 Tb per year. Detailed guides describing the hydroacoustic, infrasound, and radionuclide resources have been prepared and these are available on-line at the RDSS web site. These guides provide detailed descriptions of the stations, instructions on accessing data, and detailed information on data availability. A guide to CMR seismic resources will be prepared in the future, though usage patterns for the data archive indicate that the R&D community is generally more familiar with the existing CMR seismic resources than either the hydroacoustic or infrasound data resources.

CMR data are easily accessed from remote sites by using the AutoDRM (Automatic Data Request Manager) interface, an e-mail-based request mechanism. RDSS users are also provided access to bulletins and other data products obtained from the International Data Centre (IDC) in Vienna, Austria. The RDSS is presently developing a streamlined, web-based graphical user interface to the data archive. We expect this new interface to be online in the fourth quarter of 2002.

Special Databases

The RDSS produces a variety of special databases and data products that are useful to nuclear explosion monitoring research and development, and these are summarized in Table 1. These data products provide data and metadata

assembled in a manner to maximize their utility for research purposes. Where appropriate, data being delivered to the RDSS by DTRA-sponsored contractors are added to these databases, such that the value of both the delivered data, and the database, are increased.

Table 1. Research databases available to R&D community via the RDSS.

Radionuclide	• High-resolution gamma-ray spectroscopy • Beta-gamma coincidence spectroscopy
Ground Truth	• Nuclear and chemical explosions, industrial events, earthquakes, mixed data sets
Reference Event	• Small- to medium-sized, well located, uniformly globally distributed events
Nuclear Explosion	• Nuclear explosions (1945 – 1993), announced nuclear explosions since 1984, and Australian Geological Survey Organization database (1945 – 1996)
Lop Nor	• An extensive compilation of seismic data for events in and around the Lop Nor nuclear test site region, China

Recently, an Advanced Concept Demonstration (ACD) was performed at CMR (Kohl *et al*, 2002). This ACD focused on improving the capability for monitoring the Chinese nuclear test site at Lop Nor. As part of this ACD, an extensive data set was assembled. The RDSS has now integrated the Lop Nor ACD data set into a data product for public distribution, referred to as the Lop Nor Database (LNDB). The LNDB includes nuclear explosions and earthquakes, as well as various synthetic events. All relevant information, including parameters, waveforms, and extensive metadata, are collected together in this product. As for the other RDSS research databases, all information is loaded into a centralized relational database, with waveforms and metadata stored on local disks. Database tables have been created to store metadata that do not fit within the standard IDC database schema.

The Lop Nor Database consists of 421 events (Figure 1) in the Lop Nor ACD "box" (defined as 39°--44° N and 86°--92° E), with approximately 43,000 arrivals. For each event there are multiple data sources, and a preferred origin is chosen based on the location accuracy. Data sources for events and arrivals include:

- ACD analysis results
- PIDC Reviewed Event Bulletins (REBs)
- IDC REBs
- CMR Nuclear Explosion Database
- CMR Ground Truth Database
- International Seismological Centre
- Annual Bulletin of Chinese Earthquakes (ABCE)
- PIDC GAMMA bulletin

A total of 205 events were thoroughly analyzed during the ACD work, including 25 out of all 45 nuclear explosions. Waveform data were obtained from the CMR archive system, CMR Nuclear Explosion Database, Incorporated Research Institutions for Seismology (IRIS) Data Management Center, and Blacknest UK data archives. Synthetic seismograms for small nuclear tests were obtained by applying frequency dependent scaling relations to actual recordings of large nuclear tests and embedding the result in noise recordings. Ground truth information is available for most of the nuclear explosions and for the scaled/embedded events. There are approximately 100 Gb of waveform data in total.

There are 37 tables in the LNDB providing detailed metadata for waveforms and events. Metadata tables are developed to document data sources, references to data sources, and various computational results. This database uses unique event identifiers (evid) to identify all related solutions for an event and the associated waveforms. Metadata are also associated with each event through the metadata tables. Arrivals from the ACD analysis and from bulletin collections are associated with their corresponding origins. Additional details about the Lop Nor database, including a complete description of the schema, will be published as a CMR Technical Report (to be completed in fourth quarter, 2002).

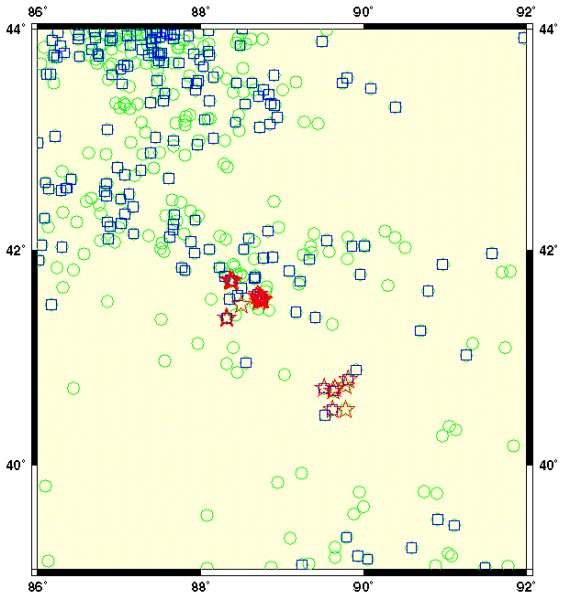

Figure 1. Preferred origin of 421 events (green circles) in the Lop Nor Database, including nuclear explosions (red stars) and events for which waveform data were analyzed (blue squares).

Commercial Satellite Imagery

A variety of high-resolution commercial satellite images are available through the RDSS (Skov *et al*, 2002). Images include 1-m panchromatic and 4-m multi-spectral satellite imagery obtained from commercial vendors. At CMR these images have been used in conjunction with re-analysis of seismic data to obtain definitive locations of historical nuclear explosions with accuracy suitable for designations as Ground Truth 1 (GT1) or GT2 events. Images have been obtained for the test sites at Novaya Zemlya, Lop Nor, India, and Pakistan.

The imagery has been analyzed to identify features in one of three categories: 1) direct evidence of disturbances resulting from nuclear detonations, typically collapse features; 2) direct evidence of test site artifacts highly correlated with locations of nuclear tests; 3) direct evidence of test site artifacts constrained to the vicinity of nuclear detonations. To estimate uncertainties, highly visible and distinct but spatially constrained features, such as the intersections of major roadways, are identified on a number of different sources. Older imagery from lower resolution sensors (SPOT, LANDSAT, KVR), digital terrain elevation data, and high resolution maps available through the National Imagery and Mapping Agency were registered with respect to one another, demonstrating variations of no more than several hundred meters.

The results of the imagery analysis are assembled in a series of imagery products that are available through the RDSS web site. The imagery products are provided in Portable Document Format (PDF) to ensure maximum portability. Table 2 presents a list of the imagery products presently available through the RDSS web site. This collection will continue to grow as new images are acquired as part of CMR's imagery acquisition program. A comprehensive discussion of the use and analysis of satellite imagery at CMR can be found in Skov *et al*. (2002).

Table 2. List of imagery products available through the RDSS web site.

Site	Acquisition Dates	Imagery Type	# of Nuclear Tests Within Area of Imagery
Novaya Zemlya	June 26, 2000 July 20, 2000 August 3, 2000	1-m panchromatic, mosaic of 3 images	31
Lop Nor	February 26, 2000	1-m pan + 4-meter multi-spectral	6
	July 1, 2000	1-m pan + 4-meter multi-spectral	13
India	August 10, 2000	1-m pan + 4-meter multi-spectral	2
Pakistan	July 9, 2000	1-m pan + 4-meter multi-spectral	1
	July 9, 2000	1-m panchromatic	1

Hypocenter Location Server

The RDSS has recently developed the Hypocenter Location Server (HLS) to provide a remotely accessible interface to the powerful hypocenter location program *EvLoc*. The *EvLoc* software is a core element of the CMR processing system and is part of the complete system provided to the IDC. *EvLoc* is capable of using any combination of seismic, hydroacoustic, and infrasound arrivals to determine hypocenters and to compute magnitudes (seismic only). The HLS is accessed by sending formatted e-mail messages to the server (in this sense it looks much like an AutoDRM server), as illustrated in Figure 2. The user provides data files, configuration files, and custom parameter files via FTP (using a flat-file structure or using XML). The HLS processes requests, with their associated input files, and then e-mails the results to the user.

EvLoc is a complex software component that relies heavily on a carefully configured database environment (e.g. Oracle) to function properly. As such, *EvLoc* is not readily portable. By providing access to *EvLoc* functionality through the Application Service Provider model as described here, researchers can readily use *EvLoc* in their analysis without worrying about software portability or configurability. Further, the capability provided by the HLS completely supercedes that provided by CMR's stand-alone hypocenter determination program *LocSAT*. Note that the HLS is fully backward compatible with *LocSAT* input files.

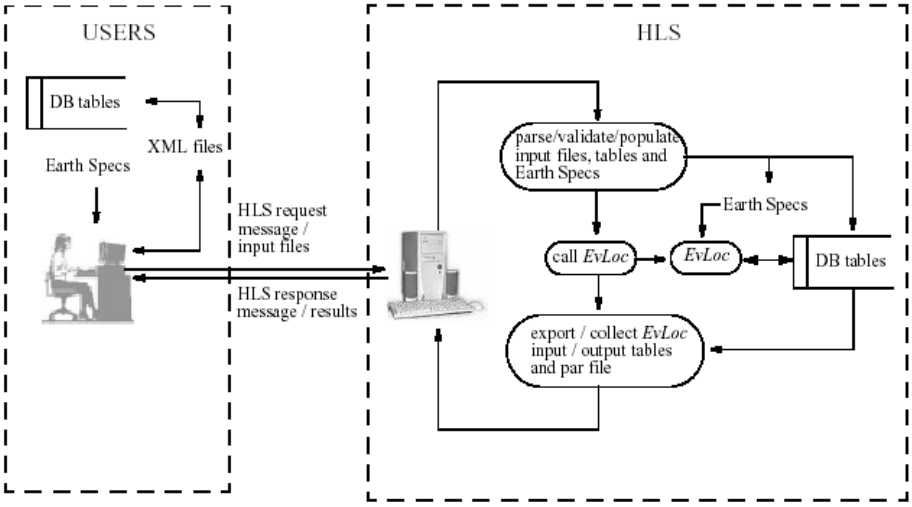

Figure 2. Data flow for the Hypocenter Location Server, showing the relationship between the user and the server.

DTRA Contract Results

A key activity of the RDSS is receiving, accepting, and testing results from the R&D community. In general, the RDSS receives three types of deliveries: technical reports, data to receive and store, and software components or parametric results to evaluate and possibly integrate into a monitoring system. All of the R&D products received by

the RDSS are archived and are made available for redistribution to the entire R&D community via the RDSS web site. Table 3 summarizes the deliveries from DTRA-sponsored researchers that have been received to date. To learn more about any of the products listed in Table 3, please consult the RDSS web site.

Table 3. Summary of research products received by the RDSS.

	Contract/Task Title	Performing Org.	P.I.	Products Received
1	Development of a Dynamic Infrasound Knowledge Database	BBN Tech.	Farrell	Software and User's Guide
2	Enhanced Depth Determination Using Cepstral Techniques	Weston Geophysical	Reiter	Report ; Software for cepstral F-stat analysis
3	Characterization of Reflected Arrivals for Hydroacoustic Test Ban Monitoring	BBN Tech.	Gibson	Final Report; database 15 events between 1965 and 1970
4	Feasibility of the Use of 3D Models to Improve Regional Locations in W. China, Central Asia, and Parts of the Middle East	Univ. of Colorado at Boulder	Ritzwoller	Final Report; database of KNET and CAB bulletins
5	Long-Period Surface Wave Dispersion and NDC Global Association Database	Boston College	Harkrider	Final Report; FORTRAN versions of travel time codes
6	Infrasound Excitation and Propagation Research	Maxwell Tech.	Stevens	Final Report; database of infrasound recordings; IDG Final Report
7	Statistical Calibration & Regionalization of China & Surrounding Region	New Mexico State Univ.	Hearn, Ni	Annual Bulletin of Chinese Earthquakes 1985, 1986, and 1991-1995
8	Collection and Analysis of Regional Seismic Data for Underground Explosions	Mission Research Corp.	Fisk	Final Report; waveform database
9	Reconnaissance of Backgound Infrasound at Selected Future IMS Locations, Atlantic Ocean	UC San Diego	Hedlin	Final Report
10	Development of Ultrahigh Sensitivity Xenon Detectors for Enhancement of Ability to Monitor Nuclear Testing	Univ. of Cincinnati	Valentine	Final Report
11	Discr., Det., Dep., Loc., and Wave Propagation Studies Using Intermed. Period Surface Waves in the Mid-East, C. Asia, and the Far East	Univ. of Colorado at Boulder	Levshin	Final Report
12	Advanced Regional Array Studies	NORSAR	Kvaerna	Final Report
13	Source Char. and Reg. Discr. of N. Idaho Rockbursts and Earthquakes	Univ. of Idaho	Sprenke	Final Report
14	Signal Det. and Estimation Directional Parameters for Multiple Arrays	UC Davis	Shumway	Final Report
15	CTBT Seismic Monitor Issues at Local Distance Ranges	Univ. Bergen	Husebye	Technical Report
16	Regionalized Velocity Models and Improved Locations for Pakistan and the Surrounding Area	Weston Geophysical	Reiter	Technical Report
17	Joint Inversion of Receiver Function and Surface Wave Dispersion for Local Crustal Structure in the Mideast	St. Louis Univ.	Herrmann, Ammon	Final Report
18	Various contracts	Columbia Univ., LDEO	Kim, Richards	Report; Borovoye digital seismogram archive
19	Development of Event Screening Procedures	Australian Geol. Survey Org.	Jepsen	Summary report; database of nuclear and chemical events, CSS3.0 format
20	Path Corrections for Regional Phase Discriminants	UC Santa Cruz	Lay	Final Report
21	Improve Monitoring of the CTBT in Middle East by Israel SeisNet	Geophysical Institute Israel	Gitterman	Final Report; data, video, etc.
22	A Ground Truth Database for Regional Seismic Research	Multimax	Henson	313 CEB events China, FSU, and N. Am
23	A Damage Mechanics Model for Underground Nuclear Explosions	Univ. Southern CA	Sammis	Final Report
24	Basic Research on Seismic Monitoring Problems	UC Berkeley	Johnson	Final Report
25	Auto Interpretation of Seismic Signals Using CUSUM-SA Algorithm	ENSCO	Der	Final Report; software – Matlab M-scripts
26	Global & Regional GIS Database Development in Support of CTBT	Cornell	Barazangi	Final Report
27	Probabilistic Integration of Seis, Hydro & Infra Data in Disc Sch	ENSCO	Der	Final Report

	Contract/Task Title	Performing Org.	P.I.	Products Received
28	Seismic Calibration for IMS Stations in North Africa and Western Asia (Group 2)	SAIC	McLaughlin	Reports; SSSCs and numerous data products
29	Integration of Enhanced Propagation, Environmental Variability, and Network Performance Models into the InfraMAP Software Toolkit	BBN Tech.	Norris	InfraMAP Users Guide, V2.1; InfraMAP V2.1 (available from BBN)
30	Constraining Depth and Source Mechanisms of Small Events at Far-regional to Teleseismic Distances	ANU	Kennett	Final Report
31	Regional GIS Databases in Support of CTBT Monitoring	Cornell	Barazangi	Final Report; GIS digital data sets
32	Physical Basis and Improved Criteria for Phase Spectral Ratio Discrimination	Columbia Univ., LDEO	Xie	Final Report
33	Integrated Study of Seismic and Infrasonic Signals from Sources in Southern Siberia, Eastern Kazakhstan, and Western China	Columbia Univ., LDEO	Kim	Final Report
34	Seismic Calibration for IMS Stations in Eastern Asia (Group 1)	Columbia Univ., LDEO	Richards	Pn SSSCs for subset of group 1 IMS stations
35	Application of Joint Inversion of Receiver Functions and Surface-Wave Dispersion for Local Crustal Structure	St. Louis University	Herrmann	Seismological software
36	Development of Improved Capabilities for Depth Determination and Research on the Frequency Dependence of Regional Seismic Phases	MRC	Fisk	Final Report; software
37	Statistical Calibration & Regionalization of China & Surrounding Region	New Mexico State Univ.	Hearn, Ni	Final Report; velocity models,; Annual Bulletin of Chinese Earthquakes, 1984-1999
38	Seismic Calibration for IMS Stations in Eastern Asia (Group 1)	SAIC	Murphy	SSSCs for group 1 IMS stations
39	Enhanced Depth Determination Using Cepstral Techniques	Weston Geophysical	Reiter	Final Report; software

Integration and Testing

Many of the deliveries to the CMR R&D Support System comprise software components, parametric results, or other components that are to be tested to determine their potential for use in large-scale monitoring systems. To perform such tests, a test plan, with evaluation criteria, is generated by the researcher in collaboration with RDSS staff.

Deliveries that require full-scale testing require special planning. For example, the DTRA IMS Location Calibration Program is funding three consortia to provide SSSCs for stations of the IMS. In this endeavor, integration, testing, and evaluation are required at CMR to ensure that the results produced by the three consortia are compatible with the CMR nuclear-explosion-monitoring system software. To date, the RDSS has performed testing for two of the consortia (Yang *et al*, 2001; Richards *et al*, 2002).

Part of the DTRA tasking to the location consortia has been to develop depth-dependent SSSCs. In the past, SSSCs have only been specified for a single source depth, typically either 0 km or 10 km. To support the consortia activities, the RDSS has now developed a new version of *EvLoc* that can utilize SSSCs that are specified for multiple source depths (Figure 3). Additionally, the new *EvLoc* will be available to the R&D community via the Hypocenter Location Server discussed earlier.

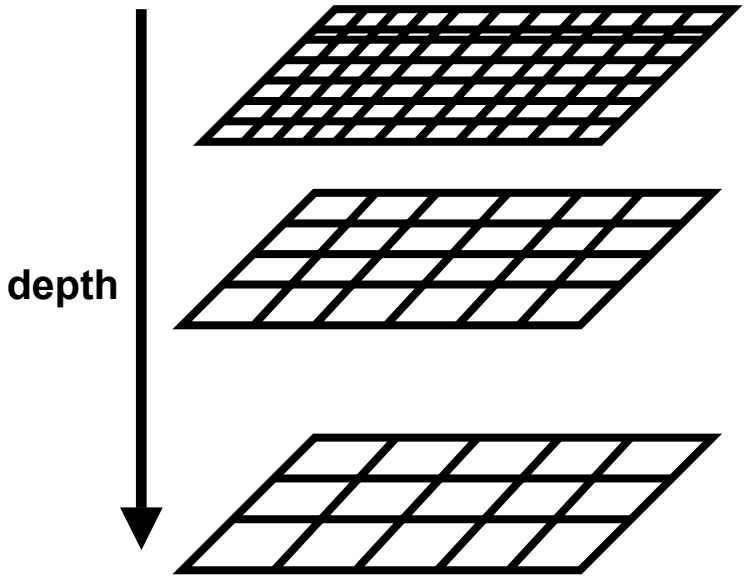

Figure 3. Depth-dependent SSSCs are parameterized as a sequence of horizontal 2-D grids at various depths. The software supports arbitrary depth sampling and variable horizontal gridding. The software is backward compatible with non-depth-dependent SSSC files.

In another testing effort at the RDSS, investigators at the University of California, Berkeley, and RDSS staff are working on a plan for integrating UCB's automated moment tensor software (Dreger *et al*, 2001) into the nuclear monitoring system developed at CMR. The purpose of the UCB effort is to develop software to automatically determine moment tensors for seismic events recorded at the IMS network stations. To support UCB, the RDSS staff have configured a dedicated test platform, with direct access to the near-real time disk loops at CMR (kept online for 20 days) and to the database containing the Reviewed Event Bulletins produced by the IDC. In this way the UCB software can access the bulletins to cue their processing and can take advantage of the high-speed access to full waveform data that is provided by the online diskloops. This dedicated test platform will allow UCB researchers to refine and tune their software by experimenting with large numbers of events in different parts of the world. Ultimately, the software will be integrated into the CMR processing pipeline architecture and will provide improved source characterization capabilities for the nuclear-explosion monitoring system.

CONCLUSIONS AND RECOMMENDATIONS

The RDSS supports R&D aimed at improving nuclear-explosion monitoring and treaty verification capabilities by drawing on the facilities, resources, and expertise of the CMR.

In summary, basic RDSS activities include:

- Supporting the R&D community, from the inception of research through to testing and archiving of results.
- Archiving research results to ensure important work is not lost and results can be shared readily amongst the R&D community.
- Providing a mechanism for the test, evaluation, and integration of R&D results.

A wide range of CMR staff, including scientific, software development, testing, and infrastructure support teams, are available to support all phases of R&D activity. Please watch for news and developments (or contact us) at: http://www.cmr.gov/rdss . The web site contains a wide range of information, such as listings of current DTRA

contracts, contract deliverables received, documents describing the access and use of the RDSS, and information on available RDSS resources.

REFERENCES

Dreger, D., B. Romanowicz, G. Clitheroe, P. Hellweg, J. Stevens (2001), Development of Automated Moment Tensor Software at the Prototype International Data Center, Proceedings of the 23rd Seismic Research Review, Vol. I, 500-508.

Kohl, B., R. North, J. Murphy, M. Fisk, and G. Beall (2002), Demonstration of Advanced Concepts for Nuclear Test Monitoring Applied to the Nuclear Test Site at Lop Nor, China, 24th Seismic Research Review (this volume).

Richards, P., R. Burlacu, M Fisk (2002), Pn SSSCs for IMS and Surrogate Stations in Asia, proposal to CMR Configuration Control Board, CCB-PRO-02/04, http://www.cmr.gov/cmrlibrarybox/ccb/ccb0204.pdf .

Skov, M., B. Kohl, R. Woodward (2002), Imagery Assets for Supporting Nuclear Explosion Monitoring Research and Development, 24th Seismic Research Review (this volume).

Yang, X., K. McLaughlin, I. Bondár, J. Bhattacharyya, H. Israelsson (2001), Pn & Sn SSSCs in Europe, North Africa, Middle East, and Western Asia, proposal to CMR Configuration Control Board, CCB-PRO-01/15, http://www.cmr.gov/cmrlibrarybox/ccb/ccb0115a.pdf.

VERSION 1.7 OF MATSEIS AND THE GNEM R&E REGIONAL SEISMIC ANALYSIS TOOLS

Christopher J. Young, Eric P. Chael, and Bion J. Merchant

Sandia National Laboratories

Sponsored by National Nuclear Security Administration
Office of Nonproliferation Research and Engineering
Office of Defense Nuclear Nonproliferation

Contract No. DE-AC04-94AL85000

ABSTRACT

To improve the nuclear event monitoring capability of the U.S., the NNSA Ground-based Nuclear Explosion Monitoring Research & Engineering (GNEM R&E) program has been developing a collection of products known as the Knowledge Base (KB). Though much of the focus for the KB has been on the development of calibration data, we have also developed numerous software tools for various purposes. The Matlab-based MatSeis package and the associated suite of regional seismic analysis tools were developed to aid in the testing and evaluation of some Knowledge Base products for which existing applications were either not available or ill-suited. This presentation will provide brief overviews of MatSeis and each of the tools, emphasizing features added in the last year.

MatSeis was begun in 1996 and is now a fairly mature product. It is a highly flexible seismic analysis package that provides interfaces to read data from either flatfiles or an Oracle database. All of the standard seismic analysis tasks are supported (e.g. filtering, 3 component rotation, phase picking, event location, magnitude calculation), as well as a variety of array processing algorithms (beaming, FK, coherency analysis, vespagrams). The simplicity of Matlab coding and the tremendous number of available functions make MatSeis/Matlab an ideal environment for developing new monitoring research tools (see the regional seismic analysis tools below). New MatSeis features include: addition of *evid* information to events in MatSeis, options to screen picks by author, input and output of *origerr* information, improved performance in reading flatfiles, improved speed in FK calculations, and significant improvements to Measure Tool (filtering, multiple phase display), Free Plot (filtering, phase display and alignment), Mag Tool (maximum likelihood options), and Infra Tool (improved calculation speed, display of an F statistic stream).

Work on the regional seismic analysis tools (CodaMag, EventID, PhaseMatch, and Dendro) began in 1999 and the tools vary in their level of maturity. All rely on MatSeis to provide necessary data (waveforms, arrivals, origins, and travel time curves). CodaMag Tool implements magnitude calculation by scaling to fit the envelope shape of the coda for a selected phase type (Mayeda, 1993; Mayeda and Walter, 1996). New tool features include: calculation of a yield estimate based on the source spectrum, display of a filtered version of the seismogram based on the selected band, and the output of codamag data records for processed events. EventID Tool implements event discrimination using phase ratios of regional arrivals (Hartse et al., 1997; Walter et al., 1999). New features include: bandpass filtering of displayed waveforms, screening of reference events based on SNR, multivariate discriminants, use of *libcgi* to access correction surfaces, and the output of discrim_data records for processed events. PhaseMatch Tool implements match filtering to isolate surface waves (Herrin and Goforth, 1977). New features include: display of the signal's observed dispersion and an option to use a station-based dispersion surface. Dendro Tool implements agglomerative hierarchical clustering using dendrograms to identify similar events based on waveform correlation (Everitt, 1993). New features include: modifications to include arrival information within the tool, and the capability to automatically add/re-pick arrivals based on the picked arrivals for similar events.

OBJECTIVE

MatSeis was originally developed to support signal-processing research for the GNEM R&E program at Sandia Labs. The initial goal was simple: to develop a graphical user interface (GUI) to help a user bring data from an Oracle database into Matlab. Once the data was in Matlab, researchers could then run various scripts and/or functions to test algorithms. This goal was quickly accomplished thanks to the tremendous range of existing Matlab functionality, but Sandia chose to extend development because it became apparent that the package had potential to be much more useful than had been expected. Within a year we had developed a simple, interactive seismic analysis package built around 4 basic data types: waveforms, arrivals, origins, and travel time curves. However, because the bulk of Sandia's development work went towards signal processing, early versions of MatSeis had an odd look and feel: the package had an extensive set of signal processing capabilities (e.g. filtering, rotation, beaming, FK, coherency, vespagrams), while at the same time it lacked many of the more common seismic analysis utilities (e.g. a locator, magnitude calculations, a quick and easy phase picker) because these were not needed for Sandia's research efforts at that time.

The second MatSeis development phase began when Sandia began to use the package as a base upon which to develop specialized regional seismic analysis tools. Over the past few decades, many studies have suggested ways to improve regional monitoring, yet relatively few of the ideas presented have found their way into operational software. The reason is that those who actually monitor have limited time and resources to put towards evaluating these ideas, and so generally only the most sure-fire get implemented. What is needed is a prototyping environment in which promising analysis techniques can be implemented and evaluated quickly and with relatively little effort. Sandia recognized that MatSeis/Matlab offered just such an environment, and taking advantage of this we began to build a set of prototypes for various regional analysis tasks, focusing first on the techniques and data sets generated by the research of our colleagues at Lawrence Livermore National Lab (LLNL) and Los Alamos National Lab (LANL). Currently the tools support phase match filtering, regional magnitude calculations, discrimination, and event clustering using waveform correlation.

An unplanned but welcome side effect of the development of these tools has been the improvement of MatSeis itself. To properly use the tools, it is necessary to add new picks, re-time picks, re-locate events, etc. Thus, Sandia was forced to fill in many of missing basic seismic analysis utilities, and to improve many of the existing ones. The result is that MatSeis is now a significantly more complete, more robust package.

RESEARCH ACCOMPLISHED

The following sections describe MatSeis, and the four regional seismic analysis tools. The important new features for Version 1.7 are highlighted for each.

MatSeis

The main MatSeis graphical window is a standard time vs. epicentral distance plot that can display waveforms, arrivals, origins, and travel time curves (Figure 1). The user can interact with this display by clicking directly on the displayed objects, by using the buttons along the bottom, by using the menus along the top, or by typing commands at the Matlab prompt. MatSeis is predominantly written as Matlab m-file functions, which are organized in a set of directories according to the general purpose of each. However, the package also includes a set of compiled C functions linked to the m-files via the Matlab cmex utility. Typically the C functions are introduced where performance of an m-file is too slow (e.g. FK calculations).

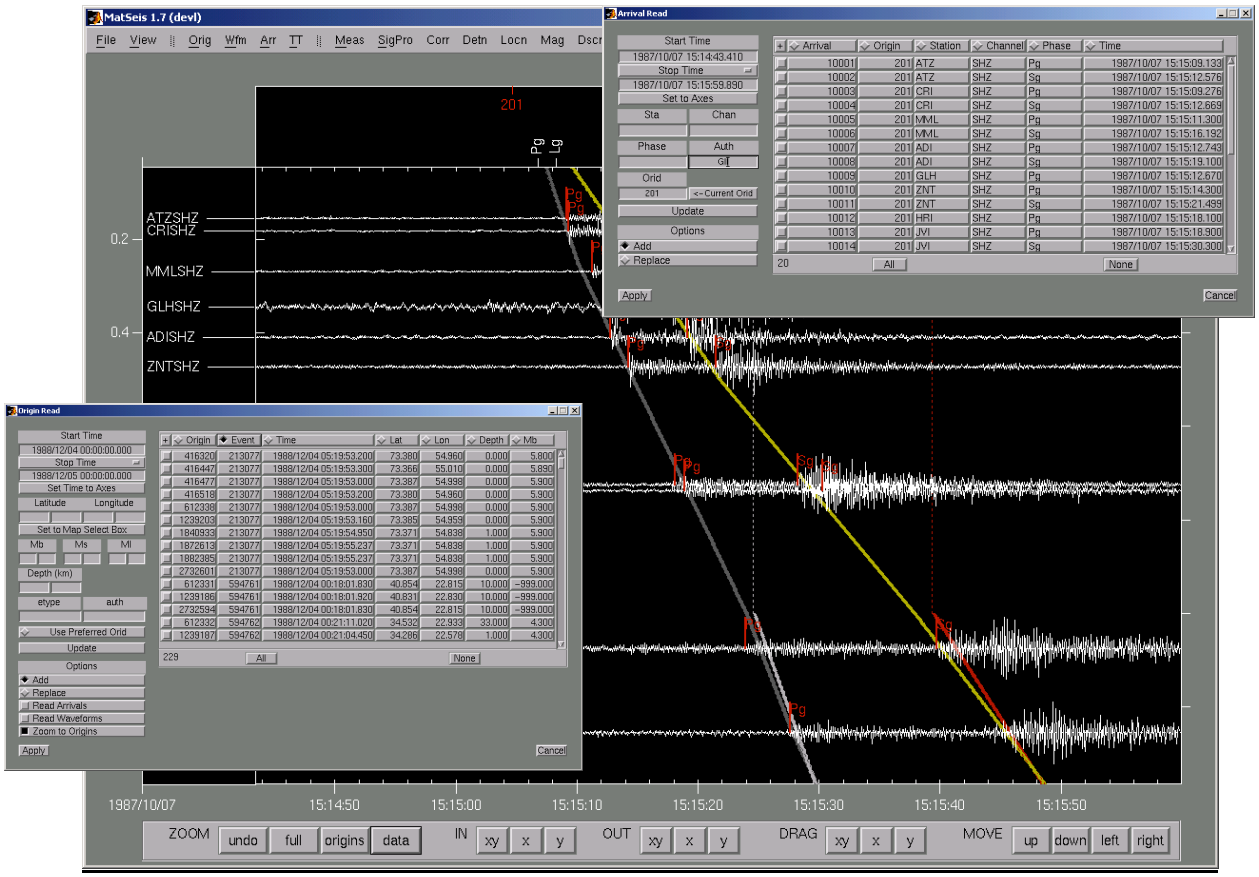

Figure 1. The main MatSeis display is a standard time vs. epicentral distance waveform profile. This figure shows all 4 data objects: waveforms, arrivals, origins, and travel time curves. Also shown are the re-designed popups to read in arrivals (upper right) and origins (lower left).

Data IO

MatSeis can read CSS3.0 format data from either an Oracle database, or flatfiles. Output is restricted to flatfiles only. The number of tables used by MatSeis has steadily expanded and now includes: *affiliation, amplitude, arrival, assoc, event, instrument, nextid, netmag, network, origerr, origin, remark, sensor, site, sitechan, stamag, wfdisc,* and *wftag*. In Version 1.7, flatfile data reads have been greatly sped up, making it practical to work with larger data sets than has been the case in the past. In order to allow the user to better control the data read into MatSeis, Version 1.7 has an extensive set of filters for both origins (*lat, lon, magnitude, etype, auth*) and arrivals (*sta, chan, phase, auth, orid*). In the origin read popup, *evid* is now displayed, which makes it more convenient to work with multiple origins for the same event.

Arrival Picking and Amplitude Measurement

Arrivals can be added, deleted, renamed, and retimed in the main MatSeis display, but it is a cumbersome process and impractical when editing more than a few arrivals. The recommended method is to use an auxiliary utility called Measure Tool (Figure 2) that can be launched from the main display. Measure Tool is designed to help analysts quickly and efficiently pick arrivals and measure amplitudes for an event. The theoretical arrival times for the TT curves in MatSeis, are shown for reference. Version 1.7 includes a set of controls to filter the waveforms, and the filtering can be toggled on or off. Once an arrival has been picked, the user can choose from a set of amplitude measurements (e.g. Peak-Peak, Zero-Peak, RMS), and the measurement is automatically made after the user sets the window. A toggle allows the user to choose whether or not to correct the measurements for instrument response.

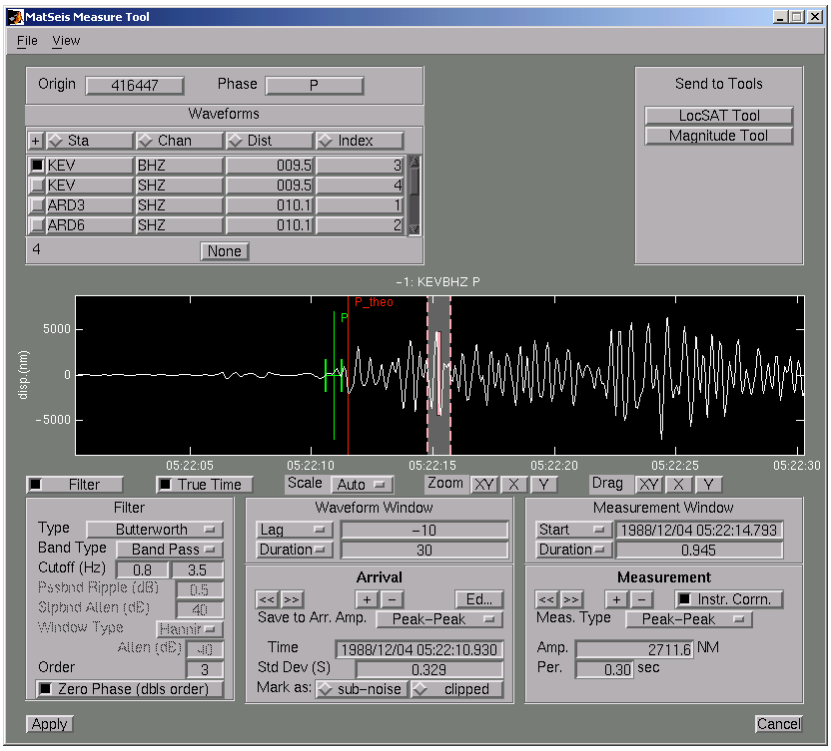

Figure 2. Measure Tool has been designed specifically to allow the analyst to quickly pick, retime, and measure amplitudes for arrivals.

Magnitude

Magnitudes can be calculated in MatSeis using either of two tools. The Magnitude Tool (Figure 3) offers a variety of standard amplitude-based magnitude formulas for local, regional, and teleseismic data. The user can screen the data used by phase, period, and distance.

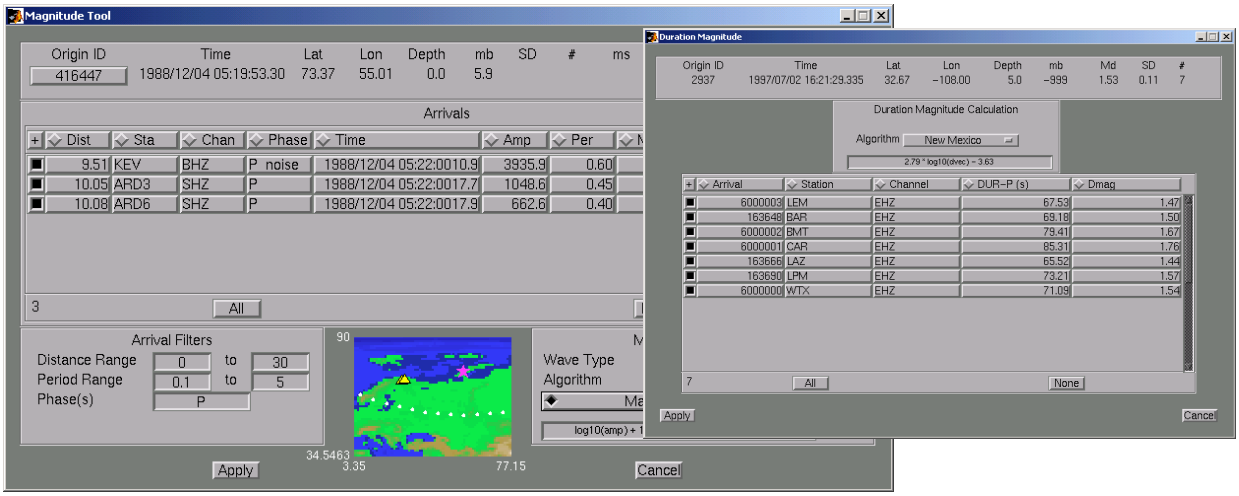

Figure 3. The Magnitude Tool (left) and Duration Mag Tool (right) allow the user to select the type of magnitude formula , and provides a clickable list to control which station measurements are used for the network magnitude.

Individual measurements can be turned on or off by clicking on their rows in a table, and a small map shows the positions of the stations relative to the source location. A new feature in Version 1.7 is an option to calculate a maximum likelihood magnitude, if some of the arrivals have been designated as sub-noise or clipped (Blandford & Shumway, 1993; Ringdal, 1976).

The Duration Magnitude Tool has a similar look and feel, but calculates magnitude base on duration of signal above noise, as picked by an analyst. The tool includes a default formula for New Mexico, and can be easily modified to include calibrated formulas for any number of other regions.

Infra Sound Analysis

MatSeis-1.7 includes Infra Tool, a tool for analysis of infrasound array data. This tool uses cross-correlations of the array channels to derive azimuth and velocity for incoming signals. The calculation is made for a short user-defined moving window, so the result is a stream of azimuth, velocity, correlation, and fstat. The tool displays these streams, along with the filtered data channels (Figure 4). The user can change the filter parameters and/or the moving window parameters (length, %overlap), and re-calculate the streams.

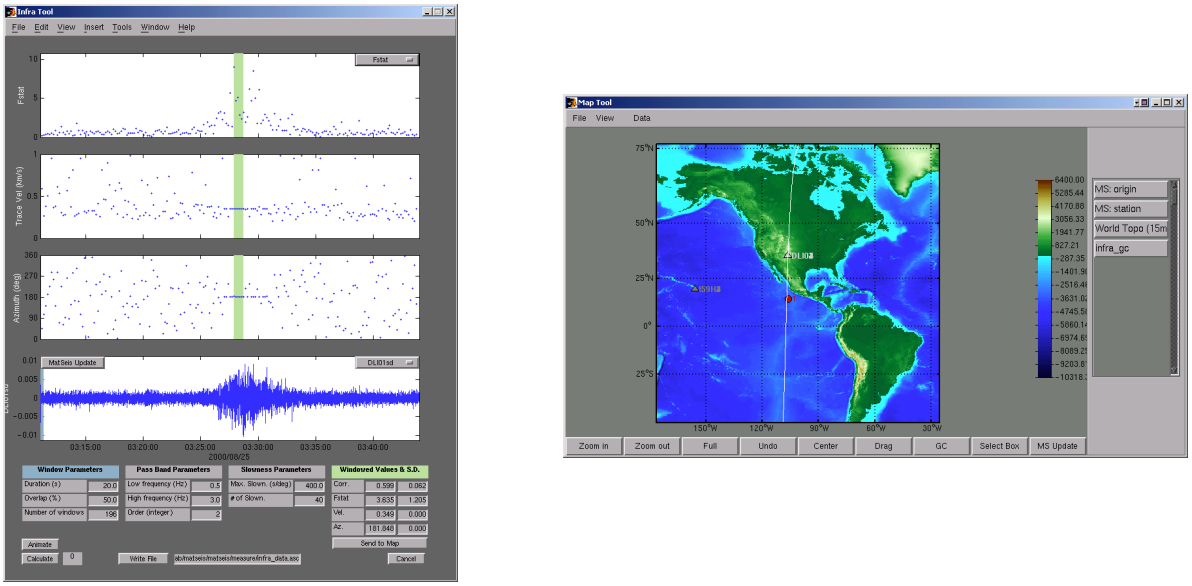

Figure 4. The Infra Tool helps the user derive great circle path information from infrasound array data (left). Great circles can be plotted using the Map Tool (right).

Once the streams have been calculated, the user can set an analysis window to measure average values and standard deviations for each of the calculated streams. The average azimuth value can then be sent to the map and plotted as a great circle. Using data from two or more infrasound arrays, events can be located by crossing the great circles.

Regional Seismic Analysis Tools

Phase Match Tool

PhaseMatch Tool is a waveform analysis interface launched from MatSeis that allows the user to calculate the predicted surface wave dispersion for a given source to receiver path by ray tracing through a model, and then use the model dispersion to generate and apply a matched filter (Herrin and Goforth, 1977). The tool (Figure 5) allows the user to view the observed waveform, the model dispersion, the predicted waveform, the cross-correlation of the predicted and observed waveforms, and the match-filtered waveform. The user can control the frequency range of the model dispersion used, as well as the time limit of the portion of the cross-correlated waveform from which the match-filtered waveform is taken. Once a satisfactory filtering has been achieved, the user can send either the

observed waveform or the filtered waveform to Measure Tool to measure surface wave amplitudes, which can then be used to determine event magnitude.

New features for the Version 1.7 include an option to display the signal's observed dispersion, and an option to use a station-based dispersion surface.

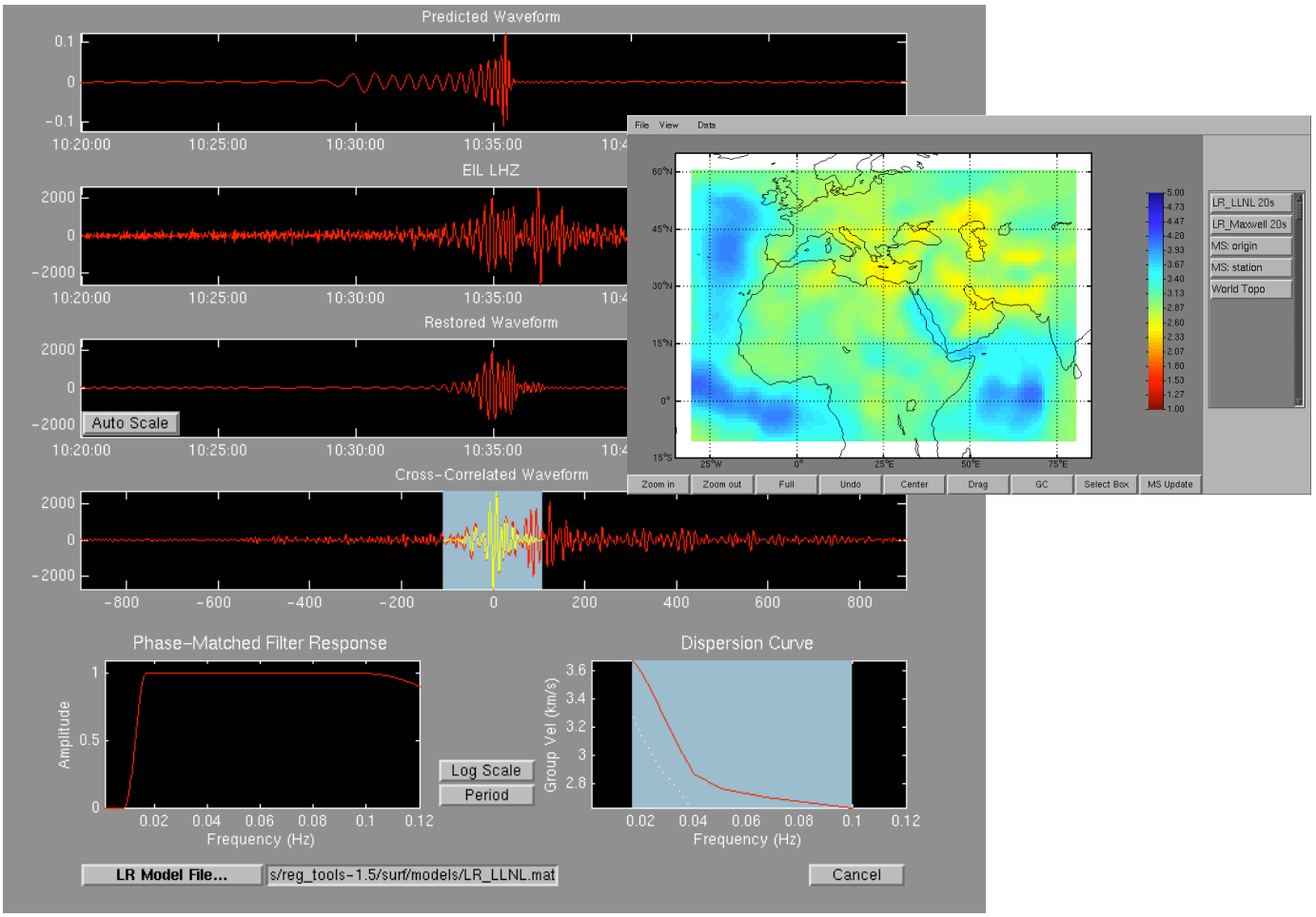

Figure 5. Phase Match Tool allows the user to use the information from a dispersion model (upper right) to design a phase-match filter to isolate surface waves.

Coda Magnitude Tool

CodaMag Tool is a waveform analysis interface launched from MatSeis that allows the user to calculate magnitudes and source spectra for an event of interest by fitting empirical decay functions to narrow-band coda envelopes of a given phase (currently Lg). The technique was developed by Mayeda and has been described in detail in several papers (Mayeda, 1993; Mayeda and Walter, 1996; Mayeda, et al., 1999). The tool consists of two displays. The main one shows the calculated moment spectrum and the derived magnitudes. The second display shows how the spectrum was derived. The user can adjust the Lg arrival window, examine the fit between the observed and synthetic envelopes, and control which frequency bands are used for the magnitude calculations. The various required parameters (frequency bands, groups velocity windows, decay curves, etc.) are read from parameter files unique to each station.

Important new features in Version 1.7 include a yield estimate based on the source spectrum, an option to display filtered seismograms in addition to the Hilbert envelopes, and the capability to write out data records to capture results.

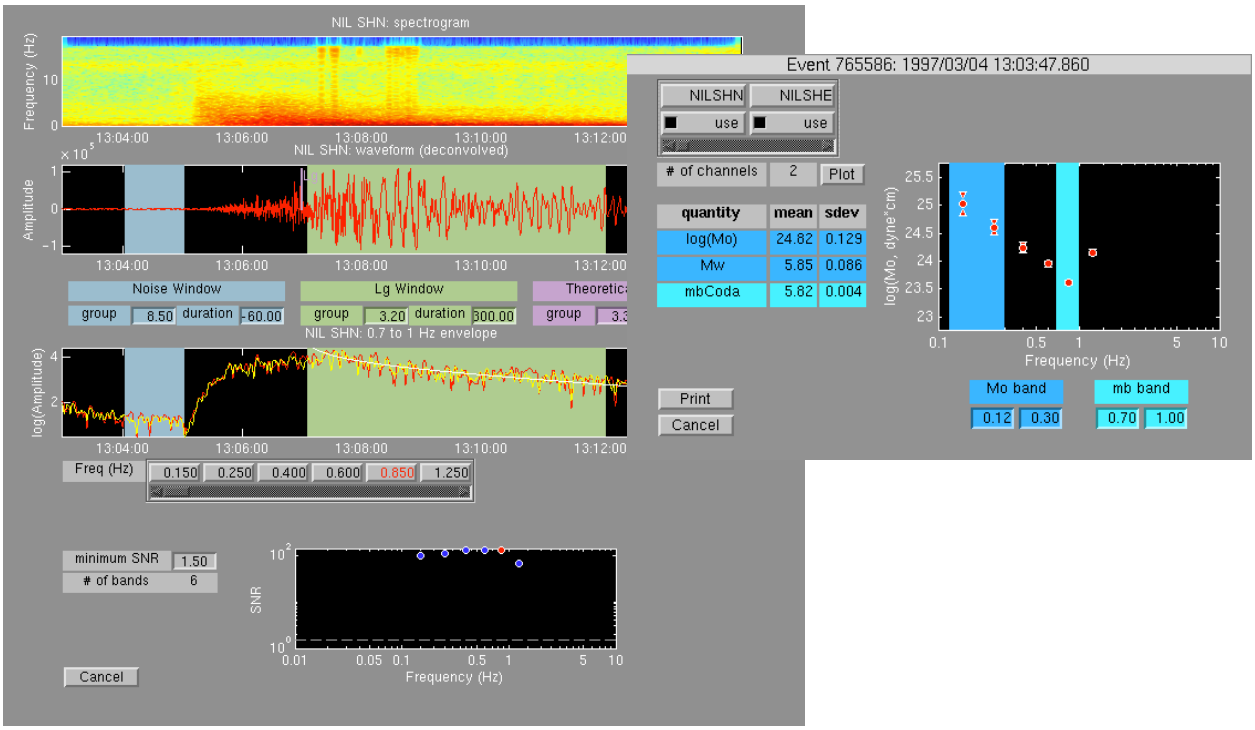

Figure 6. The Coda Mag Tool implements the methodology developed by Mayeda. Coda envelopes are fit for a series of narrow frequency bands (left), and the scaling factors are then used to derive a moment spectrum, from which various magnitudes can be taken (right).

Event Identification Tool

EventID Tool is a waveform analysis interface launched from MatSeis that allows the user to identify an event of interest (i.e. explosion or earthquake) using spectral ratios of standard regional arrivals (see Hartse et al., 1997; Walter et al., 1999). The tool (Figure 7) consists of three displays. The main display plots the phase ratio for the current event against a backdrop of the same ratio for archived events that have already been identified. The user can choose different phases and/or frequency bands to ratio to try to improve the separation of the earthquake and explosion populations, and the display will immediately update. A second display shows the user a plot of an "MDACogram" (i.e. the MDAC corrected measurements at all of the phase/frequency combinations) for the current event along with all of the archived events. This can be useful in deciding which ratio will yield the best separation. If there are questions about the amplitude measurements themselves, a third display can be brought up, and the user can easily examine group velocity windows for the phases and change them if necessary. If they are changed, the measurements will automatically be re-made and the ratios updated in the main display.

Version 1.7 has several important new features including the ability to apply MDAC2 corrections (Walter and Taylor, 2002) to the spectral measurements, as well as kriged corrections from Ground Truth events, the option to use multi-variate discriminants, the capability to screen the reference events shown, based on signal-to-noise ratio, and the capability to write out data records for processed events.

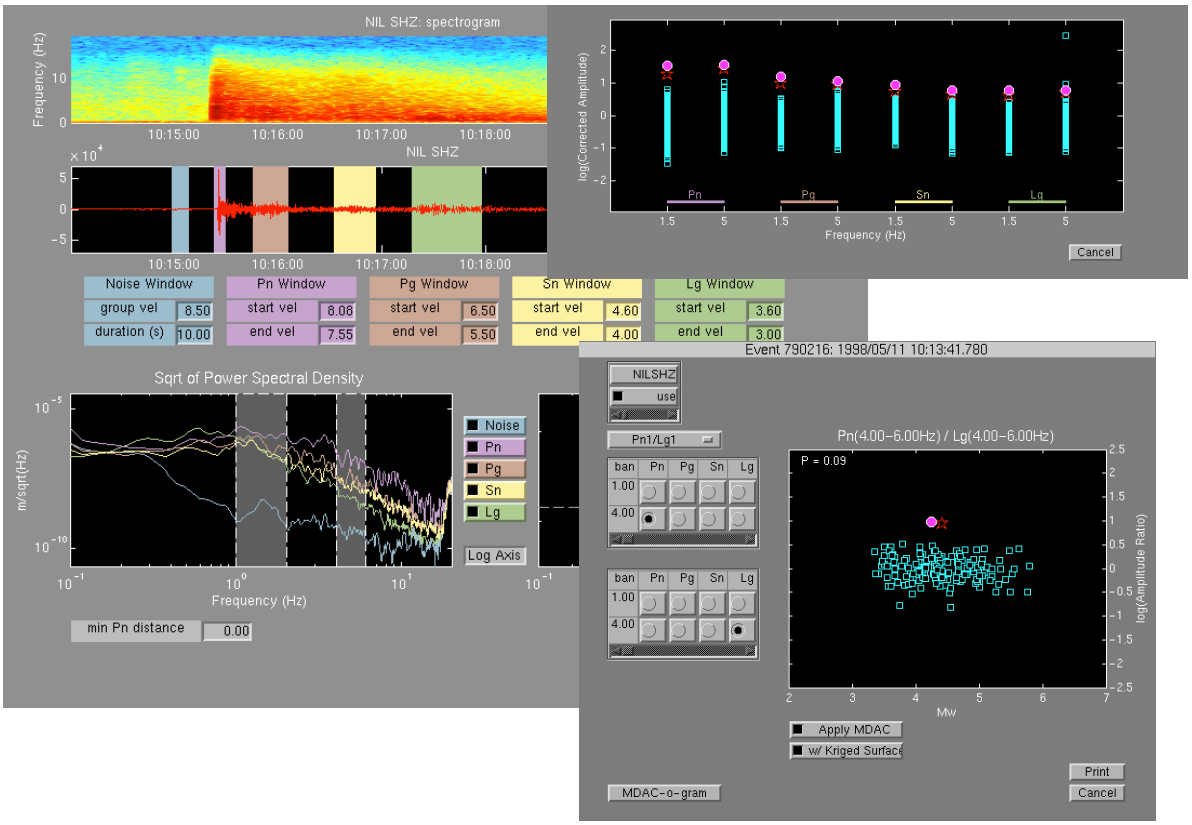

Figure 7. The EventID Tool helps the user discriminate explosions from earthquakes using standard phase-ratio methods. The user can view the overall results (lower right) or an "MDACogram" (upper right), or examine and change how the measurements for each phase were made (left).

Dendrogram Tool

The DendroTool provides a tool to perform waveform correlation-based cluster analysis techniques on seismic data. The purpose of Dendro Tool is quite simple: to allow a user to quickly and efficiently determine whether a waveform of interest matches any in the available archives. By arranging the correlations in a hierarchical dendrogram, rather than just determining the most similar waveform, the user gets a much more complete picture of how the current event fits with the archived events. For example, in regions with repeated mining explosions, the mines are often easily identified as distinct clusters, and new mining events can be readily identified as such by association with those clusters.

Dendro Tool consists of many interfaces to help the user assess the effectiveness of the clustering and to use the clusters to identify the events. The main display shows the dendrogram, along with a set of metrics that can be used to determine the correlation level to use to identify the families of events. Once a level has been chosen, the families are assigned separate, distinct colors to make them easier to see. Parameters controlling filtering and windowing of the waveforms, the method used to build the dendrogram, etc. can be set using another display, and the dendrogram will then be updated. The color-coded waveforms for any or all of the families in the dendrogram display can be sent to the MatSeis utility Free Plot for viewing to assess the validity of the families. The color-coded locations of the events in any or all of the families can be sent to the MatSeis Map Tool to see how the families agree with the locations. Within the Dendro Tool, origin times for any or all of the families can be used to generate color-coded histograms by year, month, day of year, day of week, or hour of day.

Dendro Tool can form dendrograms based on a single-phase window for a single station, or the user can choose to use multiple windows and/or multiple stations. The method of combining the multiple correlations (minimum, maximum, mean, median) is user controlled.

The significant new features for Version 1.7 are related to the newly added support for arrivals. The user can now view the picks along with the waveforms when examining the structure of the dendrograms. It is now also possible to use Dendro Tool to re-time arrivals based on lags calculated from the waveform cross-correlations. Once the current event has been added to a dendrogram, the user can then re-time the picks for that event based on the lags with other events in that group. Once the arrivals have been adjusted, they can then be sent back to MatSeis for other uses (e.g. re-locating the event).

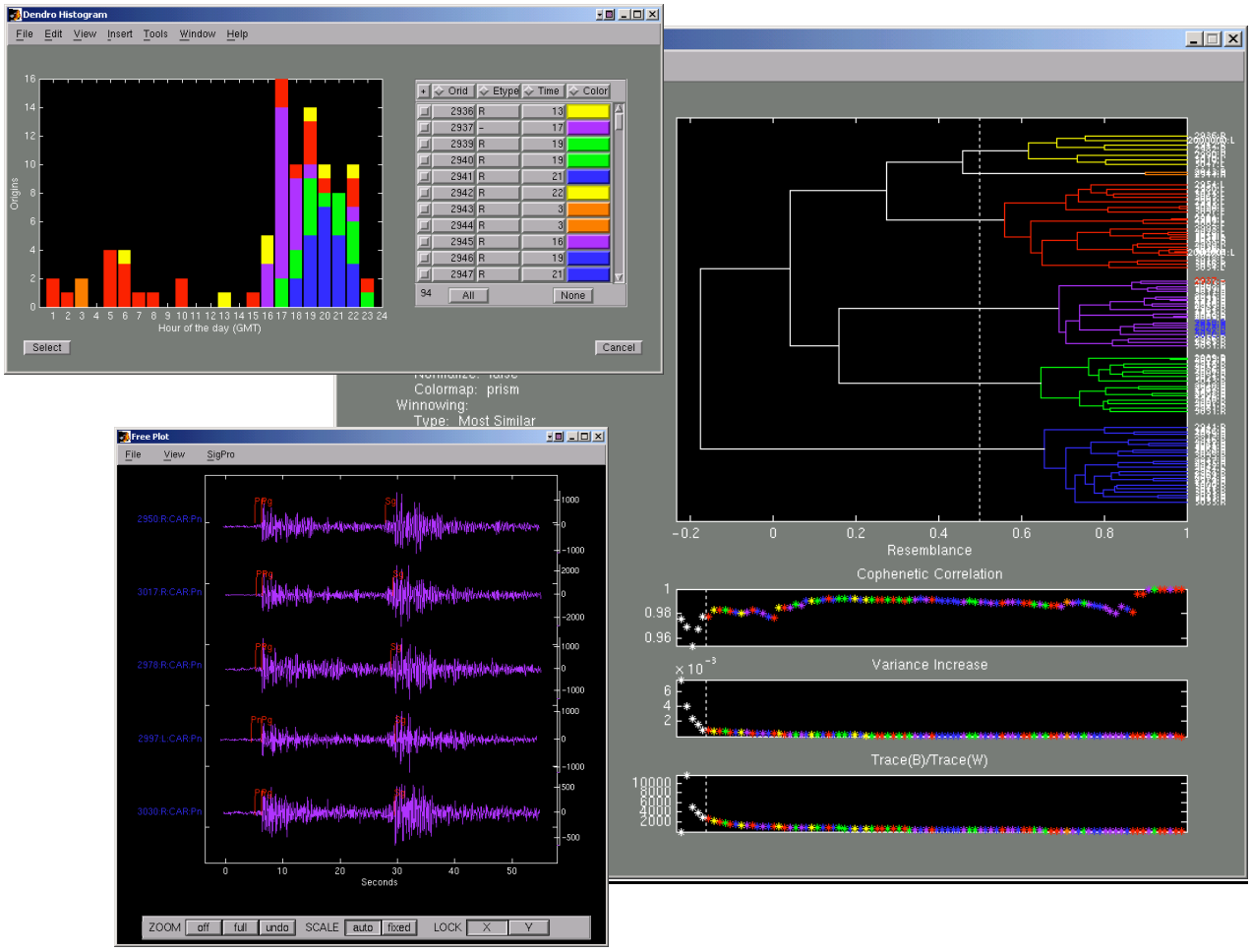

Figure 8. The Dendrogram Tool employs hierarchical cluster analysis to group similar waveforms. The main display is a dendrogram (right). The user can also view the waveforms (lower left) or histograms (upper left) for all or part of the dendrogram.

CONCLUSIONS AND RECOMMENDATIONS

Though started specifically to support signal-processing research in the GNEM program at Sandia Labs, MatSeis has now become an important part of the overall GNEM R&E program. It provides a much needed bridge between research results and operational monitoring. The ability of researchers to generate interesting new data sets and ideas continues to overmatch the resources available for testing them in an operational or quasi-operational setting. This is unfortunate both because using some of these products could immediately improve monitoring capabilities, and because feedback on the products could be used to guide further research.

To improve the situation, what is needed is a means to quickly develop realistic prototype software to test products. We believe that MatSeis offers one of the best, if not the best, platforms to do this. MatSeis handles all of the data I/O with the standard CSS3.0 format, it provides a broad range of basic seismic analysis functions, and perhaps most

importantly, it runs on top of the well-vetted, powerful, flexible, commercial Matlab product. So far, we have used MatSeis as a base to develop a suite of 4 regional seismic analysis tools – Phase Match Tool, Codamag Tool, EventID Tool, and Dendro Tool – which are being used to evaluate some of the analysis methodologies and regional calibration products produced by the GNEM R&E program. We expect to expand the use of MatSeis in the future and develop other prototype tools, where appropriate, to help evaluate promising research products.

The basic MatSeis package is available to all as a data product on the GNEM R&E web site: http://www.nemre.nn.doe.gov/nemre/

Matlab and the Signal Processing Toolbox are required to run MatSeis. Version 6.1 of Matlab or later is recommended, but the software should run with Matlab versions back as far as 5.3. MatSeis will run on Sun workstations, Windows PC's, and Linux PC's. It should run on other platforms as well, but the C code will need to be re-compiled.

ACKNOWLEDGEMENTS

We thank all of the MatSeis users who have helped us to debug and improve the software, particularly our colleagues at LANL and LLNL.

REFERENCES

Blandford, R. R. and R. H. Shumway (1982). Magnitude: yield for nuclear explosions in granite at the Nevada Test Site and Algeria: joint determination with station effects and with data containing clipped and low-amplitude signals, *Report VSC-TR-82-12*, Teledyne Geotech, Alexandria, Virginia.

Everitt, B. S. (2001). Cluster analysis, Arnold, London.

Hartse, H. E., Taylor, S. R., Phillips, W. S., and G. E. Randall (1997). A preliminary study of regional seismic discrimination in central Asia with emphasis on western China, *Bull. Seism. Soc. Am.*, 87, 551-568.

Herrin, E. and T. Goforth (1977). Phase-matched filters: application to the study of rayleigh waves, *Bull. Seism. Soc. Am.*, 67, 1259-1275.

Mayeda, K. (1993). Mb(LgCoda): a stable single station estimator of magnitude, *Bull. Seism. Soc. Am.*, 83, 851-861.

Mayeda, K. and W. R. Walter (1996). Moment, energy, stress drop, and source spectra of western United States earthquakes from regional coda envelopes, *J. Geophys. Res.*, 101, 11,195-11,208.

Mayeda, K., R. Hofstetter, A. J. Rodgers and W. R. Walter (1999). Applying coda envelope measurements to local and regional waveforms for stable estimates of magnitude, source spectra, and energy, *21st Annual Seismic Research Symposium on Monitoring a CTBT*, Vol I, 527-533.

Ringdal, F. (1976). Maximum-likelihood estimation of seismic magnitude, *Bull. Seism. Soc. Am.*, 66, 789-802.

Walter, W. R. and S. R. Taylor (2002). A revised magnitude and distance amplitude correction (MDAC2) procedure for regional seismic discriminants: theory and testing at NTS, *LLNL Report UCRL-ID-146882*.

Walter, W. R., A. J. Rodgers, A. Sicherman, W. Hanley, K. Mayeda, S. C. Myers and M. Pasyanos (1999). LLNL's regional seismic monitoring research, *21st Annual Seismic Research Symposium on Monitoring a CTBT*, Vol I, 294-302.